Aus dem Max von Pettenkofer-Institut

Lehrstuhl für Medizinische Mikrobiologie und Krankenhaushygiene

der Ludwig-Maximilians-Universität München

Vorstand: Prof. Dr. med. Sebastian Suerbaum

Exploring the role of *Mucispirillum schaedleri* in enteric *Salmonella enterica* serovar Typhimurium infection

Dissertation

zum Erwerb des Doktorgrades der Naturwissenschaften

an der Medizinischen Fakultät

der Ludwig-Maximilians-Universität München

vorgelegt von

Simone Herp

aus Offenburg

2018

Gedruckt mit Genehmigung der Medizinischen Fakultät
der Ludwig-Maximilians-Universität München

Betreuerin: Prof. Dr. Barbara Stecher-Letsch

Zweitgutachterin: Prof. Dr. Gabriele Rieder

Dekan: Prof. Dr. med. dent. Reinhard Hickel

Tag der mündlichen Prüfung: 19.02.2019

Eidesstattliche Erklärung

Ich, Simone Herp, erkläre hiermit an Eides statt, dass ich die vorliegende Dissertation mit dem Thema:

Exploring the role of *Mucispirillum schaedleri* in enteric *Salmonella enterica* serovar Typhimurium infection

selbständig verfasst, mich außer der angegebenen keiner weiteren Hilfsmittel bedient und alle Erkenntnisse, die aus dem Schrifttum ganz oder annähernd übernommen sind, als solche kenntlich gemacht und nach ihrer Herkunft unter Bezeichnung der Fundstelle einzeln nachgewiesen habe.
Ich erkläre des Weiteren, dass die hier vorgelegte Dissertation nicht in gleicher oder in ähnlicher Form bei einer anderen Stelle zur Erlangung eines akademischen Grades eingereicht wurde.

München, den 07.03.2019 Simone Herp

Table of Contents

Table of Contents

Table of Contents

Table of Contents

List of abbreviations

AAM	Akkermansia medium
ABTS	2,2'-Azino-di-(3-ethylbenzthiazolin-6-sulfonsäure)
AGR2	Anterior gradient homolog 2
Amp	Ampicillin
ANOVA	Analysis of variance
ArcBA	Aerobic respiratory control two-component system
ASF	Altered Schaedler Flora
ATP	Adenosine triphosphate
BHQ1	Black whole quencher 1
bp	Base pairs
BSA	Bovine serum albumin
BSH	Bile salt hydrolase
°C	Degrees Celsius
CA	Cholic acid
CD	Crohn`s disease
CDCA	Chenodeoxycholic acid
cfu	Colony forming units
Cm	Chloramphenicol
Cq	Quantification cycle
CR	Colonization resistance
DAPI	4',6-diamidino-2-phenylindole
DC	Dendritic cell
DCA	Deoxycholic acid
ddH_2O	Double-distilled water (Ampuwa)
dH_2O	Distilled water
Diam.	Diameter
DMSO	Dimethyl S-oxide
DNA	Deoxyribonucleic acid
DNRA	Dissimilatory nitrate reduction to ammonia
ds	Double-stranded
DSMZ	Deutsche Sammlung von Mikroorganismen und Zellkulturen
DTL	Limit of detection
EDTA	Ethylenediaminetetraacetic acid
EGTA	Ethylene glycol tetraacetic acid
ELISA	Enzyme-linked immunosorbent assay
EPEC	Enteropathogenic *Escherichia coli*
ETHZ	Eidgenössische Technische Hochschule Zürich
FAM	6-carboxyfluoresceine

List of abbreviations

FCS	Fetal calf serum
FISH	Fluorescence *in situ* hybridization
FNR	Fumarate nitrate reduction regulator
FRT	Flippase recognition target sites
Flp	Flippase
gDNA	Genomic DNA
GF	Germ-free
HDCA	Hyodeoxycholic acid
H&E	Hematoxylin and eosin
HEX	6-carboxyhexafluoresceine
HPLC	High-performance liquid chromatography
HRP	Horseradish peroxidase
IBD	Inflammatory bowel disease
ID	Identity
IL	Interleukin
iNOS	Inducible nitric oxide synthase
IVC	Individually ventilated cage
Kan	Kanamycin
LB	Luria-Bertani
LCA	Lithocholic acid
LCN2	Lipocalin-2
NapABCGH	Periplasmic nitrate reductase
NarGHI	Nitrate reductase A
NarZYV	Nitrate reductase Z
MCA	Muricholic acid
MGB	Minor groove binder
MHH	Medizinische Hochschule Hannover
mLN	Mesenteric lymph node
MOI	Multiplicity of infection
MUC2	Mucin 2
MvP	Max von Pettenkofer-Institut
nr	Nitrate reductase
n.s.	Not significant
nt	Nucleotide
OligoMM	Oligo-Mouse-Microbiota
OD_{600}	Optical density of 600 nm
p.a.	Pro analysi
PBS	Phosphate buffered saline
PCoA	Principal Coordinate Analysis
PCR	Polymerase chain reaction
PFA	Paraformaldehyde
p.i.	Post infection

List of abbreviations

PMN	Polymorphonuclear neutrophil
QIIME	Quantitative Insights Into Microbial Ecology
qPCR	Quantitative real-time polymerase chain reaction
RAST	Rapid Annotations using Subsystems Technology
RegIIIγ	Regenerating islet-derived protein III-gamma
RNA	Ribonucleic acid
RNAseq	RNA sequencing
RNS	Reactive nitrogen species
ROS	Reactive oxygen species
rpm	Revolutions per minute
RT	Room temperature
SCFA	Short chain fatty acids
SCV	*Salmonella*-containing vacuole
SD	Standard deviation
SDS	Sodium dodecyl sulfate
SPF	Specific pathogen-free
SPI	*Salmonella* pathogenicity island
SPI1-T3SS	T3SS encoded by SPI-1
SPI2-T3SS	T3SS encoded by SPI-2
sp.	Species
S. Tm	*Salmonella enterica* serovar Typhimurium
Strep	Streptomycin
TCA	Taurocholic acid
Tir	Translocated intimin receptor
TLR	Toll-like receptor
TMAO	Trimethylamin-N-oxide
TMCA	Tauromuricholic acid
T3SS	Type three secretion system
T6SS	Type six secretion system
UC	Ulcerative colitis
UPLC-MS	Ultra performance liquid chromatography - mass spectrometer
WHO	World Health Organization
wt	Wildtype

List of publications

Work conducted during the PhD thesis:

Loy A, Pfann C, Steinberger M, Hanson B, **Herp S**, Brugiroux S, Gomes Neto JC, Boekschoten MV, Schwab C, Urich T, Ramer-Tait AE, Rattei T, Stecher B and Berry D. **"Lifestyle and Horizontal Gene Transfer-Mediated Evolution of *Mucispirillum schaedleri*, a Core Member of the Murine Gut Microbiota"** mSystems 00171-16 **2017**

Brugiroux S, Beutler M, Pfann C, Garzetti D, Ruscheweyh HJ, Ring D, Diehl M, **Herp S**, Lötscher Y, Hussain S, Bunk B, Pukall R, Huson DH, Münch PC, McHardy AC, McCoy KD, Macpherson AJ, Loy A, Clavel T, Berry D and Stecher B. **"Genome-guided modular design of a novel defined mouse microbiota that confers colonization resistance against *Salmonella enterica* serovar Typhimurium."** Nature Microbiology 2: 16215 **2016**

Other publications:

Rosenbaum M, Andreani V, Kapoor T, **Herp S**, Flach H, Duchniewicz M, Grosschedl R. **"MZB1 is a GRP94 cochaperone that enables proper immunoglobulin heavy chain biosynthesis upon ER stress"** Genes & Development gad.240762.114 **2014**

Summary

The intestinal tract is home of trillions of bacteria which are essential for our health as they provide us with nutrients, are important for a balanced and mature immune system and protect us from enteric pathogens. The majority of the bacteria in the gut are obligate anaerobes which are fastidious and not easy to isolate or even culture. Though much progress has been made in the field of microbiome research in the past decade, still, our knowledge on lifestyle and functions of the mammalian gut bacteria is insufficient today. While many insights on the role of the microbiota for human health have been gained from comparative microbiome analyses in humans, the causative role of individual microbes in health and disease can only be addressed using gnotobiotic animal models. We can follow changes in the microbiota composition and distribution in the intestine, as well as resulting metabolic changes and the influence on the host immune system. Furthermore, the protective effect of specific microbiota alterations during enteric infections can be monitored. In this thesis I investigated the impact of *Mucispirillum schaedleri* ASF457 on *Salmonella enterica* serovar Typhimurium (*S*. Tm), a major cause of human gastroenteritis. *S*.Tm is transmitted via ingestion of contaminated food or via the fecal-oral route. After ingestion, *S*.Tm colonizes the intestinal tract, invades the intestinal epithelial cells and triggers inflammation by employing its type three secretion system (T3SS) encoded on *Salmonella* pathogenicity island 1 (SPI-1) (SPI1-T3SS). *S*.Tm is recognized by the innate immune system and induces a self-limiting gastroenteritis accompanied with diarrhea, fever, nausea and abdominal pain in healthy individuals. In a previous study with mucus-deficient *Agr2*$^{-/-}$ mice it was reported that *Agr2*$^{-/-}$ mice were protected from *S*. Tm colitis compared to littermate *Agr2*$^{+/-}$ control mice (Brugiroux, 2016). *M. schaedleri* was identified by comparative microbiome analysis as a candidate bacterium for protection from *S*. Tm colitis (Brugiroux, 2016).

Employing a gnotobiotic mouse model with a low complex microbiota consisting of 3 different bacterial species (*Clostridium* sp., *Parabacteroides goldsteinii* and *Lactobacillus murinus*) I could show that the mouse-derived bacterium *M. schaedleri* is localized in close proximity to the epithelium. While *M. schaedleri* had no effect on *S.* Tm gut colonization, it protected mice efficiently against *S*. Tm induced gut inflammation. This protective phenotype could be recapitulated in another gnotobiotic mouse model with a more complex microbiota, the

OligoMM^{12} mouse model. The microbial consortium of those mice consists of 12 different species representing the main 5 phyla inhabiting the murine gut (Firmicutes, Bacteroidetes, Verrucomicrobia, Proteobacteria and Actinobacteria) (Brugiroux *et al.*, 2016).

Microarray analysis revealed that *M. schaedleri* had no effect on suppression of the pro-inflammatory host response (Loy *et al.*, 2017). Further tissue invasion of *S.* Tm was drastically reduced in protected mucus-deficient *Agr2*$^{-/-}$ mice (Brugiroux, 2016). However, *M. schaedleri* did not block access to the epithelium. Finally, I could show that in the presence of *M. schaedleri* the *S.* Tm SPI1-T3SS is downregulated utilizing a *gfp*-reporter strain for SPI1-T3SS expression. Transcriptome data from *S.* Tm in gnotobiotic mice with and without *M. schaedleri* confirmed this result and further suggested a potential role of nitrate in SPI1-T3SS regulation *in vivo*.

Expression of *S.* Tm SPI1-T3SS is regulated by a complex network of transcription factors, two-component regulatory systems and environmental stimuli. Using a luciferase reporter strain for *S.* Tm SPI1-T3SS expression I could identify nitrate as a previously unknown stimulus for SPI1-T3SS induction under anaerobic conditions *in vitro*. This is an important finding as nitrate is formed from NO, a product of the gut epithelium by oxidation and reaches the gut lumen by diffusion.

Previously it was found that *M. schaedleri* is able to utilize alternative electron acceptors like nitrate, nitrite, trimethylamin-N-oxide (TMAO) and dimethyl S-oxide (DMSO) (Loy *et al.*, 2017) indicating competition with *S.* Tm. Employing *S.* Tm mutants unable to perform nitrate respiration (*S.* Tm$^{\Delta nr3}$) or anaerobic respiration of nitrate, TMAO, DMSO, tetrathionate and fumarate (*S.* Tm$^{\Delta moaA}$), I showed that the protective effect of *M. schaedleri* is independent of utilization of those alternative electron acceptors by *S.* Tm, suggesting that other environmental factors like nitrite or O_2 could be involved in regulation of SPI1-T3SS.

M. schaedleri was described as a mucus dwelling bacterium and protection of *Agr2*$^{-/-}$ mice from *S.* Tm colitis was attributed to *M. schaedleri* (Brugiroux, 2016). So far the role of mucus-deficiency on *M. schaedleri* colonization and function is unclear. Employing mucus-deficient gnotobiotic mice (OligoMM^{12} *Agr2*$^{-/-}$) I found that *M. schaedleri* colonized OligoMM^{12} *Agr2*$^{-/-}$ mice and protected mice from *S.* Tm colitis independently of the host genotype.

Summary

With this study I identified *M. schaedleri*, a low abundant member of the murine microbiota, as a protective bacterium against *S.* Tm infection. The *S.* Tm SPI1-T3SS was found to be downregulated in the presence of *M. schaedleri,* suggesting that *M. schaedleri* directly affects SPI1-T3SS regulation or alters the environmental conditions which are important for SPI1-T3SS expression. Competition for nitrate, oxygen and H_2 may be involved in virulence interference by *M. schaedleri*. Currently, genetic manipulation of *M. schaedleri* is not possible which limited further mechanistic analysis of the protective phenotype.

Zusammenfassung

Der Magen-Darm-Trakt beherbergt eine Vielzahl an Mikroorganismen – die Mikrobiota. Sie erfüllt essentielle Aufgaben wie den Aufschluss von Nährstoffen, die Entwicklung eines gesunden Immunsystems und den Schutz vor Krankheitserregern. Die Darm-Mikrobiota setzt sich vor allem aus obligat anaeroben Bakterien zusammen, welche komplexe Anforderungen an die Kultivierung und Isolierung stellen. In den letzten zehn Jahren wurden große Fortschritte im Bereich der Mikrobiom-Forschung gemacht, allerdings ist unser Wissen über die Lebensweise und Funktionen der einzelnen Darmbakterien bis heute sehr begrenzt. Die vergleichende Mikrobiom-Analyse gewährt uns erste Einblicke auf die wichtige Rolle der Darm-Mikrobiota im Zusammenhang mit der menschlichen Gesundheit. Die kausalen Zusammenhänge einzelner Bakterien auf den Schutz vor Krankheiten kann allerdings nur mit Hilfe gnotobiotischer Modelle untersucht werden. In diesen können Veränderungen der Mikrobiota-Zusammensetzung als auch die daraus resultierenden Auswirkungen auf das Metabolom sowie auf das Immunsystem des Wirts betrachtet werden. Zusätzlich kann der Beitrag einzelner Bakterien auf den Schutz vor Krankheitserregern analysiert werden. In dieser Doktorarbeit wurde der Einfluss des Bakteriums *Mucispirillum schaedleri* ASF457 auf die Infektion mit *Salmonella enterica* serovar Typhimurium (*S*. Tm) untersucht. Eine Infektion mit *S*. Tm erfolgt durch die Aufnahme verunreinigten Essens und ist die Hauptursache für Gastroenteritis beim Menschen. *S*. Tm besiedelt den Darm und wandert in die Epithelzellen ein wofür ein Typ-3-Sekretionssystem (T3SS) genutzt wird, welches auf der *Salmonella* Pathogenitätsinsel-1 (SPI1) codiert ist. Das angeborene Immunsystem erkennt *S*. Tm und löst eine selbstbegrenzende Gastroenteritis aus, welche sich durch Durchfall, Fieber, Erbrechen und Bauchschmerzen kennzeichnet. Eine Studie mit Mucus-defizienten *Agr2*$^{-/-}$ Mäusen zeigte, dass *Agr2*$^{-/-}$ Mäuse vor einer *S*. Tm induzierten Gastroenteritis geschützt waren (Brugiroux, 2016). Vergleichende Mikrobiom-Analyse identifizierte *M. schaedleri* als potentielles Bakterium, welches Schutz vor *S*. Tm Kolitis vermittelt (Brugiroux, 2016).

In gnotobiotischen Mäusen mit einer minimalen Mikrobiota bestehend aus drei Spezies (*Clostridium* sp.; *Parabacteroides goldsteinii* und *Lactobacillus murinus*) konnte gezeigt werden, dass *M. schaedleri* sich nahe des Darmepithels ansiedelt. Bei einer Infektion mit *S*.Tm verhindert *M. schaedleri* nicht die Besiedlung von *S*. Tm, allerdings schützte es vor

einer Entzündung des Zökums. Die Protektion von *M. schaedleri* gegenüber *S.* Tm Kolitis konnte zusätzlich in einem weiteren gnotobiotischen Model, der OligoMM^{12} Maus, gezeigt werden. Die OligoMM^{12} setzt sich aus 12 verschiedenen Bakterienarten zusammen, welche den fünf Hauptphyla (Firmicutes, Bacteroidetes, Verrucomicrobia, Proteobacteria und Actinobacteria) der Mausmikrobiota angehören (Brugiroux *et al.*, 2016).

Durch Microarray Analysen konnte gezeigt werden, dass *M. schaedleri* keinen Einfluss auf die pro-inflammatorische Immunantwort ausübt (Loy *et al.*, 2017). Weiterhin wurde festgestellt, dass in geschützte mucus-defizienten *Agr2*$^{-/-}$ Mäuse weniger *S.* Tm in das Epithel eindrangen (Brugiroux, 2016). Allerdings blockiert *M. schaedleri* nicht den Zugang zum Epithel. Mit Hilfe eines *gfp*-Reporters für SPI1-T3SS Expression konnte ich zeigen, dass *S.*Tm in der Gegenwart von *M. schaedleri* das SPI1-T3SS herunter reguliert. *In vivo* Transkriptom Daten von *S.*Tm bestätigen die verringerte Expression von SPI1-T3SS in Mäusen mit *M. schaedleri*.

Die Expression von *S.* Tm SPI1-T3SS ist durch ein komplexes Netzwerk von Transkriptionsfaktoren, Zweikomponentensystem und Umwelteinflüssen reguliert. Mittels eines Luziferase-Reportersystems für SPI1-T3SS Expression konnte gezeigt werden, dass Nitrat unter anaeroben Bedingungen eine induzierende Wirkung auf das SPI1-T3SS ausübt.

M. schaedleri besitzt die Fähigkeit alternative Elektronenakzeptoren wie Nitrat, Nitrit, Trimethylamin-N-oxid (TMAO) und Dimethylsulfoxid (DMSO) zu nutzen (Loy *et al.*, 2017). Dies könnte zu einer Kompetition mit *S.* Tm führen. Mit Hilfe von *S.* Tm Mutanten, welche keine funktionelle Nitratatmung besitzen (*S.* Tm$^{\Delta nr3}$) oder keine anaerobe Atmung von Nitrat, DMSO, TMAO, Tetrathionat und Fumarat betreiben können (*S.* Tm$^{\Delta moaA}$), wurden für *in vivo* Infektionsstudien genutzt. Dadurch konnte gezeigt werden, dass der protektive Effekt von *M. schaedleri* unabhängig von diesen alternativen Elektronakzeptoren ist und weiter Umweltfaktoren wie O_2 und Nitrit eine wichtige Rolle spielen könnten.

In mucus-defizienten *Agr2*$^{-/-}$ Mäusen wurde *M. schaedleri* eine schützende Wirkung vor *S.* Tm Kolitis zugeschrieben (Brugiroux, 2016). Allerdings ist die Bedeutung der Mucusschicht auf die Besiedlung und Funktion von *M. schaedleri* im Darm noch nicht erforscht. Mittels gnotobiotischer mucus-defizienter Mäuse (OligoMM^{12} *Agr2*$^{-/-}$) konnte ich

zeigen, dass *M. schaedleri* auch OligoMM^{12} *Agr2*$^{-/-}$ Mäuse kolonisiert und diese Mäuse unabhängig ihres Genotypes vor *S.* Tm induzierten Gastroenteritis schützt.

Mit dieser Arbeit konnte gezeigt werden, dass das Bakterium *M. schaedleri* protektiv gegenüber *S.* Tm Kolitis ist. Das *S.* Tm SPI1-T3SS ist in der Gegenwart von *M. schaedleri* herunter reguliert, was darauf hindeutet, dass *M. schaedleri* entweder direkt die SPI1-T3SS Regulation beeinflusst oder aber die Umweltbedingungen verändert welche für die SPI1-T3SS Expression essentiell sind. Kompetition um Nitrat, Sauerstoff und Wasserstoff könnten eine wichtige Rolle einnehmen. Zurzeit ist es nicht möglich *M. schaedleri* genetisch zu verändern, was weiter mechanistische Analysen erschwert.

1 Introduction

1.1 The intestinal microbiota: keeper of homeostasis and health

Our intestine is the natural habitat for trillions of bacteria with which we maintain a mutualistic relationship beginning directly at birth. Those bacteria provide us with nutrients such as vitamins and short chain fatty acids (SCFA) essential for the metabolism and protect us from invading pathogens. Studies showed that antibiotic intake disrupts the microbiota and increases the susceptibility to intestinal pathogens like *Salmonella enterica* serovar Typhimurium (*S*.Tm), *Clostridium difficile* and vancomycin-resistant *Enterococcus* (Buffie *et al.*, 2012; Ubeda *et al.*, 2010) which can have severe outcomes.

Therefore it is of enormous importance that we study and understand how individual commensal bacteria and pathogens interact with each other and with their host.

1.1.1 Mechanisms of colonization resistance (CR)

The intestinal microbiota confers protection against enteric pathogens which is called colonization resistance (CR) (Buffie & Pamer, 2013; Stecher *et al.*, 2013). This is mediated by multiple mechanisms. Direct CR is conferred by secretion of harmful bacteriocins or attacking other bacteria with a type 6 secretion system (T6SS) (Corr *et al.*, 2007; Donohoe *et al.*, 2011; Hecht *et al.*, 2016; Sassone-Corsi *et al.*, 2016). It was also shown that bacteria can compete for the same nutrients, and therefore limit colonization (Deriu *et al.*, 2013; Leatham *et al.*, 2009) (Fig. 1B). Furthermore, the microbiota modulates the host's immune system by enhancing secretion of antimicrobial peptides like RegIIIγ and strengthens our epithelial barrier (Cash *et al.*, 2006; Rakoff-Nahoum *et al.*, 2004) which is termed indirect or immune-mediated colonization resistance (Buffie & Pamer, 2013) (Fig. 1A). Further, *Clostridium scindens* was shown to be a secondary bile acid producer. Those secondary bile acids prevent vegetative growth of *C. difficile* (Buffie *et al.*, 2015; Studer *et al.*, 2016) (Fig. 1A).

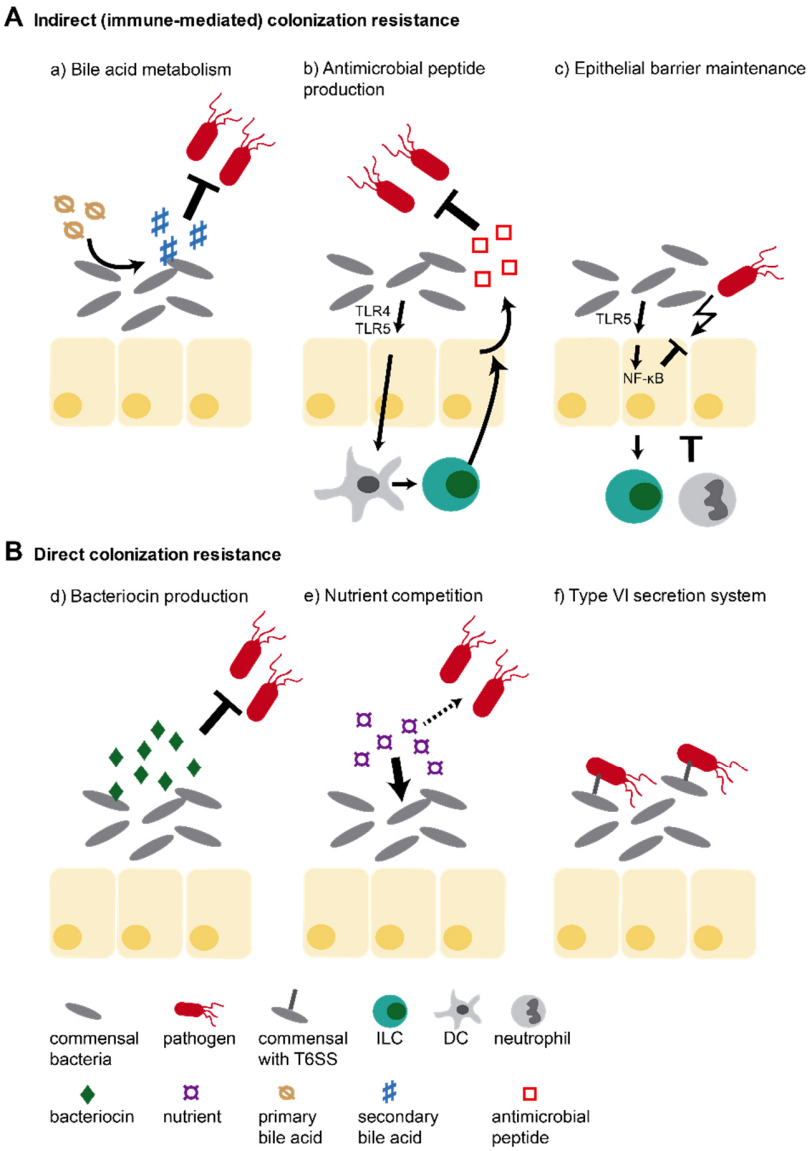

Fig. 1. Mechanisms of colonization resistance. A) Indirect (immune-mediated) CR. a) The commensal bacterium *Clostridium scindens* can convert primary bile acids in secondary bile acids. Those inhibit the vegetative growth of the pathogen *Clostridium difficile*. b) Commensal bacteria stimulate continuously the innate immune system via flagellin or LPS leading to the secretion of antimicrobial peptides (e.g. RegIIIγ) by paneth and epithelial cells. This leads to pore formation in Gram positive bacteria (e.g. Vancomycin resistant *Enterococcus* or *Listeria monocytogenes*). c) Pathogens like *C. difficile* lead to disruption of the epithelial barrier. The microbiota induces the NF-κB pathway in epithelial cells via TLR5 signaling. This pathway leads to induction of anti-apoptotic factors which results in cell proliferation and enhancement of tight junctions. The recruitment of innate immune cells further stabilizes epithelial integrity. **B)** Direct colonization resistance. d) The probiotic *E. coli* Nissle 1917 can secrete bacteriocins which reduce colonization of pathogenic bacteria like *Salmonella enterica* serovar Typhimurium and therefore leads to lower intestinal inflammation. e) The commensal bacteria can compete with invading pathogens for essential nutrients like iron or carbohydrates and therefore limit colonization. f) Commensal *Bacteroides* spp. can employ their T6SS and deliver toxic effector proteins in a contact dependent manner to pathogenic *Bacteroides* spp.. This leads to reduced intestinal inflammation. Adapted from (Buffie & Pamer, 2013; Kim *et al.*, 2017).

1.1.2 SCFAs are important for our intestinal health

The majority of the intestinal bacteria are obligate anaerobes which meet their energy demands by fermentation of indigestible carbohydrates, thereby producing SCFA like butyrate, acetate, propionate, succinate, formate and lactate (Macfarlane & Macfarlane, 2003; Macfarlane *et al.*, 1998; Miller & Wolin, 1996). These SCFAs have extremely diverse and pivotal functions for the host. They serve as an energy source for colonocytes (Donohoe *et al.*, 2011), play an important role in immune regulation (Calo *et al.*, 2015; Furusawa *et al.*, 2013; Trompette *et al.*, 2014), improve barrier integrity via tight junctions and regulate the pH of the intestine (den Besten *et al.*, 2013; Peng *et al.*, 2009).

1.1.3 Host produced bile acids are modified by the intestinal microbiota

Another important group of metabolites in the gut are bile acids. They are produced in the liver from cholesterol were they are conjugated to taurine or glycine to primary bile acids. Mice and humans harbor a different set of bile acids. Primary bile acids in mice are α-muricholic acid (MCA) and β-MCA. Both in mouse and human we find cholic acid (CA) as well as chenodeoxycholic acid (CDCA)). Those primary bile acids are secreted into the gallbladder and released into the intestine upon ingestion of food (Falany *et al.*, 1994; Vessey, 1978; Wahlstrom *et al.*, 2016). They are needed to facilitate the uptake of lipids and fat-soluble vitamins. The gut microbiota has the capacity to modify the primary bile acids by deconjugation using bile salt hydrolases (BSH) or form secondary bile acids by dehydroxylation. Secondary bile acids in mouse and human are lithocholic acid (LCA) and deoxycholic acid (DCA) whereas only in mouse hyodeoxycholic acid (HDCA) and ω-MCA are present. Bile acids recirculate to the liver via the enterohepatic route (de Aguiar Vallim *et al.*, 2013). BSHs are found in a variety of different bacterial species belonging to the genera *Bacteroides*, *Clostridium*, *Lactobacillus* and *Bifidobacterium* (Chand *et al.*, 2017; Moser & Savage, 2001). Bile acids can directly harm sensitive bacteria by membrane disruption and DNA damage (Begley *et al.*, 2005; Devlin & Fischbach, 2015; Merritt & Donaldson, 2009; Sung *et al.*, 1993), but plenty of enteric pathogens evolved mechanisms to survive bile salt exposure and even managed to use them as signals for virulence gene expression (Sistrunk *et al.*, 2016). For example, *S.* Tm employs several efflux pumps to fend off intracellular bile acids (Buckley *et al.*, 2006; Nishino *et al.*, 2006) and uses DNA adenine methylase to cope with bile acid induced DNA damage (Prieto *et al.*, 2004). On the other hand, *S.* Tm responds to bile acids by regulating its virulence factors. Its SPI1-T3SS and flagella biosynthesis are downregulated in the presence of a mixture of bile acids which

could be an adjustment to decreasing bile salt concentrations along the intestinal tract (Prouty & Gunn, 2000; Sistrunk *et al.*, 2016; Wohlgemuth *et al.*, 2011).

1.2 *Mucispirillum schaedleri*, a commensal bacterium in the murine gut

Mucispirillum schaedleri, a member of the family *Deferribacteraceae* (Robertson *et al.,* 2005) is Gram$^-$, flagellated, spiral shaped and a obligate anaerobic bacterium (Robertson *et al.*, 2005). It is a common member of the mouse gut microbiota (Rosshart *et al.*, 2017) and also found in the intestine of several different species like turkey, pigs, lizards and occasionally also in humans (Harrell *et al.*, 2012; He *et al.*, 2016; Rausch *et al.*, 2011; Scupham *et al.*, 2008; Zhang *et al.*, 2018). Interestingly, in the family *Deferribacteraceae*, *M. schaedleri* is the only species known to inhabit the intestine, whereas the other members were isolated from waste water, hot springs and sediments (Loy *et al.*, 2017). *M. schaedleri* is enriched in mice suffering from acute colitis (Berry *et al.*, 2012; Rooks *et al.*, 2014; Selvanantham *et al.*, 2016; Song *et al.*, 2018) and is also elevated in obese mice (Ravussin *et al.*, 2012; Serino *et al.*, 2012). Recently, genome and transcriptome analysis gave us a deeper insight into the lifestyle of *M.schaedleri* (Loy *et al.*, 2017). Several genes important for anaerobic respiration of nitrate, fumarate, TMAO or tetrathionate are present (Loy *et al.*, 2017). Its capacity to use nitrate as electron acceptor and perform full dissimilatory nitrate reduction to ammonia (DNRA) was verified in *in vitro* cultures (Fig. 2B) (Loy *et al.*, 2017). Furthermore, this bacterium occupies a niche close to the epithelium and genes for the defense against oxidative stress (e.g. catalase, superoxide reductase and cytochrome c peroxidase) were found (Loy *et al.*, 2017). Despite *M.schaedleri* was shown to colonize close to the mucus layer no enzymes for mucus degradation were found (Loy *et al.*, 2017). Predicted genomic features are visualized in (Fig. 2A) (Loy *et al.*, 2017).

M. schaedleri (ASF457) is also a component of the Altered Schaedler Flora (ASF). The ASF is a bacterial consortium established in 1965 by Russel W. Schaedler and consisted initially of five bacterial isolates from the murine gut (Schaedler *et al.*, 1965). Later this consortium was revised by Roger Orcutt to enclose eight different species (Orcutt *et al.*, 1987), two lactobacilli (*L. intestinalis* ASF360 and *L. murinus* ASF361), *Parabacteroides goldsteinii* (ASF519), *Eubacterium plexicaudatum* (ASF492), *Pseudoflavonifactor* sp. (ASF500), *M. schaedleri* (ASF457) and two *Clostridium* spp. (ASF356 and ASF502) (Dewhirst *et al.*, 1999; Wymore Brand *et al.*, 2015).

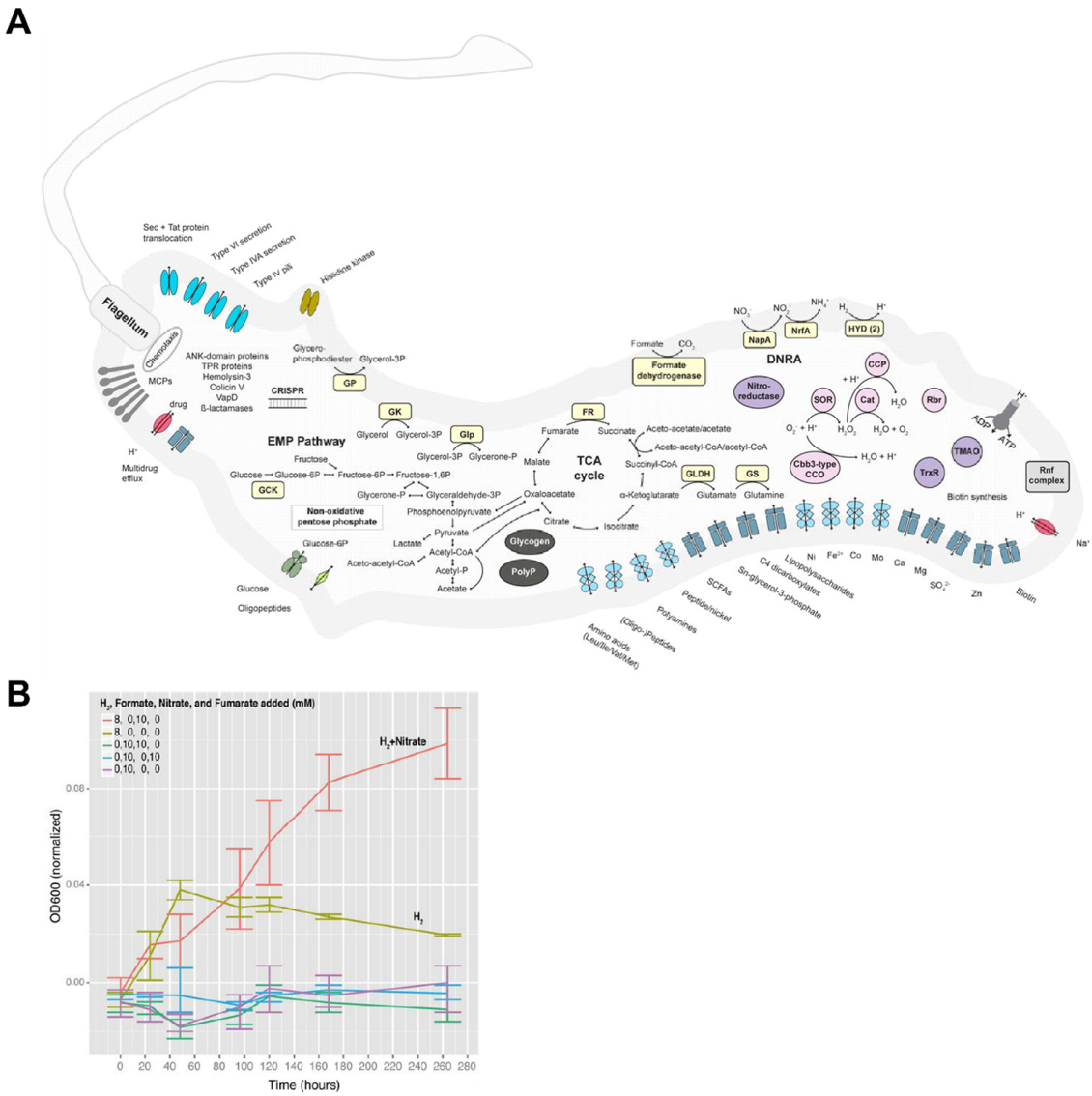

Fig. 2. Genomic features of *M. schaedleri*, based on prediction from genome annotations (Loy *et al.*, 2017). A) Model of metabolic features of *M. schaedleri.* Abbreviations: Cat: Catalase; CCO: Cytochrome c oxidase; CCP: Cytochrome c peroxidase; DNRA: Dissimilatory nitrate reduction to ammonium; EMP: Embden-Meyerhof-Parnas; FR: Fumarate reductase; GCK: Glucokinase; GK: Glycerol kinase; GLDH; Glutamate dehydrogenase; Glp: Sn-glycerol-3-phosphate dehydrogenase; GP: Glycerolphosphodiester phosphodiesterase; GS: Glutamine synthetase; HK: Histidine kinase; HYD: Hydrogenase; Hyb: Hydrogenase 2; MCP: Methyl-accepting chemotaxis protein; NapA: Periplasmic nitrate reductase; NrfA: Cytochrome c nitrite reductase; PolyP: Polyphosphate; Rbr: Rubrerythin; Rnf: Ferredoxin:NAD^+ oxidoreductase; SOR: Superoxide reductase; TMAO: Trimethylamine-N-oxide reductase; TrxR: Thioredoxin reductase; TCA: Tricarboxylic acid. **B)** Growth of *M.schaedleri* under anaerobic conditions in the presence of either 10 mM nitrate and 8 % H_2 (red); only 8 % H_2 (light green); 10 mM formate and 10 mM nitrate (dark green); 10 mM formate and 10 mM fumarate (blue) or only 10 mM formate (violet) monitored by OD_{600} measurement. *M. schaedleri* can use nitrate as electron acceptor and H_2 as electron donor under anaerobic conditions (Loy *et al.*, 2017). Figures from (Loy *et al.*, 2017).

1.3 *Salmonella enterica* serovar Typhimurium (*S*.Tm)

1.3.1 *S*.Tm is a major cause of gastroenteritis

The non-typhoidal *Salmonella* Typhimurium (*S*.Tm), a Gram$^-$ rod shaped bacterium of the family *Enterobacteriaceae*, is the cause of foodborne Salmonellosis. It is transmitted via ingestion of contaminated food but can also be passed directly person-to-person via the fecal-oral route (WHO, 2018). After ingestion, *S.* Tm induces a localized and self-limiting gastroenteritis, accompanied with diarrhea, fever, nausea and abdominal pain in healthy individuals (Coburn *et al.*, 2006). Immunocompromised people can suffer from an invasive disease resulting in high mortality (Gordon, 2008; Uche *et al.*, 2017). To establish disease, *S.* Tm needs to colonize the intestinal tract and invade the epithelium where it is recognized by the immune system which subsequently triggers inflammation (Hapfelmeier *et al.*, 2005; Lawley *et al.*, 2008). When *S.* Tm is close to the epithelial barrier it employs a needle like structure, its type 3 secretion system, encoded on the *Salmonella* Pathogenicity Island 1 (SPI1-T3SS), to invade the epithelial cells (Laughlin *et al.*, 2014; Lorkowski *et al.*, 2014). Once inside a host cell, *S.* Tm uses its second T3SS, located on the *Salmonella* Pathogenicity Island 2 (SPI2), to survive and multiply intracellularly (Hensel *et al.*, 1998; Laughlin *et al.*, 2014; Ochman *et al.*, 1996).

1.3.2 Experimental models for studying *S*.Tm induced colitis

1.3.2.1 The streptomycin mouse model

For a long time it has been challenging to decipher mechanisms important for *S*.Tm pathogenesis *in vivo*, as the most common experimental model, the mouse, is resistant to *S*.Tm induced gastroenteritis. Instead mice develop systemic disease resembling the course of human typhoid fever (Santos *et al.*, 2001). Studies by Barthel and colleagues found that this protection is dependent of the microbiota and established the streptomycin mouse model (Barthel *et al.*, 2003). The antibiotic streptomycin disrupts the colonization resistance against *S*. Tm. Mice treated with a high dose of streptomycin one day prior to infection are efficiently colonized by *S*. Tm and develop gastroenteritis one day post infection (p.i.) with symptoms resembling human disease (diarrhea, submucosal edema, epithelial ulceration, infiltration of polymorphonuclear cells (PMNs) and loss of goblet cells) (Barthel *et al.*, 2003; Day D *et al.*, 1978).

1.3.2.2 Gnotobiotic low complex microbiota models

Another possibility to study *S.* Tm infection is the use of gnotobiotic mouse models, harboring a microbiota with reduced complexity which does not confer colonization resistance to *S.* Tm. One of these mouse models are mice colonized with the ASF (1.2) consisting of 8 bacterial species. This consortium does not confer colonization resistance to *S.* Tm and the mice develop colitis without disruption of the microbiota by antibiotic pretreatment (Stecher *et al.*, 2010). A more complex consortium consisting of 12 bacterial species (OligoMM^{12}; Table 22, Fig. 3A) was recently published (Brugiroux *et al.*, 2016). This consortium maintains a stable composition over mouse generations and confers intermediate colonization resistance (Brugiroux *et al.*, 2016) which is ideal to study the different stages of *S.* Tm colonization and onset of inflammation. The use of this model makes it possible to explore *S.* Tm induced microbiota changes over time (Beutler, 2016). Onset of inflammation is observed at day 3 post infection and severe colitis is established one day later, 4 days post infection (Fig. 3C) (Beutler, 2016).

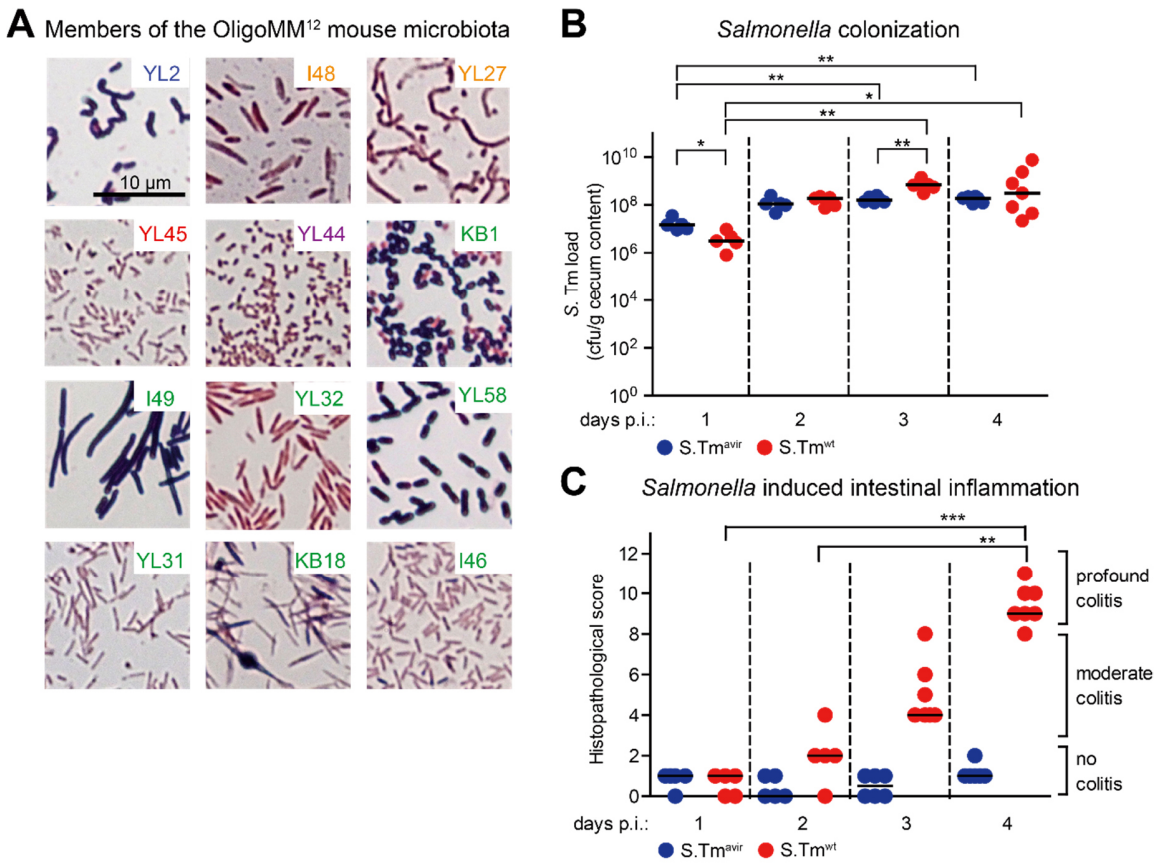

Fig. 3. The gnotobiotic OligoMM^{12} mouse microbiota model. A) Images of Gram stainings from each individual strain of the OligoMM^{12} microbiota. Actinobacteria: YL2, *Bifidobacterium longum* subsp. *animalis;* Bacteroidetes*:* I48*, Bacteroides caecimuris;* YL27*, Muribaculum intestinale;* Proteobacteria: YL45*, Turicimonas muris;* Verrucomicrobia*:* YL44*, Akkermansia muciniphila;* Firmicutes: KB1*, Enterococcus faecalis; I49, Lactobacillus reuteri;* YL32*, Clostridium clostridioforme;* YL58*, Blautia coccoides;* YL31*, Flavonifractor plautii;* KB18*, Acutalibacter muris;* I46*, Clostridium innocuum;* scale bar: 10 µm. Picture from (Brugiroux *et al.*, 2016). **B)** Colonization of an attenuated *S*.Tm^{avir} (blue dots) and a virulent *S*.Tm^{wt} (red dots) over time in mice associated with the OligoMM^{12} consortium (Beutler, 2016). **C)** Histopathological score of cecal tissue after infection with an attenuated *S*.Tm^{avir} and a virulent *S*.Tm^{wt} over time. *S*.Tm^{wt} induces inflammation at day 3 p.i. (Beutler, 2016). The degree of submucosal edema, neutrophil infiltration, loss of goblet cells and epithelial damage was scored in a double-blinded manner. 0-3: no pathological changes; 4-7: moderate inflammation; above 8: severe inflammation. Each dot represents one mouse. Kruskal-Wallis test with Dunn's multiple comparison test, no significant difference $p \geq 0.05$, *$p < 0.05$, **$p < 0.01$, ***$p < 0.001$. Adapted from (Beutler, 2016).

1.3.3 The *Salmonella* pathogenicity island 1 type 3 secretion system (SPI1-T3SS)

For full pathogenicity, *S.* Tm requires its major virulence factor, the SPI1-T3SS (Hapfelmeier *et al.*, 2005). The SPI1-T3SS consists of a multitude of structural proteins that form a needle like structure. With this apparatus, *S.* Tm can deliver a cocktail of effector proteins into host cells and facilitate pathogen uptake by rearrangement of the host cell's cytoskeleton (Burkinshaw & Strynadka, 2014). Furthermore, by invasion into host cells, the innate immune response is triggered and a pro-inflammatory milieu is established (cf. 1.3.4.3). As SPI1-T3SS fulfills an essential role, it was already studied extensively, but due to its complex regulatory networks little is known on the environmental factors influencing its expression. Induction of SPI1-T3SS under laboratory conditions is extremely influenced by osmolarity of the medium, oxygen concentration and growth phase (Bajaj *et al.*, 1996; Galan & Curtiss, 1990; Lee & Falkow, 1990; Steele-Mortimer *et al.*, 1999; Tartera & Metcalf, 1993). Standard SPI1-inducing conditions are reported as high salt (0.3 M NaCl) and microaerobic growth (1 % O_2) (Lee & Falkow, 1990; Song *et al.*, 2004). In contrast, highest invasiveness was reached when *S.*Tm was grown in fully aerated cultures to late exponential phase (Ibarra *et al.*, 2010). Under oxygen limiting conditions (1 % oxygen) highest invasion was observed when bacteria reach the stationary phase but where still reduced in their invasive capacity compared to fully aerated cultures (Ibarra *et al.*, 2010). Furthermore, Gunn and Poutry showed that *S.* Tm is reduced in its invasiveness in the presence of bile salts which could give an insight for the regulation *in vivo* (Prouty *et al.*, 2004; Prouty & Gunn, 2000). Another family of metabolites shown to regulate SPI1-T3SS expression are SCFAs. Acetate induces SPI1-T3SS expression whereas butyrate and propionate show an inhibitory effect (Durant *et al.*, 2000; Lawhon *et al.*, 2002).

The SPI1-T3SS is expressed in a bistable manner. In the gut, two subpopulations are found, a slow growing SPI1-T3SS$^+$ population, important for induction of inflammation, and a fast growing SPI1-T3SS$^-$ population which can colonize effectively the intestine (Diard *et al.*, 2013). The exact mechanism of SPI1-T3SS regulation and the influence of the microbiota and the host remains still elusive and needs further consideration.

1.3.4 The gut is an oxygen limited environment

1.3.4.1 Sensing of environmental oxygen by *S.*Tm

As *S.* Tm is a facultative anaerobic bacterium it can cope with changes of the available oxygen in the environment. When oxygen is present, *S.* Tm uses preferentially O_2 as terminal electron acceptor as it is the most potent to drive efficient ATP production and rapid growth (Barrow *et al.*, 2015; Unden & Dunnwald, 2008). In the gastrointestinal tract *S.* Tm faces an oxygen limited environment (Albenberg *et al.*, 2014) and has to switch to an anaerobic lifestyle, which is mainly regulated by the aerobic respiratory control two-component system (ArcBA) and the global fumarate nitrate reduction regulator (FNR) (Evans *et al.*, 2011; Fink *et al.*, 2007; Wallace *et al.*, 2016). When oxygen concentrations are low ArcA acts as a repressor of aerobic metabolism, energy generation, amino acid and fatty acid transport (Evans *et al.*, 2011). On the other hand, it is an activator of flagella biosynthesis, motility, chemotaxis and anaerobic metabolism (ethanolamine and propanediol utilization, nitrite reductase) (Evans *et al.*, 2011). FNR is a transcription factor which is inactive under aerobiosis due to its oxidized iron-sulfur cluster. Anaerobic conditions result in formation of FNR dimers and DNA binding (Lazazzera *et al.*, 1996) which leads to upregulation of genes which are essential for anaerobic respiration (DMSO reductase, ethanolamine utilization), flagella biosynthesis and the SPI1-T3SS (Fink *et al.*, 2007). It also acts as a repressor of aerobic metabolism (cytochrome c-oxidase, NADH-dehydrogenase, cytochrome cd-complex) (Fink *et al.*, 2007). Using these sensors, *S.* Tm can efficiently adapt its metabolism to changing oxygen environments.

1.3.4.2 Utilization of alternative electron acceptors during inflammation: advantage of *S.* Tm over the commensal microbiota

Under anaerobic conditions *S.* Tm can undergo fermentative metabolism of complex carbohydrates and produce energy by substrate-level phosphorylation. This is not energetically favorable for *S.* Tm as it only yields two ATP per mol glucose (Gunsalus & Park, 1994). *S.* Tm adopts several different pathways to utilize alternative electron acceptors (in order of preference: nitrate, nitrite, DMSO, TMAO, tetrathionate and fumarate) in an anaerobic environment which increases energy yield (Unden & Dunnwald, 2008). *S.* Tm possesses three nitrate reductases, the constitutively produced NarZYV, the high affinity periplasmic NapABCGH and the low affinity cytosolic NarGHI, which reduce nitrate to nitrite. Nitrite is then further reduced to ammonia by the nitrite reductase NrfABCD (Unden &

Dunnwald, 2008). For DMSO, TMAO, fumarate and tetrathionate, *S.* Tm encodes the respective reductases in the *dmsABC*, *torCAD*, *frdABCD* and *ttrBCA* operons (Unden & Dunnwald, 2008). All these reductases contain a molybdopterin co-factor which is essential for their function (Hille, 1996). Therefore by deletion of *moaA*, an essential gene for molybdopterin synthesis, anaerobic respiration is prevented (Mehta *et al.*, 2014). Winter and colleagues showed that a *moaA E. coli* mutant exhibits a growth disadvantage with nitrate, TMAO and DMSO in an anaerobic co-culture assay (Rivera-Chavez *et al.*, 2013).

As mentioned above, most obligate anaerobic bacteria ferment complex carbohydrates to meet their energy demands. Instead, *M. schaedleri* is able to use nitrate as alternative electron acceptor for anaerobic respiration (Loy *et al.*, 2017) (Fig. 2B). Further, a putative TMAO reductase, tetrathionate reductase and DMSO reductase were found by genome analysis (Loy *et al.*, 2017). As those are all metabolites which are more abundant in the inflamed gut (Winter, Lopez*, et al.*, 2013; Winter, Winter*, et al.*, 2013), it is not astonishing that *M. schaedleri* is found in increased abundance in mouse models associated with acute colitis (cf. 1.2), but also in a dementia mouse model which is associated with inflammation in the brain cortex (Gao *et al.*, 2018).

1.3.4.3 *S.* Tm creates a favorable environment by induction of an inflammatory response

When *S.* Tm enters the gut it has to compete with the commensal microbiota and reach a critical density to induce inflammation and allow further transmission via the fecal-oral route (Lawley *et al.*, 2008). Compared to the resident microbiota, *S.* Tm has a growth advantage in the presence of anaerobic electron acceptors (nitrate, nitrite, DMSO, TMAO, tetrathionate and fumarate) (1.3.4.2). Those metabolites are increased in the inflamed gut, due to the host's immune response (Winter, Lopez*, et al.*, 2013). After *S.* Tm is ingested, it can attach to the epithelial cells via adhesins and the SPI1-T3SS which facilitates invasion into the host cells (Gerlach *et al.*, 2007; Hapfelmeier *et al.*, 2005). *S.*Tm triggers the intracellular NAIP/NLRC4 inflammasome which elicits IL18, a proinflammatory cytokine (Muller *et al.*, 2016; Sellin *et al.*, 2014). This leads to epithelial damage, submucosal edema and attraction of cells of the innate immune system like macrophages and neutrophils (Barthel *et al.*, 2003). Those cells release harmful reactive oxygen species (ROS) (Winterbourn *et al.*, 2016). Further the inducible nitric oxide synthase (iNOS) of intestinal epithelial cells and macrophages produce nitric oxide (NO) which reacts with ROS to form reactive nitrogen

species (RNS) which creates an antibacterial environment (Aviello & Knaus, 2017). Reactive oxygen / nitrogen species lead to DNA damage, lipid peroxidation and protein modification which are mechanisms of the innate immune system to prevent spread of pathogenic bacteria (Maier *et al.*, 2014; Tharmalingam *et al.*, 2017). In addition these ROS/RNS boost also the formation of alternative electron acceptors by oxidation. Microbial released hydrogen sulfide (H_2S), trimethylamine and NO react with the present ROS and form the alternative electron acceptors tetrathionate, TMAO, nitrate and nitrite respectively (Rivera-Chavez & Baumler, 2015). Recently, it was shown that during *S.* Tm infection, *Clostridia* spp. are depleted in a SPI1-T3SS dependent manner which leads to reduced butyrate concentration and subsequently to oxygenation of the intestinal epithelium. Therefore, oxygen becomes available, which can be readily consumed by *S.* Tm and reinforces its colonization (Rivera-Chávez *et al.*, 2016). Taken together *S.* Tm establishes a beneficial milieu for its growth by induction of gut inflammation which allows efficient replication in the gut.

1.4 Role of the intestinal mucus layer: protection and supply of nutrients

1.4.1 Architecture of the intestinal mucus layer

The epithelial border of the intestine is lined with a layer of mucus that protects from environmental challenges. This intestinal mucus layer consist mainly of the mucin MUC2, which is heavily O-glycosylated in the endoplasmatic reticulum of goblet cells and is secreted into the lumen (Arike & Hansson, 2016). In the large intestine, mucus consists of two distinct layers, the outer loosely attached and the inner firm layer strongly attached to the epithelium. The outer layer is permeable to bacteria whereas the inner layer is densely packed and devoid of bacteria (Johansson *et al.*, 2008).This mucus protects the epithelium from pathogens and bacterial derived products but also serves as a nutrient source (e.g. sialic acid, fucose, galactose, amino acids). Commensal bacteria such as *Bacteroides thetaiotaomicron* or *Akkermansia muciniphila*, harbor multiple glycoside hydrolases which they employ to forage the mucus layer (Derrien *et al.*, 2004; Sonnenburg *et al.*, 2005). The released nutrients can not only be used by themselves but also by other co-localized bacteria by cross-feeding (Backhed *et al.*, 2005; Belzer *et al.*, 2017; Derrien *et al.*, 2004; Sonnenburg *et al.*, 2005). Although *M.schaedleri* colonizes the outer mucus layer it does not possess any known genes for mucus degradation (Loy *et al.*, 2017). To summarize, the intestinal mucus layer is essential for human health and offers a complex niche for the microbiota.

1.4.2 *Agr2*$^{-/-}$ mice, lacking secreted MUC2, are protected against *S.* Tm induced colitis

Previous work in the group employed the *Agr2*$^{-/-}$ mouse model to study the role of the mucus layer in *S.* Tm infection (Brugiroux, 2016). *Agr2*$^{-/-}$ mice lack the protein disulfide isomerase anterior gradient homolog 2 (AGR2) which is important for correct folding and secretion of MUC2. Mice deficient in AGR2 (*Agr2*$^{-/-}$) lack MUC2 in the intestine but exhibit no adverse health effects during the early life stages (up to 4 months) (Bergström *et al.*, 2014; Park *et al.*, 2009). Histology and microarray data showed that the intestine of *Agr2*$^{-/-}$ mice harbors an increased amount of mast cells and proinflammatory cytokines (Park *et al.*, 2009). Still, mice do not develop spontaneous colitis but are more susceptible to chemically induced DSS colitis (Park *et al.*, 2009).

Agr2$^{-/-}$ mice, pretreated with the antibiotic streptomycin, showed reduced inflammation after one day of infection with *S.* Tm, compared to *Agr2*$^{+/-}$ mice (Brugiroux, 2016). On the contrary, when mice are pretreated with ampicillin instead of streptomycin, *S.* Tm colitis was induced in *Agr2*$^{-/-}$ as well as *Agr2*$^{+/-}$ mice (Brugiroux, 2016) (Fig. 4A). Microbiota analysis revealed, that *M. schaedleri* is enriched in the protected *Agr2*$^{-/-}$ streptomycin treated mice compared to the three unprotected groups (Brugiroux, 2016) (Fig. 4B). Thus it was hypothesized that *M. schaedleri* is protective against *S.*Tm induced colitis. The aim of my PhD thesis was to further investigate the protective effect of *M. schaedleri* in *S.* Tm colitis.

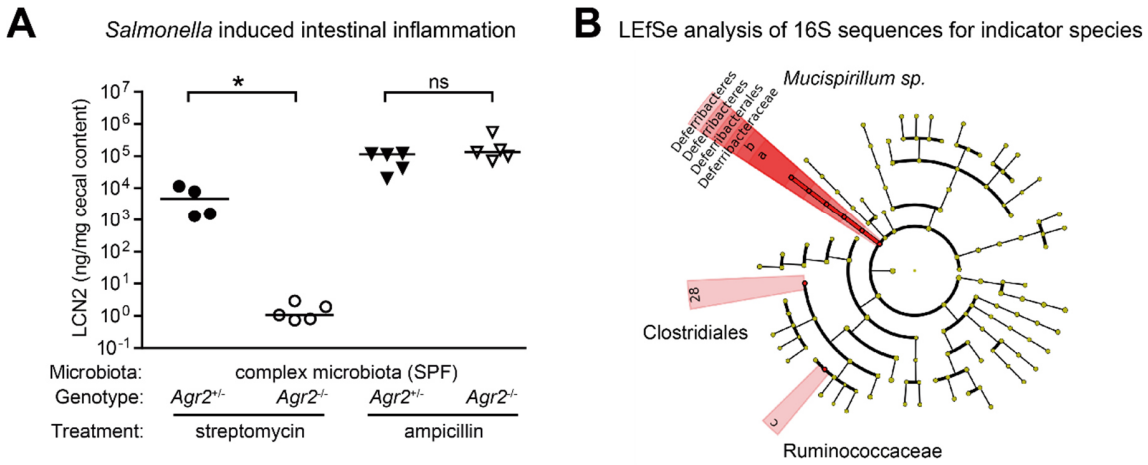

Fig. 4. Streptomycin treated *Agr2*$^{-/-}$ mice are protected from *S.*Tm induced colitis (Brugiroux, 2016). *Agr2*$^{-/-}$ and *Agr2*$^{+/-}$ mice were treated with streptomycin or ampicillin one day before infection with *S.*Tm and LCN2 levels at day 1 post infection is shown as a measure of intestinal inflammation. Mann–Whitney U test; ns, no significant difference $p \geq 0.05$, *$p < 0.05$, **$p < 0.01$, ***$p < 0.001$. **B)** DNA from cecal samples was extracted, sequenced and bioinformatic analysis on the 16S rRNA genes was performed. The cladogram shows indicator species, which are enriched in the protected mice compared to all other three unprotected groups using LEfSe algorithm (Segata *et al.*, 2011). Adapted from (Brugiroux, 2016).

2 Aims of this PhD thesis

To identify the causal role of one bacterial species and its contribution to or protection from disease is still a challenging task. In a previous study *Mucispirillum schaedleri,* a member of the Deferribacteres, was identified by comparative microbiome analysis as a candidate bacterium for protection from *S*. Tm colitis (Brugiroux, 2016).

In order to investigate, if *M. schaedleri* plays a protective role in *S*. Tm infection, I plan to employ gnotobiotic mouse models colonized with different microbial consortia, associated in addition with *M. schaedleri* or control, where the impact of *M. schaedleri* on the microbiome, the host and *S*. Tm infection can be causally addressed.

Streptomycin treated mucus-deficient *Agr2*$^{-/-}$ mice exhibit increased levels of *M. schaedleri* and are protected from *S*. Tm colitis (Brugiroux, 2016). So far the role of mucus-deficiency on *M. schaedleri* colonization and function is unclear. By generating gnotobiotic *Agr2*$^{-/-}$ mice I want to analyze if protection of conventional streptomycin treated *Agr2*$^{-/-}$ mice is mediated by the microbiota or the host's genotype.

Last, I want to elucidate the protective mechanism of *M. schaedleri* in *S*.Tm colitis by using metabolite analysis and infection studies with *S*.Tm mutants defective in different pathways which may be involved in competition with *M. schaedleri*.

3 Materials and Methods

3.1 Materials

3.1.1 Media and buffer

Table 1. Luria-Bertani (LB) medium

Components	Per liter
NaCl	5 g
Yeast extract	5 g
Tryptone	10 g

All components were dissolved in dH_2O.

Table 2. LB agar

Components	Per liter
NaCl	5 g
Yeast extract	5 g
Tryptone	10 g
Agar	15 g

All components were dissolved in dH_2O.

Table 3. LB 0.3 M NaCl

Components	Per liter
NaCl	17.53 g
Yeast extract	5 g
Tryptone	10 g

All components were dissolved in dH_2O.

Table 4. Peptone-glycerol broth (P/G)

Components	Per liter
Peptone	20 g
Glycerol	50 ml

All components were dissolved in dH_2O.

Table 5. 10 x Phosphate Buffered Saline (PBS)

Components	Per liter
NaCl	80 g
KCl	2 g
Na_2HPO_4	6.1 g
KH_2PO_4	2.4 g

All components were dissolved in dH_2O.

Table 6. *Akkermansia* medium (AAM) without mucin, supplemented with $NaNO_3$

Components	Per liter medium
Brain Heart Infusion	18.5 g
Trypticase soy broth	15 g
Yeast extract	5 g
K_2HPO_4	2.5 g
Hemin	1 mg
Glucose	0.5 g
$NaNO_3$	0.85 g
Autoclave and add the following components under sterile conditions:	
Na_2CO_3¤	0.4 g
Cysteine hydrochloride#	0.5 g
Menadione#	0.5 g
Complement inactivated FCS#	3 %

Hemin, resuspended in ethanol p.a. and supplemented with NaOH until dissolved; menadione, was resuspended in ethanol p.a.; Cysteine hydrochloride and Na_2CO_3 were dissolved in dH_2O. After addition of supplements, the still warm media was imported under the anaerobic tent. ¤ Autoclaved. # Sterile filtered.

Table 7. 4 % Paraformaldehyde (PFA)

Components	Per liter
ddH_2O	300 ml
PFA	40 g
1 M NaOH	100 µl
10 x PBS in ddH_2O, pH 7.4	100 ml

Components were heated up to 60 °C and stirred vigorously until PFA is dissolved. ddH_2O (Ampuwa) was filled up to 1 l, pH was adjusted, afterwards sterile filtered and stored at -20 °C.

Table 8. 50 x TAE buffer

Components	Per 5 l
Tris	1,210 g
Glacial acetic acid	285.5 ml
0.5 M EDTA pH 8.0	500 ml
dH_2O	ad 5 l

Table 9. 10 x loading dye

Components	Final concentration
Sucrose	40 %
Bromphenol blue	0.25 %
Xylene Cyanol	0.25 %

Table 10. SOC medium

Components	Per 250 ml
Tryptone	5 g
Yeast extract	1.25 g
NaCl	0.125 g
250 mM KCl	2.5 ml
Ad 250 ml with ddH_2O (Ampuwa), adjust pH to 7.0 with 5 M NaOH and autoclave.	
1 M glucose (sterile filtered)	5 ml

Table 11. 20 % glycerol-palladium solution

Components	Per 50 ml
100 % glycerol	10 ml
Palladium crystals	Tip of spatula
ddH_20	40 ml

After autoclaving, the warm solution (60 °C) was imported in the anaerobic tent.

Table 12. PBT

Components	Per 200 ml
BSA fraction V	200 mg
TM 10 tergitol	200 µl
1 x PBS	ad 200 ml

Solution was sterile filtered and stored at -20°C.

Table 13. Lysis buffer for DNA extraction (Stool kit, Qiagen)

Components	Final concentration
Tris	20 mM
EDTA	2 mM
Triton X 100	1 %
Adjust pH to 8.0 with HCl, autoclave and add:	
Lysozyme	20 mg/ml

Components were dissolved in ddH_2O (Ampuwa).

Table 14. CTAB/NaCl

Components	Final concentration
CTAB	10 %
NaCl	0.7 M

All components were dissolved in Ampuwa water.

Table 15. TE buffer

Components	Final concentration
Tris-Cl	10 mM
EDTA	1 mM

All components were dissolved in ddH_2O (Ampuwa) and pH was adjusted to pH 8.0 with HCl

Table 16. Extraction buffer for DNA extraction (Turnbaugh/Ubeda)

Components	Final concentration
Tris	200 mM
NaCl	200 mM
EDTA	20 mM

Components were dissolved in ddH_20 (Ampuwa). pH was adjusted to 8.0 using HCl and the solution was finally autoclaved.

Table 17. Hybridization buffers (HB) for FISH

Component	Volume
5 M NaCl	180 µl
1 M Tris / HCl	20 µl
ddH_2O	449 µl
Formamide	350 µl
10 % SDS	1 µl

Table 18. Washing buffer (WB) for FISH

Component	Volume
5 M NaCl	0.7 ml
1 M Tris / HCl	1 ml
0.5 M EDTA	0.5 ml
ddH_2O	To 50 ml

Table 19. Lysis buffer (Luciferase assay)

Component	Final concentration
K_2HPO_4	100 mM
KH_2PO_4	100 mM
EDTA	2 mM
Triton X-100	1 %
BSA (PAA)	5 mg/ml
Solution was sterile filtered (0.22µm) and stored at -20 °C. Following ingredients were added freshly per 10 ml:	
PIC	100µl of 5x Protease inhibitor cocktail
DTT	1 mM
Lysozyme	5 mg/ml

All components were dissolved in ddH_2O (Ampuwa).

Table 20. Luciferase reagent

Component	Final concentration
Tricine	20 mM
$(MgCO_3)_4Mg(OH)_25H_2O$	1 mM
EDTA	0.1 M
D(-) Luciferin	470 µM
DTT	33 mM
Li_3-Coenzym A	270 µM
Mg-ATP	530 µM
Glycylglycin	125 µM
Tricine	5 mg/ml

All components were dissolved in ddH_2O (Ampuwa) and stored at -20 °C.

3.1.2 Strains and plasmids

3.1.2.1 Strains

Table 21. *S.* Tm and *C. rodentium* strains

Strain	Lab-internal strain designation	Genotype	Resistances	Reference
S. Tm^{wt}	SB300	*S.* Tm strain SL1344	Strep	(Hoiseth & Stocker, 1981)
S. Tm^{avir}	M2702	SL1344 Δ*invG*; Δ*ssaV*	Strep	(Maier *et al.*, 2013)
S. Tm^{SPI1}	SB161	SL1344 Δ*invG*	Strep	(Kaniga *et al.*, 1994)
S. Tm^{avir}p*sicAgfp*	M2702_pM974	*S.* Tm^{avir} with plasmid pM974	Strep; Amp	(Brugiroux, 2016)
S. Tm^{avir}pM1419	M2702_pM1419	*S.* Tm^{avir} with plasmid pM1419	Strep; Amp	This study
S. Tm$^{avir\ hyd3}$	M3087	ΔSL1467-SL1468, SL1714-SL1715::aphT, SL3121-SL3124::cat Δ*invG*; Δ*ssaV*	Strep; Cm; Kan	(Maier *et al.*, 2013)
S. Tm$^{\Delta narZ}$	MBE1	SL1344 *narZ::cat*	Strep; Cm	(Beutler, 2016)
S. Tm$^{\Delta narG}$	MBE2	SL1344 *narG::cat*	Strep; Cm	(Beutler, 2016)
S. Tm$^{\Delta napA}$	MBE3	SL1344 *napA::aphT*	Strep; Kan	(Beutler, 2016)
S. Tm$^{\Delta nr3}$	MBE7	Δ*narZ*; *narG::cat; napA::aphT*	Strep; Cm; Kan	(Beutler, 2016)
SHE1	SHE1	Δ*invG*; Δ*ssaV* *narZ::cat* (P22-phage lysate of MBE1 on M2702)	Strep; Cm	This study
SHE2	SHE2	Δ*narZ* (pCP20 in SHE1)	Strep	This study
SHE3	SHE3	Δ*narZ*; *narG::cat* (P22-phage lysate of MBE2 on SHE2)	Strep; Cm	This study
S. Tm$^{avir\ \Delta nr3}$	SHE4	Δ*narZ*; *narG::cat; napA::aphT* (P22-phage lysate of MBE3 on SHE3)	Strep; Cm; Kan	This study
S. Tm $^{avir\ \Delta nr3\ sicA-luc}$	SHE5	Δ*narZ*; *narG::cat; napA::aphT* pagC::pM1471 (PsicA-luc) (P22-phage lysate of M971 on SHE4)	Strep; Cm; Kan; Amp	This study
S. Tm$^{sicA-luc}$	M971	pagC::pM1471 (PsicA-luc)	Strep; Amp	(Häberli, 2005)
S. Tm$^{avir\ sicA-luc}$	SHE11	pagC::pM1471 (PsicA-luc) (P22-phage lysate of M971 on M2702)	Strep; Amp	This study
SHE13	SHE13	*moaA::aphT*	Strep; Kan	This study
S. Tm$^{\Delta moaA}$	SHE14	*moaA::aphT* (P22-phage lysate of SHE13 on SB300)	Strep; Kan	This study
C. rodentium	DBS100			(Schauer & Falkow, 1993)

Table 22. Mouse derived bacterial strains

Strain	Taxonomy (species level)	DSM No.	Reference
	OligoMM[12]		
YL2	*Bifidobacterium longum* subsp. *animalis*	26074	(Brugiroux *et al.*, 2016)
YL27	*Muribaculum intestinale*	28989	(Brugiroux *et al.*, 2016)
YL31	*Flavonifractor plautii*	26117	(Brugiroux *et al.*, 2016)
YL32	*Clostridium clostridioforme*	26114	(Brugiroux *et al.*, 2016)
YL44	*Akkermansia muciniphila*	26127	(Brugiroux *et al.*, 2016)
YL45	*Turicimonas caecimuris*	26109	(Brugiroux *et al.*, 2016)
YL58	*Blautia coccoides*	26115	(Brugiroux *et al.*, 2016)
I46	*Clostridium innocuum*	26113	(Brugiroux *et al.*, 2016)
I48	*Bacteroides caecimuris*	26085	(Brugiroux *et al.*, 2016)
I49	*Lactobacillus reuteri*	32035	(Brugiroux *et al.*, 2016)
KB1	*Enterococcus faecalis*	32036	(Brugiroux *et al.*, 2016)
KB18	*Acutalibacter muris*	26090	(Brugiroux *et al.*, 2016)
	ASF[3]		
ASF356	*Clostridium* sp.		Charles River Laboratories
ASF519	*Parabacteroides. goldsteinii*		Charles River Laboratories
ASF361	*Lactobacillus murinus*		Charles River Laboratories
ASF457	*Mucispirillum schaedleri*		Charles River Laboratories

3.1.2.2 Plasmids

Table 23. Plasmids in *S.* Tm

Plasmid	Genotype	Reference
pM974	T3SS-1 (SPI-1) promotor of the *sicAsipBCDA* operon coupled with GFP*mut2* coding sequence Amp^R	(Ackermann *et al.*, 2008)
pM1419	Temperature sensitive plasmid, variant of pHSG422 lacking Km^R Cm^R resistances; Amp^R	(Stecher *et al.*, 2008)

Table 24. Plasmids for lambda Red recombination in *S.* Tm

Plasmid	Function	Genotype	Reference
pKD3	Harbors a chloramphenicol resistance gene (*cat*)	*cat* with FRT sites, Amp^R	(Datsenko & Wanner, 2000)
pKD4	Harbors a kanamycin resistance gene (*aphT*)	*aphT* with FRT sites, Amp^R	(Datsenko & Wanner, 2000)
pKD46	Harbors 2,154 nt (31088–33241) of phage λ, enzymes for recombination	*araC*, ParaB γ, β and exo, $repA101^{ts,}$ Amp^R	(Datsenko & Wanner, 2000)
pCP20	Harbors FLP-recombinase	FLP^+, λ $cI857^+$, λ p_R Rep^{ts}, Amp^R, Cm^R	(Cherepanov & Wackernagel, 1995)

3.1.3 Oligonucleotides

Table 25. Oligonucleotides and hydrolysis probes for qPCR

Primers and corresponding probe (targeted strain)	Sequence 5' - 3'	Reference
Isol46_Exonucl.2_fwd	CGGATCGTAAAGCTCTGTTGTAAG	(Brugiroux *et al.*, 2016)
Isol46_Exonucl.3_rev	GCTACCGTCACTCCCATAGCA	
Probe3_Isol46	FAM-AAGAACGGCTCATAGAGG-BHQ1	
(*Clostridium innocuum* I46)		
Isol49_Exonucl._fwd	GCACTGGCTCAACTGATTGATG	(Brugiroux *et al.*, 2016)
Isol49_Exonucl._rev	CCGCCACTCACTGGTGATC	
Probe_Isol49	HEX-CTTGCACCTGATTGACGA-BHQ1	
(*Lactobacillus reuteri* I49)		
YL58_Exonucl._fwd	GAAGAGCAAGTCTGATGTGAAAGG	(Brugiroux *et al.*, 2016)
YL58_Exonucl._rev	CGGCACTCTAGAAAAACAGTTTCC	
Probe_YL58	FAM-TAACCCCAGGACTGCAT-BHQ1	
(*Blautia coccoides* YL58)		
YL27_Exonucl.2_fwd	TCAAGTCAGCGGTAAAAATTCG	(Brugiroux *et al.*, 2016)
YL27_Exonucl.2_rev	CCCACTCAAGAACATCAGTTTCAA	
Probe2_YL27	HEX-CAACCCCGTCGTGCC-BHQ1	
(*Muribaculum intestinale* YL27)		
YL31_Exonucl.2_fwd	AGGCGGGATTGCAAGTCA	(Brugiroux *et al.*, 2016)
YL31_Exonucl.3_rev	CCAGCACTCAAGAACTACAGTTTCA	
Probe2_YL31	FAM-CAACCTCCAGCCTGC-BHQ1	
(*Flavonifractor plautii* YL31)		
YL32_Exonucl.2_fwd	AATACCGCATAAGCGCACAGT	(Brugiroux *et al.*, 2016)
YL32_Exonucl.2_rev	CCATCTCACACCACCAAAGTTTT	
Probe2_YL32	HEX-CGCATGGCAGTGTGT-BHQ1	
(*Clostridium clostridioforme* YL32)		
KB1_Exonucl._fwd	CTTCTTTCCTCCCGAGTGCTT	(Brugiroux *et al.*, 2016)
KB1_Exonucl._rev	CCCCTCTGATGGGTAGGTTACC	
Probe_KB1	FAM-CACTCAATTGGAAAGAGGAG-BHQ1	
(*Enterococcus faecalis* KB1)		
YL2_Exonucl._fwd	GGGTGAGTAATGCGTGACCAA	(Brugiroux *et al.*, 2016)
YL2_Exonucl._rev	CGGAGCATCCGGTATTACCA	
Probe_YL2	HEX-CGGAATAGCTCCTGGAAA-BHQ1	
(*Bifidobacterium longum* subsp. *animalis* YL2)		

Primers and corresponding probe (targeted strain)	**Sequence 5' - 3'**	**Reference**
KB18_Exonucl.2_fwd KB18_Exonucl.2_rev Probe2_KB18 (*Acutalibacter muris* KB18)	TGGCAAGTCAGTAGTGAAATCCA TCACTCAAGCTCGACAGTTTCAA FAM-CTTAACCCATGAACTGC-BHQ1	(Brugiroux *et al.*, 2016)
YL44_Exonucl._fwd YL44_Exonucl._rev Probe_YL44 (*Akkermansia muciniphila* YL44)	CGGGATAGCCCTGGGAAA GCGCATTGCTGCTTTAATCTTT HEX-TGGGATTAATACCGCATAGTA-BHQ1	(Brugiroux *et al.*, 2016)
YL45_Exonucl._fwd YL45_Exonucl._rev Probe_YL45 (*Turicimonas caecimuris* YL45)	AGACGGCCTTCGGGTTGTA CGTCATCGTCTATCGGTATTATCAA FAM-ACCACTTTTGTAGAGAACGA-BHQ1	(Brugiroux *et al.*, 2016)
Isol48_Exonucl._fwd Isol48_Exonucl._rev Probe_Isol48 (*Bacteroides caecimuris* I48)	GGCAGCATGGGAGTTTGCT TTATCGGCAGGTTGGATACGT HEX-CAAACTTCCGATGGCGAC-BHQ1	(Brugiroux *et al.*, 2016)
ASF356_Exonucl.2_fwd ASF356_Exonucl.2_rev Probe2_ASF356 (*Clostridium* sp. ASF356)	CGGCAAGGTAAGCGATATGTG CGCTTTCCTCTCCTGTACTCTAGCT FAM-TAACTTAAGGATAGCATAACGAAC T-BHQ1	(Brugiroux *et al.*, 2016)
ASF361_Exonucl._fwd ASF361_Exonucl._rev Probe_ASF361 (*Lactobacillus murinus* ASF361)	TCGGATCGTAAAACCCTGTTG ACCGTCGAAACGTGAACAGTT HEX-TAGAGAAGAAAGTGCGTGAGAG-BHQ1	(Brugiroux *et al.*, 2016)
ASF457_Exonucl._fwd ASF457_Exonucl._rev Probe_ASF457 (*Mucispirillum schaedleri* ASF457)	GACTGGAACAACTTACCGAAAGGT CAGGTCTCCCCAACTTTTCCT FAM-TAATGCCGGATGAGTTATA-BHQ1	(Brugiroux *et al.*, 2016)
ASF519_Exonucl._fwd ASF519_Exonucl._rev Probe_ASF519 (*Parabacteroides goldsteinii* ASF519)	TGTGGCTCAACCATAAAATTGC GCATTCCGCCTACCTCAAATAT HEX-TTGAAACTGGTTGACTTGAG-BHQ1	(Brugiroux *et al.*, 2016)
Salmo_Exonucl._fwd Salmo_Exonucl._rev Probe_Salmo (*Salmonella* SL1344)	TGGGAAACTGCCTGATGGA CTTGCGACGTTATGCGGTATT FAM-ATAACTACTGGAAACGGTGGC-BHQ1	(Brugiroux *et al.*, 2016)

Primers and corresponding probe (targeted strain)	Sequence 5' - 3'	Reference
Univ_Exonucl.3_fwd	TGCAYGGYYGTCGTCAGC	(Brugiroux *et al.*, 2016)
Univ_Exonucl.3_rev	CRTCRTCCYCRCCTTCCTC	
Probe2_Univ	HEX-AACGAGCGCAACCC-BHQ1	

* FAM (6-carboxyfluoresceine); HEX (6-carboxyhexafluoresceine); BHQ1 (black hole quencher 1).

Table 26. Primers used for construction of *S.* Tm mutants

Designation	Sequence 5' - 3'	Construction of strain	Amplicon size (bp)
narZ-fwd-ko	AATGGTTTAACGCCAAATCGACAGGATGGCGGA AAATTTATCGAAGCAGGAGAAATGTCatatgaatatc ctccttagtt		
narZ-rev-ko	GGTGTGACAGCCAATACATTTATCGAGATTCAG TACCATCCCAACCTGTGAGCGTATTTtgtgtaggctg gagctgcttc	MBE1 (*narZ::cat*)	
narZ fwd-check up	GCGTCGTAAGCCTAAACA		
narZ rev-check up	CCGGTCCAGACGTTTTTA		3948
narG-fwd-ko	CTTAGTTAAGCAATGTCGATTTATCAGAGAGCC GTAAGGTTCCACACAGGAGAAACCCGatatgaatat cctccttagtt		
narG-rev-ko	GGTATGACAGCCGATGCACTTATCGAGATTCAG CACCATGCCGACTTGTGAACGAATTTtgtgtaggctg gagctgcttc	MBE2 (*narG::cat*)	
narG fwd-check up	TTCTCACGCCCATTCAGC		
narG rev-check up	CCAGACGTTTTTACAGGT		3921
napA-fwd-ko	GGCGTACTGGCGGTGTCGCTGGTTTATCACCA GCAGGATGAGCAAGGTGAGGAAACACCatatgaat atcctccttagtt		
napA-rev-ko	ACATCACGCAGGAAGCGGCGGCGGCCATTTTG GGGTTTCGCTGTACGGGACATAACGCGtgtgtagg ctggagctgcttc	MBE3 (*napA::aphT*)	
napA fwd-check up	ACAATTGAGTCAGTACGC		
napA rev-check up	GCTGGCGAAGACATTTTC		2756
moaA-fwd-ko	CGTTTGCCACCAGGGCGCAGGAAGAAATGACT CCGCCTCCCGTATTTGGAAAGGTGTACatatgaata tcctccttagtt		
moaA-rev-ko	ATGCGGGTCGGGATAAATTCAGCGCTGACCTG ACTCATCTGAAATCTCCTTATTAAGGAtgtgtaggctg gagctgcttc	SHE13 *(moaA::aphT)*	
moaA fwd-check up	CACGTATTCTGTCGCTAAA		
moaA rev-check up	CGGTTCTCTTTAACGATGG		1405

Genes of interest were replaced by either chloramphenicol (*cat*) or kanamycin (*aphT*) resistance genes using the λ Red recombination system (Datsenko & Wanner, 2000). PCR products were generated with primers harboring a homology region adjacent to the gene of interest (capital letters) and a sequence targeting the plasmids pKD3 (*cat*) and pKD4 (*aphT*, small letters) (Table 24). Check-up primers were used to verify correct insertion of the antibiotic cassette.

Table 27. Further oligonucleotides used in this study

Designation	Sequence 5' - 3'	Purpose	Reference
fD1	CGATATCTCTAGAAGAGTTTGATCCTGG CTCAG	Amplification of bacterial 16S rRNA genes	(Weisburg *et al.*, 1991)
fD2	CGATATCTCTAGAAGAGTTTGATCATGG CTCAG	Amplification of bacterial 16S rRNA genes	(Weisburg *et al.*, 1991)
rP1	GATATCGGATCCACGGTTACCTTGTTAC GACTT	Amplification of bacterial 16S rRNA genes	(Weisburg *et al.*, 1991)
ssaV_check_fwd	GGA GCT CTG GTT ACG ATT	confirm Δ*ssaV* genotype in M2702	(Nedialkova, 2014)
ssaV_check_rev	ATA TTT CAG CCT CAG ACG	confirm Δ*ssaV* genotype in M2702	(Nedialkova, 2014)
pagC_pLB02_for	GGTCCTGGGGGTCTAGAGAT	confirm integration of *pagC::pM1471*	(Häberli, 2005)
pagC_chrom_rev	AATTGTCGTTGTTGAGCGTTT	confirm integration of *pagC::pM1471*	(Häberli, 2005)

Table 28. Probes for FISH

Designation	Sequence 5' - 3'	Target	Reference
Msc487_correct (2xCy3)	CAG TCA CTC CGA ACA ACG CT	*M. schaedleri*	(Loy *et al.*, 2017)
Eub338 I (2xCy5)	GCT GCC TCC CGT AGG AGT	Most bacteria	(Amann *et al.*, 1990)
Eub338 III (2xCy5)	GCT GCC ACC CGT AGG TGT	Verrucomicrobiales	(Daims *et al.*, 1999)

3.1.4 Chemicals and antibiotics

Table 29. Chemicals used in this study

Compound	Supplier
ABTS substrate	Merck (Darmstadt)
Acetic acid	Roth (Karlsruhe)
Agar	BD (Heidelberg)
Agarose	Bio&Sell (Feucht)
L-(+)-arabinose	Sigma-Aldrich (Munich)
Brain Heart Infusion	Oxoid, Thermo Fisher Scientific biosciences (St. Leon-Rot)
Bromphenol blue	Sigma-Aldrich (Munich)
Bovine serum albumin (BSA)	PAA Laboratories GmbH (Austria)
BSA fraction V	Roth (Karlsruhe)
$CaCl_2$	Roth (Karlsruhe)
$CaCl_2 \cdot 2H_2O$	Merck (Darmstadt)
Chloroform	Roth (Karlsruhe)
CloneJET™ PCR Cloning kit	Fermentas, Thermo Scientific (USA)
$CoCl_2 \cdot 6H_2O$	Merck (Darmstadt)
$CuSO_4 \cdot 5H_2O$	Merck (Darmstadt)
Cysteine (-L) Hydrochloride Monohydrate	Sigma-Aldrich (Munich)
ddH_2O (Ampuwa)	Fresenius Kabi (Bad Homburg)
ddH_2O used for qPCR reactions	Gibco, Life Technologies (UK)
dNTPs	Fermentas, Thermo Scientific (USA)
DAPI	Roth (Karlsruhe)
DreamTaq PCR Master Mix (2x)	Fermentas, Thermo Scientific (USA)
DTPA	Sigma-Aldrich (Munich)
EDTA	Biomol (Hamburg)
EGTA	Sigma-Aldrich (Munich)
Eosin Y solution	Sigma-Aldrich (Munich)
Ethanol p.a.	Roth (Karlsruhe)
Ethidium bromide	Sigma-Aldrich (Munich)
FastStart Essential DNA Probes Master	Roche (Mannheim)
FastStart Taq polymerase	Roche (Mannheim)
FCS	Biochrom AG (Berlin)
$FeCl_3 \cdot 6H_2O$	Merck (Darmstadt)
$FeSO_4 \cdot 7H_2O$	Roth (Karlsruhe)
Formamide	Sigma-Aldrich (Munich)

Compound	Supplier
GeneRuler 1kb DNA Ladder	Thermo Fisher Scientific biosciences (St. Leon-Rot)
GeneRuler DNA ladder mix (100bp)	Thermo Fisher Scientific biosciences (St. Leon-Rot)
D-glucose	Roth (Karlsruhe)
Glycerol	Roth (Karlsruhe)
HCl	Roth (Karlsruhe)
Hemin	Sigma-Aldrich (Munich)
Histidine	Sigma-Aldrich (Munich)
H_2O_2	Merck (Darmstadt)
HRP-streptavidin	IBA (Göttingen)
K_2HPO_4	Roth (Karlsruhe)
KCl	Fluka, Sigma-Aldrich (Munich)
KH_2PO_4	Roth (Karlsruhe)
Lipocalin-2 standard	R&D Systems (Wiesbaden-Nordenstadt)
Lysozyme from hen egg	Sigma-Aldrich (Munich)
MacConkey agar	Oxoid, Thermo Fisher Scientific Biosciences (St. Leon-Rot)
Menadione	Sigma-Aldrich (Munich)
$MgSO_4$	Roth (Karlsruhe)
$MnSO_4 \cdot H_2O$	Roth (Karlsruhe)
$MnCl_2 \cdot 4H_2O$	Merck (Darmstadt)
NaCl	Roth (Karlsruhe)
Na_2CO_3	Merck (Darmstadt)
Na_2HPO_4 unhydrated	Roth (Karlsruhe)
$Na_2HPO_4 \cdot 2H_2O$	Roth (Karlsruhe)
$Na_2MoO_4 \cdot 2H_2O$	Merck (Darmstadt)
$NaNO_2$	Sigma-Aldrich (Munich)
$NaNO_3$	Roth (Karlsruhe)
NaOH	Roth (Karlsruhe)
NaOH pellets	Merck (Darmstadt)
$Na_2O_6S_4 \cdot 2H_2O$	Sigma-Aldrich (Munich)
Na_2SeO_3	Sigma-Aldrich (Munich)
Na_2SO_4	Merck (Darmstadt)
NH4Cl	Merck (Darmstadt)
N-naphthylethylenediamine dihydrochloride monomethanolate (NEDD)	Sigma-Aldrich (Munich)
Normal goat serum	Biozol (Eching)
O.C.T.	Sakura Finetek (Torrance)
Palladium chloride	Sigma-Aldrich (Munich)

Compound	Supplier
Paraformaldehyde (PFA)	Roth (Karlsruhe)
Phenol:chloroform:isoamylalcohol (25:24:1)	Roth (Karlsruhe)
Potassium acetate	Roth (Karlsruhe)
Protease inhibitor cocktail	Sigma-Aldrich (Munich)
Oligonucleotides	Metabion (Martinsried)
Peptone	Oxoid, Thermo Fisher Scientific Biosciences (St. Leon-Rot)
$Q5^{Tm}$ Hot Start High-Fidelity polymerase	New England BioLabs (Frankfurt am Main)
Rotimount	Roth (Karlsruhe)
Sabouraud dextrose agar	Oxoid, Thermo Fisher Scientific Biosciences (St. Leon-Rot)
Sodium acetate	Roth (Karlsruhe)
Sodium dodecyl sulfate (SDS)	Serva (Heidelberg)
Sucrose	Sigma-Aldrich (Munich)
Sulfanilamide	Merck (Darmstadt)
Thiamine hydrochloride	Roth (Karlsruhe)
TM 10 tergitol	Chemika (Australia)
Tricine	AppliChem (Darmstadt)
Tris	MP Biomedicals (Eschwege)
Triton	Roth (Karlsruhe)
Trypticase soy broth	Oxoid, Thermo Fisher Scientific biosciences (St. Leon-Rot)
Tryptone	Roth (Karlsruhe)
Tween	Sigma-Aldrich (Munich)
VCL_3	Sigma-Aldrich (Munich)
Vectashield	Enzo life science (UK)
Vector’s Hämalaun solution	Roth (Karlsruhe)
VirkonS	V.P. Produkte (Schlüchtern)
Xylene	Roth (Karlsruhe)
Xylene Cyanol	Sigma-Aldrich (Munich)
Yeast extract	MP Biomedicals (Eschwege)
Yeast t-RNA	Roche (Mannheim)
$ZnSO_4 \cdot 7H_2O$	Merck (Darmstadt)

Table 30. Antibiotics used in this study

Antibiotic	Supplier	Final concentration
Ampicillin	Roth (Karlsruhe)	100 µg/ml
Chloramphenicol	Roth (Karlsruhe)	30 µg/ml
Kanamycin sulfate	Roth (Karlsruhe)	15 or 30 µg/ml
Streptomycin sulfate	Roth (Karlsruhe)	50 or 100 µg/ml

3.1.5 Antibodies

Table 31. Antibodies used for lipocalin-2 ELISA (mouse lipocalin-2/NGAL detection kit (R&D, DY1857)

Antibody	Origin	Supplier	Dilution
Lipocalin-2 capture antibody	rat	R&D, Part 842440	1:200
Lipocalin-2 detection antibody (biotinylated)	rat	R&D, Part 842441	1:200

Table 32. Antibodies used for immunofluorescence staining

Antibody	Origin	Supplier	Dilution
α-*Salmonella* B test serum anti-O	rabbit	Becton Dickinson (New Jersey, US)	1:400
α-rabbit DyLight 649	goat	Jackson ImmunoResearch (Baltimore, US)	1:400

3.1.6 Devices and specific materials

Table 33. Devices and specific materials

Items	Supplier
Acid washed glass beads (<106 µm)	Sigma-Aldrich (Munich)
Aluminum crimp seals (diam. 11 mm)	Supelco (USA)
Aluminum crimp seals (diam. 20 mm)	Supelco (USA)
Amp for agarose gels (Power Pac)	Bio Rad (Munich)
BioPhotometer	Eppendorf (Wesseling-Berzdorf)
BreatheEasy membrane	Sigma-Aldrich (Munich)
Butyl-rubber stoppers (diam. 11 mm)	Supelco (USA)
Butyl-rubber stoppers (diam. 20 mm)	Geo-Mocrobial Technologies (USA)
Cannulas	B. Braun (Melsungen)
Cell strainer (40 µm pore size)	SPL Life Sciences (Korea)
Crimper (diam. 11 mm)	VWR (Darmstadt)
Crimper (diam. 20 mm)	VWR (Darmstadt)
Confocal microscope (TCS SP5)	Leica (Wetzlar)
Cryotome	Leica Biosystems (Wetzlar)
Cryo-tubes	Thermo Fisher Scientific biosciences (St. Leon-Rot)
Decrimper (diam. 20 mm)	VWR (Darmstadt)
Dialysis membrane (pore size: 0.025 µm)	Merck, Millipore (Darmstadt)
Diagnostic slides (10 wells, 76 x 25 x 1 mm)	Thermo Fisher Scientific biosciences (St. Leon-Rot)
1.5 ml DNA loBind tubes	Eppendorf (Wesseling-Berzdorf)
Electroporation cuvette (1mm)	Peqlab (Erlangen)
Electroporation device (MicroPulser)	Bio Rad (Munich)
Epi Centrifuge (5430 R)	Eppendorf (Wesseling-Berzdorf)
ezDNase	Thermo Fisher Scientific biosciences (St. Leon-Rot)
Filter Millex (0.22 µm; PES membrane)	Merck (Darmstadt)
Filter Millex (0.45 µm; PVDF membrane)	Merck (Darmstadt)
Gammex® Latex glove	Ansell (Brussels)
Gel documentation chamber	Bio Rad (Munich)
GeneJET RNA cleanup and Concentration Micro Kit	Thermo Fisher Scientific biosciences (St. Leon-Rot)
Glass slides (cover)	Marienfeld Laboratory Glassware (Lauda-Königshofen)
Gnoto cages	Han, Bioscape (Emmendingen)
Incubator (Heraeus oven)	Thermo Fisher Scientific biosciences (St. Leon-Rot)
Laminar flow (Safe 2020)	Thermo Fisher Scientific biosciences (St. Leon-Rot)
LightCycler96	Roche (Mannheim)
40 µm mesh (cell strainer)	BD Falcon™ (USA)

Items	Supplier
Microplate reader (CLARIOstar ®)	BMG LABTECH (Ortenberg)
NanoDrop	Thermo Fisher Scientific biosciences (St. Leon-Rot)
NEBNext Ultra RNA library prep for Illumina	New England Biolabs (Ipswich, MA)
NucleoSpin gDNA Clean-up kit	Macherey-Nagel (Düren)
NucleoSpin Gel and PCR Clean-up kit	Macherey-Nagel (Düren)
NucleoSpin Plasmid kit	Macherey-Nagel (Düren)
Parafilm	BEMIS (USA)
Peqstar 2x gradient cycler	Peqlab (Erlangen)
Plasmid Plus Midi Kit	Qiagen (Hilden)
Screw cap plastic tubes	A. Hartenstein (Würzburg)
1.5 ml plastic tubes (PCR grade)	Eppendorf (Wesseling-Berzdorf)
2 ml plastic tubes (PCR grade)	Eppendorf (Wesseling-Berzdorf)
15 ml plastic tubes	Greiner Bio-One (Frickenhausen)
50 ml plastic tubes	Greiner Bio-One (Frickenhausen)
Petri dishes	Greiner Bio-One (Frickenhausen)
Qiagen DNA (fast) stool kit	Qiagen (Hilden)
Quant-iT™ RiboGreen™ RNA Assay Kit	Thermo Fisher Scientific biosciences (St. Leon-Rot)
Ribo-Zero kit	Illumina (San Diego, CA)
Shaker (Certomat R)	B. Braun Biotech international (Melsungen)
Spectrophotometer (Sunrise)	Tecan (Crailsheim)
Stainless steel beads (5 mm)	Hübsch Industrietechnik (Blaibach)
Superfrost Plus slides (75 x 25 x 1 mm)	A.Hartenstein (Wuerzburg)
Syringes	B. Braun (Melsungen)
Tissue lyzer	Qiagen (Hilden)
Vortex	Scientific industries (USA)
96-well ELISA plates (Brandplates)	Brand (Wertheim)
96-well plate for standard assays	TPP (Trasadingen)
96-well plate black with white wells	Porvair Sciences Ltd (King's Lynn UK)
Wheaton glass serum bottles (1.5 ml)	Sigma-Aldrich (Munich)
Wheaton glass serum bottles (100 ml)	Sigma-Aldrich (Munich)
Zirconia/silica beads (0.1 mm)	Roth (Karlsruhe)
Zirconia-beads (0.7 mm)	Roth (Karlsruhe)

3.2 Methods

3.2.1 Anaerobic cultivation of *M. schaedleri* (ASF457)

All work was performed under anoxic conditions using an anaerobic chamber (3 % H_2, rest N_2) and all material was pre-reduced at least for two days in this environment. 10 ml of pre-reduced AAM media (supplemented with 10 mM $NaNO_3$) were distributed in 100 ml Wheaton serum bottles, inoculated with 1 ml of *M. schaedleri* (Table 22) cryostock (3.2.2) and sealed with butyl rubbers. The gas phase was exchanged by three times application of vacuum and gas atmosphere (7 % H_2, 10 % CO_2, rest N_2). Cultures were grown statically for 48 h to 72 h at 37 °C.

3.2.2 Preparation of cryostocks from anaerobic cultures

Cryostocks were prepared by mixing fresh cultures (3.2.1) at a 1:1 ratio with a pre-reduced 20 % glycerol solution containing palladium crystals (Table 11) directly in 1.5 ml glass vials and were frozen at -80 °C. Purity of cryostocks was checked by 16S rRNA gene sequencing of PCR fragments generated with primers fD1, fD2 and rP1 (Table 27). PCR fragments were purified (NucleoSpin Gel and PCR Cleanup kit, Macherey Nagel) and analyzed by Sanger sequencing (GATC Biotech, Konstanz). Sequences were compared to reference sequence of *M. schaedleri* (accession number: NR_042896) using CLC DNA Workbench 6.0.2.

3.2.3 Construction of *Salmonella enterica* serovar Typhimurium (*S.* Tm) mutants by λ Red recombination

3.2.3.1 PCR fragment

In frame deletions were performed by using the λ Red system (Datsenko & Wanner, 2000). PCR was performed in a Peqstar 2x gradient cycler using a FastStart Taq polymerase (Roche) with 10x $MgCl_2$ reaction buffer, dNTPs (200 µM of each nucleotide), 5 - 50 ng of template DNA (plasmid pKD3, chloramphenicol resistance [*cat*] or pKD4, kanamycin resistance [*aphT*] (Table 24)) and oligonucleotides (200 nM each) (Table 26) in a total volume of 200 µl. The following cycling conditions were used: one initial denaturation step at 95 °C for 6 min followed by: (i) 15 cycles with one cycle at 95 °C for 30 s, 55 °C for 30 s and 72 °C for 2 min, (ii) 35 cycles 95 °C for 30 s, 65 °C for 30 s and 72 °C for 2 min and (iii) a final elongation step at 72 °C for 10 min. Oligonucleotides were designed to amplify the

antibiotic resistance cassette and the FRT sites essential for later removal of the antibiotic cassette by FLP recombinase using plasmid pCP20 (Table 24). Furthermore, sequences of 59 bp homologous upstream to the adjacent start codon and downstream of the stop codon of the gene of interest, were attached to the oligonucleotides. PCR product was purified by ethanol precipitation. Therefore, 1/10 volume of 3 M NaAcetate and 2 volumes of ice cold 96 % p. a. EtOH were added, mixed and centrifuged (14,000 rpm, 15 min, 4 °C). The pellet was washed in 500 µl of ice-cold 70% EtOH, centrifuged (14,000 rpm, 15 min, 4 °C) and the supernatant was discarded. The pellet was dried at 37 °C and resuspended in 22 µl H_2O (Gibco). Dialysis against Ampuwa H_2O was performed for desalting. Therefore, PCR product was placed for 60 min on a dialysis membrane (pore size: 0.025 µm (Millipore)) in Ampuwa H_2O. The DNA was quantified by NanoDrop.

3.2.3.2 Electroporation of PCR product in *S.* Tm pKD46

A liquid culture of *S.* Tm containing the plasmid pKD46 (encoding the λ Red recombinase) (Datsenko & Wanner, 2000) was set up by inoculating one colony in 20 ml LB (ampicillin 100 µg/ml) and incubation for 12 h at 30 °C at 180 rpm. Overnight culture was diluted 1:200 in 100 ml fresh LB (ampicillin 100 µg/ml) supplemented with 10 mM L-(+)-arabinose to induce expression of recombinase and was grown to an OD_{600} of app. 0.5 with constant shaking at 180 rpm at 30 °C. The culture was distributed in 50 ml conical tubes, centrifuged (4,500 rpm, 4 °C, 15 min) and supernatant was removed. Electrocompetent cells were prepared by resuspending bacteria in 1 ml 10 % glycerol solution, transferring the solution to a 1.5 ml tube and centrifugation at full speed 4 °C, 1 min. This washing step was repeated five times and after the last washing step bacteria were resuspended in 80 µl of ice-cold 10 % glycerol solution. 5 - 10 µl of PCR product (3.2.3.1) was gently mixed with electrocompetent cells and added to precooled electroporation cuvettes (1 mm; Peqlab). Bacteria were electroporated with 1.8 kV for 5 ms (MicroPulser (Bio-Rad)), immediately recovered in 1 ml prewarmed SOC media (Table 10) and incubated for 1.5 h at 37 °C at 500 rpm. 500 µl of bacterial suspension was spun down, plated on LB plates with selective antibiotics (kanamycin (100 µg/ml) or chloramphenicol (30 µg/ml)) and incubated o. n. at 37 °C. Residual bacterial suspension was kept overnight at RT and was plated the next day. Colonies were picked and re-streaked, cryostocks were prepared and clones were checked

by PCR using Dreamtaq Mastermix (ThermoFisher) with 500 nM of each check-up primer (Table 26). Correct insert size was verified by agarose gel electrophoresis.

3.2.3.3 P22 phage transduction

Phage lysates were produced by mixing 1 ml of an o. n. culture (3 ml LB, 5 mM $CaCl_2$ and antibiotics (Table 30)) of the donor strain (3.2.3.2) with 10 µl of P22 stock solution, static incubation at 37 °C for 15 min and transfer in an Erlenmeyer flask containing 10 ml LB. This culture was grown for 6 h at 37 °C, 180 rpm and afterwards 50 µl of chloroform was added and incubated under constant shaking at RT for 30 min before it was filtered (0.45 µm; Merck). Sterility was checked by plating 50 µl on LB plates and phage lysate was stored at 4 °C. For transduction, the generated phage lysate (1 - 10 µl) was mixed with 100 µl of an o. n. culture (3 ml LB, 5 mM $CaCl_2$, antibiotics (Table 30)) of the recipient strain, statically incubated (15 min, 37 °C) to allow phage absorption before adding 900 µl of fresh LB supplemented with 10 mM EGTA and subsequent shaking for 1 h (500 rpm, 37 °C). Bacteria were centrifuged (10,000 rpm, 3 min), supernatant was reduced to app. 50 µl in which pellet was resuspended and all liquid was plated on selective LB plates supplemented with 10 mM EGTA. After incubation o. n. at 37 °C, colonies were picked and re-streaked three times on selective LB plates supplemented with 10 mM EGTA to remove phages. Clones were checked by PCR and stocked.

3.2.3.4 Generation of *S*.Tm$^{avir\Delta nr3}$

Single mutants of *narZ::cat* (MBE1), *narG::cat* (MBE2) and *napA::apHT* (MBE3) were generated by Dr. Markus Beutler in *S*. Tm^{wt} background and P22 phage lysates were prepared (3.2.3.3). Subsequently, *narZ::cat* allele was transferred by P22 transduction (3.2.3.3) in an attenuated *S*. Tm^{avir} strain background yielding SHE1. The chloramphenicol resistance gene was removed by electroporation of plasmid pCP20 (containing FLP recombinase) into SHE1, induction of recombinase at 43 °C and double picking on selective and non-selective plates to identify antibiotic sensitive clones (SHE2). In this strain, *narG::cat* and *napA::apHT* alleles were subsequently transferred by P22 transduction with lysate from strains MBE2 and then MBE3 (Table 21). This led to the generation of the triple mutant *S*. Tm$^{avir\Delta nr3}$ (SHE4).

3.2.3.5 Generation of *S.* Tm$^{\Delta moaA}$

The kanamycin resistance cassette was amplified from plasmid pKD4 (Table 24) using moaA_KO_fwd and moaA_KO_rev (Table 26) and PCR product was electroporated in *S.* Tm^{wt} harboring pkD46 (3.2.3.2) from which *S.* Tm$^{\Delta moaA}$ (SHE13) was obtained. A P22 lysate was prepared (3.2.3.3) and transduction of the *moaA::apHT* allele was performed into fresh *S.* Tm^{wt} strain background yielding *S.* Tm$^{\Delta moaA}$ (SHE14). Cryostocks were done and clones were checked by PCR (Table 26).

3.2.4 Fluorescence *In Situ* Hybridization (FISH)

The distal part of the cecum was fixed in 4 % paraformaldehyde (PFA) (o. n at 4 °C), incubated in 20 % sucrose solution (o. n. 4 °C) and then embedded in tissue-tek O.C.T. (Sakura), flash frozen in liquid nitrogen and stored at -80 °C. 7 µm tissue sections were cut and dried o. n. at RT. Sections were dehydrated in 50 %, 80 % and 95 % ethanol for 3 min each. Hybridization buffer (Table 17) with 35 % formamide was prepared, fluorescently labelled probes (Table 28) were added to a final concentration of 5 ng/µl, pipetted on the sections and incubated at 46 °C for 3 h. Slides were washed in prewarmed wash buffer (Table 18) for 10 min at 48 °C, then dipped in ice-cold Ampuwa water and air-dried. 4',6-diamidino-2-phenylindole (DAPI) staining was performed with a 1 µg/ml solution (in Ampuwa H_2O) for 30 min at 4 °C. Before mounting with Vectashield and sealing with nail polish, slides were washed three times in ice-cold Ampuwa water and air dried. Afterwards, slides were kept at 4°C until analysis using a confocal TCS SP5 microscope (Leica).

3.2.5 Immunofluorescence staining

As described earlier (3.2.4), 7 µm cryosections were prepared and dried o. n.. Slides were washed one minute in PBS and afterwards blocked with 10% normal goat serum in PBS for 60 min at RT. Blocking solution was removed and primary antibody (Table 32) in 10 % normal goat serum was added for another 60 min at RT. Slides were washed three times 5 min in PBS and incubated for 30 min with secondary antibody (Table 32) and DAPI (final concentration of 1 µg/ml) in 10 % normal goat serum. Finally, slides were washed again three times 5 min, air dried, mounted with Vectashield and sealed with nail polish. Slides were stored at 4 °C until analysis with a TCS SP5 microscope (Leica). For analysis of GFP$^+$ *S.* Tm (*S.*Tm^{avir}p^{sicAgfp}), images with 2 x Zoom were made (1028 x 1028 resolution). These

were imported into ImageJ (Rasband, W.S., ImageJ 1.48v, U. S. National Institutes of Health, Bethesda, Maryland, USA, https://imagej.nih.gov/ij/, 1997-2016), inverted and the number of all *α-Salmonella B test serum anti-O* (Table 32) stained bacteria were determined. Afterwards, the number of all double positive bacteria (α-*Salmonella* and GFP^+ bacteria) was determined and the percentage of GFP^+ bacteria was calculated.

3.2.6 Luciferase assay

S.Tm, harboring a chromosomal luciferase reporter gene, were grown under anaerobic conditions in 100 ml serum glass bottles with 10 ml AAM (Table 6) supplemented with 0.3 M NaCl for 12 h at 37 °C and appropriate antibiotics. Cultures were removed from serum bottles with a sterile needle and syringe under laminar flow and imported into anaerobic tent where 96 well plates for anaerobic and microaerophilic conditions were prepared. Overnight cultures were directly diluted 1:20 in fresh LB media into 96 well plates in duplicates. Plates were sealed with BreatheEasy membrane (Sigma-Aldrich), placed in an anaerobic jar, exported from anaerobic tent and a vacuum / gas cycle was applied three times (anaerobic: 7 % H_2, 10 % CO_2, rest N_2; microaerophilic: 0.8 % O_2, 5 % CO_2, rest N_2). For aerobic incubation, plates were prepared at ambient air with non-reduced media. All plates were incubated at 37 °C for 4 h, OD_{600} was measured (Sunrise Spectrophotometer, Tecan) and cultures were transferred in 1.5 ml plastic tubes, centrifuged (20 min, 14,000 rpm 2 °C), supernatant was discarded and pellet was stored at -80 °C. To measure luciferase activity, bacteria were lysed with Luc-lysis buffer (Table 19, 15 min at RT, vortexed every 2 min). Lysate was frozen for 1 hr at -20 °C and thawed again. Thereafter samples were briefly vortexed and centrifuged for 30 s to pellet cell debris. 25 µl of supernatant was pipetted in black 96 well plates with white wells (Porvair science) and luminescence was measured using Clariostar microplate reader (BMGLabtech). 50 µl of luc-reagent (Table 20) was directly injected before measurement to each well and luciferase signal was quenched with 100 µl EtOH after each measurement.

3.2.7 Hematoxylin and eosin staining (HE staining)

Cecal tissue, directly frozen in O.C.T was cut in 5 µm sections by using a cryotome (Leica) and mounted onto Superfrost Plus glass slides (Hartenstein). Sections were dried o. n. and fixed for 30 s in Wollman solution (95 % ethanol, 5 % acetic acid), washed in flowing tap water (1 min) and rinsed in dH_2O. Afterwards, slides were incubated for 20 min in Vectors's

Hämalaun (Roth) washed in flowing tap water (5 min), dipped one time in de-staining solution (70 % ethanol with 1 % HCl), washed again in flowing tap water (5 min) and rinsed in dH_2O with subsequent rinses in 70 % and 90 % ethanol. Slides were then dipped for 15 s in alcoholic eosin (90 % ethanol) with Phloxin (Sigma-Aldrich), rinsed in dH_2O followed by dehydration in 90 % ethanol, 100 % ethanol and xylene. Sections were directly mounted with Rotimount and thoroughly dried.

Histopathological scoring of cecal tissue was performed as described previously (Stecher *et al.*, 2007). Submucosal edema (0-3), infiltration of polymorphonuclear neutrophils (PMNs) (0-4), loss of goblet cells (0-3) and epithelial damage (0-3) was evaluated and all individual scores were summed up to give a final pathology score: 0-3 no inflammation; 4-8 mild inflammation; 9-13 profound inflammation. For experiments with $Agr2^{-/-}$ mice, scoring was performed without taking into account loss of goblet cells as $Agr2^{-/-}$ mice do not possess goblet cells.

3.2.8 Lipocalin-2 (LCN2) Elisa

ImmunoGrade™ 96-well plates (Brand) were coated with 50 µl lipocalin-2 capture antibody (1:200 in PBS) (Table 31) over night at 4 °C in a humid chamber. Plates were washed three times in wash buffer (0.05 % Tween-20 in PBS) and blocked for one hour at RT with 100 µl blocking buffer (2 % BSA in PBS). Again, plates were washed three times and 50 µl of sample (undiluted (resuspended in PBT (Table 12)); 1:20 and 1:200 dilutions in PBS) were added in duplicates. For quantification a standard with a starting concentration of 50 ng/ml lipocalin-2 was added and serially diluted 1:3 in blocking buffer. After one hour of incubation at RT and six times washing, 50 µl of lipocalin-2 detection antibody (1:200 in blocking buffer) (Table 31) was added, subsequently incubated for one hour at RT and washed six times. With 100 µl of HRP-streptavidin (1:1,000 in PBS) the plate was incubated for one hour at RT, six times washed and developed 30 min at RT with 100 µl substrate (1 mg ABTS in 10 ml 0.1 M NaH_2PO_4 pH 4, 5 µl H_2O_2) in the dark. Absorbance was measured at 405 nm with a spectrophotometer (Sunrise, Tecan).

3.2.9 Invasion assay of *S.* Tm in HuTu80 cells

Invasion assay was performed by Stefanie Walther (RKI, Wernigerode). Briefly, from overnight cultures a 1:31 subculture of each individual *S.*Tm strain was set up in LB with

10 mM KNO_3 LB and cultured for 3.5 h in a roller drum under aerobic or microaerophilic conditions (0.5 % O_2). HuTu80 cells (ATCC: HTB-40), a human duodenum adenocarcinoma cell line, were seeded 24 h prior to infection and infected with *S.*Tm strains with an MOI of 5 for 10 min. Non-adherent bacteria were removed by washing and cells were incubated with gentamicin for 1 h to kill external bacteria. Afterwards, cells were lysed and invaded bacteria were quantified by plating. Invasion is presented as percentage of gentamicin-protected bacteria relative to the inoculum.

3.2.10 gDNA extraction from Gram negative bacteria

DNA was extracted following a standard phenol/chloroform/isoamylalcohol protocol. Briefly, bacterial pellets were resuspended in 567 µl TE buffer, 30 µl of a 10 % SDS solution and 3 µl of 20 mg/ml proteinaseK were added, briefly vortexed and tube was incubated for 60 min at 55 °C. 100 µl of a 5 M NaCl solution and 80 µl of CTAB/NaCl was added, mixed and further incubated for 10 min at 65 °C. Equal volume of phenol:chloroform:isoamylalcohol (25:24:1) was added, thoroughly mixed and centrifuged (5 min, RT, 12,000 x g). The aqueous phase was transferred into a new tube, 0.7 x vol isopropanol and 1/10 vol. 3 M NaAcetate were added, the tube was inverted three times and centrifuged (30 min, 4 °C, 20.817 x g). The supernatant was discarded, pellet was washed with 500 µl ice-cold 70 % EtOH and centrifuged (15 min, 4 °C, 20,817 x g). Again, the supernatant was removed, pellet was air dried and resuspended in 50 µl TE buffer. DNA was stored at 4 °C for Illumina sequencing or stored at -20 °C.

3.2.11 gDNA extraction from feces and cecal content

3.2.11.1 QIAamp Fast DNA Stool Kit (Qiagen)

DNA extraction was performed as described in the manual of the QIAamp Fast DNA Stool kit with some modification. Briefly, Intestinal content was resuspended in 700 µl InhibitEx buffer and three small spoons of each Zirconia-beads (0.7 mm) and acid washed glass beads (≤ 106 µm) were added. Bacteria were lysed by bead beating (TissueLyser LT, Qiagen; 3 min, 50 Hz) and heating to 95 °C for 5 min followed by a second bead beating step (TissueLyser LT,Qiagen; 3 min, 50 Hz). After centrifugation (15,000 x g, 1 min, RT), the supernatant was transferred into a new tube and kept on ice. The pellet was supplemented

with 200 µl lysis buffer for Gram⁺ bacteria (Table 13) and incubated for 30 min, 37 °C. 500 µl InhibitEx buffer was added and stool sample was re-extracted as before (bead beating, 5 min 95 °C, bead beating) and centrifuged. Supernatant was pooled with the one obtained earlier. 15 µl proteinaseK were added to 400 µl supernatant and then mixed with 400 µl AL buffer, vortexed for 15 s and incubated for 10 min at 70 °C. Afterwards, 400 µl EtOH p. a. (96 %) was mixed with the lysate and applied to a QIAamp spin column (15,000 x g, 1 min, RT). Columns were washed with 500 µl AW1 (15,000 x g, 1 min, RT) and 500 µl AW2 (15.000 x g, 3 min, RT) followed by a drying step (15,000 x g, 3 min, RT) to remove residual AW2. DNA was eluted with 100 µl ATE buffer (preheated to 70 °C). DNA was diluted in Gibco H_2O to a final concentration of 2 ng/µl and stored at -20 °C.

3.2.11.2 gDNA extraction (Turnbaugh *et al.*, 2009)

DNA extraction was performed as described previously (Turnbaugh *et al.*, 2009; Ubeda *et al.*, 2012). Intestinal content or feces was resuspended in 500 µl extraction buffer (Table 16) and 210 µl 20 % SDS, 500 µl phenol:chloroform:isoamylalcohol (25:24:1, pH 7.9) and 20 small spoons of 0.1 mm-diameter zirconia / silica beads were added. Bacteria were lysed with a bead beater (TissueLyser LT, Qiagen) for 4 min, 50 Hz and afterwards spun down (14,000 x g, 5 min, RT). Aqueous phase was transferred into a new tube and 500 µl of phenol : chloroform : isoamylalcohol (25 : 24 : 1, pH 7.9) was added, gently inverted and again spun down (14,000 x g, 5 min, RT). After repeated transfer of aqueous phase into a new tube, 1 ml 96 % ethanol and 50 µl of 3 M sodium acetate were added, gently inverted 2 - 3 times and centrifuged for 30 min (14,000 x g, 4 °C). Supernatant was discarded and DNA pellet was washed by inversion with 500 µl ice-cold 70 % ethanol and again centrifuged (14,000 x g, 4 °C; 15 min). Supernatant was discarded, pellet air-dried and DNA was resuspended in 150 µl 10 mM Tris-HCL pH 8. After DNA was properly dissolved, it was purified using the NucleoSpin gDNA clean-up kit (Macherey-Nagel, 740230). DNA was eluted with 100 µl of preheated (70 °C) DE buffer (11.000 x g, 30 s) and diluted to a final concentration of 2 ng/µl in H_2O (Gibco). DNA was stored at -20 °C.

3.2.12 Hydrolysis-probe based quantitative real-time PCR (qPCR)

Duplex-assays were established and optimized in a Roche LightCycler96® system by Dr. Markus Beutler (Brugiroux *et al.*, 2016). Probes and primers are listed in (Table 25). Briefly, DNA extracted from feces or cecal content was diluted to a final concentration of 2 ng/µl and 5 ng were used per analysis. Samples were added as duplicates in 96 well plates (Roche) mixed with 0.2 µl of respective primer (30 µM) and hydrolysis probe (25 µM), 10 µl 2 x FastStart Essential DNA Probes Master (Roche) and 5.5 µl H_2O (Gibco). The following cycler conditions were used: preincubation for 10 min at 95 °C, followed by 45 cycles of 15 s 95 °C and 60 s 60 °C. Fluorescence was recorded after each cycle. Data were analyzed with the LightCycler96® software package (Roche).

3.2.13 Animal experiments

All animal experiments were performed at the Max von Pettenkofer-Institute, Munich and were approved by the Regierung Oberbayern (55.2-1-54-2532-13-15 and 55.2-1-54-2532-145-14).

3.2.13.1 Mice used in this study

C57BL/6J mice associated with a reduced Altered Schaedler Flora (ASF) colonized with three of the eight ASF members are termed ASF^3 mice (*Clostridium* sp., ASF356; *Lactobacillus murinus,* ASF 361 and *Parabacteroides goldsteinii,* ASF 519) (Brugiroux *et al.*, 2016).

C57BL/6J mice harboring the $OligoMM^{12}$ microbiota (*Clostridium innocuum* I46, *Bacteroides caecimuris* I48, *Lactobacillus reuteri* I49, *Enterococcus faecalis* KB1, *Acutalibacter muris* KB18, *Bifidobacterium longum* subsp. *animalis* YL2, *Muribaculum intestinale* YL27, *Flavonifractor plautii* YL31, *Clostridium clostridioforme* YL32, *Akkermansia muciniphila* YL44, *Turicimonas muris* YL45, *Blautia coccoides* YL58) were generated as described (Brugiroux *et al.*, 2016) and are termed $OligoMM^{12}$ mice.

Agr2$^{tm1.2Erle}$ mice were obtained from David Erle (Park *et al.*, 2009). Germ-free mice (*Agr2*^{GF}) mice were re-derived by Prof. Bleich and Dr. Basic at the germ-free mouse facility of the Hannover medical school (MHH). Mating pairs of *Agr2*^{GF} from MHH were imported to the mouse facility of the Max von Pettenkofer-Institute in Munich. There they were colonized with the $OligoMM^{12}$ bacteria mix as described (Brugiroux *et al.*, 2016). From these mating pairs a stable $OligoMM^{12}$ *Agr2* mouse colony was obtained.

All three different mouse colonies were kept and bred under sterile conditions in separate flexible film isolators (Harlan Laboratories) at the Max von Pettenkofer-Institute in Munich. Mice were supplied with autoclaved ddH_2O and a standard diet (V1124-300 SSniff Spezialdiäten GmbH, Soest) ad libitum.

3.2.13.2 Handling of gnotobiotic mice

$OligoMM^{12}$, ASF^3 and *Agr2*-$OligoMM^{12}$ mice were maintained and bred in flexible film isolators (Harlan Laboratories). For experiments, mice were exported in gnotocages (Han, Bioscape) supplied with sterile ddH_2O (Ampuwa), bedding, nestlet and food. All work was conducted under a laminar flow, disinfected for 30 min with Virkon®S, and additional equipment needed (gavage needles, handling cage; wrapped in sterile cloth and separately autoclaved) was brought under the laminar flow. Two person were needed to conduct an

experiment, one equipped with sterile latex surgical gloves (GAMMEX®) and sterile gown, able to handle mice in a germ-free manner and a second person assisting for the non-sterile working steps. Mice were treated according to experimental protocol.

3.2.13.3 Colonization of gnotobiotic mice with *M. schaedleri*

M. schaedleri (ASF457) was grown under anaerobic conditions for 2 days in 10 ml AAM media (supplemented with 10 mM $NaNO_3$) (3.2.1). On day of colonization, purity of culture was verified by Gram staining. *M. schaedleri* or sterile control media was administered rectally (100 µl) and by oral gavage (50 µl). To verify purity of culture, residual amount of *M. schaedleri* was pelleted, gDNA extracted (3.2.10) and checked by Sanger sequencing of the PCR amplified 16S rRNA gene (3.2.1).

3.2.13.4 Growth of *S.* Tm for mouse infections

Three colonies of respective *S.* Tm strain were picked with a sterile inoculation loop, transferred in a glass tube containing 3 ml LB with 0.3 M NaCl (Table 3) and grown in a roller drum for 12 h at 37 °C without antibiotics (antibiotics were only supplemented for plasmid selection). After 12 h, 100 µl of overnight culture was added to 2 ml fresh LB 0.3 M NaCl (Table 3) and incubated for further 4 h rotating at 37 °C. Then, 1 ml of this subculture was taken, centrifuged (2 min at 12,000 rpm), 4 °C, supernatant was removed and pellet was resuspended in an equal amount of ice-cold PBS. Aliquots of 50 µl were prepared and kept on ice until infection.

3.2.13.5 Infection of mice with a single *S.* Tm strain

If required, mice were pretreated with 25 mg of streptomycin by oral gavage one day prior to infection. *S.* Tm was administered by oral gavage at a dose of 10^7 cfu as indicated in section 3.2.13.4. *S.* Tm loads in cecal content, feces, mesenteric lymph nodes, liver and spleen were quantified by plating 50 µl suspension on MacConkey (Oxoid) with indicated antibiotics. Therefore, collected material was resuspended in PBT and disrupted with a bead beater (TissueLyser LT, Qiagen; 5 min 50 Hz). For mesenteric lymph nodes, spleen and liver a stainless steel bead (5 mm) was added for homogenization of tissue. The distal part of the cecum was ligated with dental floss, fixed overnight in 2 ml 4 % PFA (4 °C), incubated in 2 ml 20 % sucrose (4 °C) overnight and embedded in tissue-tek O.C.T. (Sakura), flash frozen in

liquid N_2 and stored at -80 °C until preparation for immunofluorescence staining or FISH. For haematoxylin/eosin staining, a part from liver (1/3) and spleen (1/2), one part of duodenum, jejunum and ileum, cecal tissue, colon and rectum were embedded in tissue-tek O.C.T. (Sakura) and directly flash frozen in liquid N_2.

3.2.13.6 Competitive infection experiments

Competitive infections were performed as described by (Maier *et al.*, 2013) in the uninflamed gut. The avirulent strain (*S.* Tm^{avir}) and the mutant strain in *S.* Tm^{avir} background (*S.* $Tm^{avir\ hyd3}$ or *S.* $Tm^{avir\ \Delta nr3}$) were grown as described in 3.2.13.4. OD_{600} of each strain was measured, if necessary adjusted and both strains were mixed in a 1:1 ratio, centrifuged 2 min at 12000 rpm, 4 °C, supernatant was removed and pellet was resuspended in an equal amount of ice-cold PBS. Bacteria were kept on ice until infection. Inoculum, feces and cecum were plated on selective MacConkey (Oxoid) plates (all *Salmonella*: $Strep^{100}$; mutant: $Strep^{100}Cm^{30}$) and counted. The competitive index was calculated as follows: Number of mutant *Salmonella* (*S.* $Tm^{avir\ hyd3}$ or *S.* $Tm^{avir\Delta nr3}$) divided by the number of the avirulent strain (*S.* Tm^{avir}) corrected by competitive index of inoculum.

3.2.13.7 Measuring the replicative capacity of *S.* Tm *in vivo*

To measure the replicative index of *S.* Tm *in vivo, S.* Tm^{avir} harboring the temperature sensitive plasmid pM1419 (Amp^R) (Table 23), was grown and prepared as described in 3.2.13.4 with exception that ampicillin (50 µg/ml) was added to the overnight and subculture. Growth was performed at 30 °C to facilitate maintenance of the plasmid. Mice were pretreated with 25 mg streptomycin and feces 5 h p. i. and cecum 20 h p. i. were plated on selective MacConkey (Oxoid) plates (all *S.* Tm: $Strep^{100}$; *S.* Tm^{avir}pM1419: $Strep^{100}Amp^{100}$) and counted. Replicative index was calculated as described by (Stecher *et al.*, 2008) and is the number of *S.* $Tm^{avir}pM1419^{+}$ divided by the number of total *S.* Tm^{avir}.

3.2.13.8 Analysis of short chain fatty acids (SCFAs) in cecal content

SCFAs in cecal content of ASF^3 mice with *M.schaedleri* and control (n = 8 / 8) were analyzed by Dr. Buck Hanson (DOME, University of Vienna) using capillary electrophoresis. Cecal content was harvested 10 days post colonization and snap frozen in liquid N_2. Samples were thawed on ice and 50 mg were resuspended in deionized water to a concentration of 0.25 mg/µl. Particulate matter was pelleted at 4 °C for 10 min, supernatants were diluted

1:10 and 1:20 in 0.01 M NaOH, 0.5 mM $CaCl_2$, and 0.1 mM caproate (hexanoate, internal standard) and each sample was screened in triplicate technical replicates. SCFA were quantified by capillary electrophoresis on a P/ACE MDQ Molecular Characterization System (Beckman Coulter) using methods previously described (Koch *et al.*, 2015). Acetate was separated by using the CEofix Anions 5 kit (Analis Technologies) on a fused silica column (TSP075375; 75 µm ID, Polymicro Technologies). External standards of formate, succinate, acetate, lactate, propionate, and butyrate (50 µm, 100 µm and 250 µM) were used to quantify analytes with each individual run (~25 samples/run). All standards and samples were normalized to the 0.1 mM caproate internal standard.

3.2.13.9 Quantification of bile acids in cecal content

For quantification of bile salts in cecal content, non-targeted metabolomics was performed using a UPLC-MS approach by Dr. Alesia Walker (Helmholtz Zentrum, München). Same samples were used as for SCFA analysis (3.2.13.8).

3.2.13.10 Transcriptome analysis

ASF^3 mice (n = 4 / 4) were pre-colonized with *M. schaedleri* or control for 10 days and infected with *S.* Tm^{avir}pM1419. Cecal content was harvested one day post infection, flash frozen in liquid N_2 and stored at -80 °C until further analysis. Samples were shipped on dry ice to Dr. David Berry (DOME, University of Vienna) were RNA was extracted, library preparation and sequencing and analysis was performed. Detailed description can be found in (Loy *et al.*, 2017). Briefly, RNA was extracted with a standard phenol:chloroform method, additionally treated with ezDNase (Invitrogen, Carlsbad, CA) and cleaned up and concentrated using the GeneJET RNA cleanup and Concentration Micro Kit (Thermo Scientific). rRNA was removed with the Ribo-Zero bacterial kit (Illumina, San Diego, CA) and RNA was evaluated with the RiboGreen assays (Quant-iT™ RiboGreen™ RNA Assay Kit, Invitrogen). Library was prepared for RNAseq on the HiSeqV4 SR100 with the NEBNext Ultra RNA library prep kit for Illumina (New England Biolabs, Ipswich, MA).

The raw reads were quality filtered using Trimmomatic (Bolger *et al.*, 2014) and mapped to the *S.* Tm reference genome (accession number: FQ312003; plasmids: HE654724, HE654725, HE654726) obtained from MicroScope (SALTS.1) (http://www.genoscope.cns.fr/agc/microscope/mage/index.php) using BWA (Li & Durbin, 2009). Differential gene expression was analyzed using EdgeR (Robinson *et al.*, 2010).

RNAseq analysis was performed by Dr. David Berry (DOME, University of Vienna) and Dr. Lara Jochum (MvP, Ludwig-Maximilians-University, Munich).

3.2.14 Statistical analysis

S. Tm loads (cfu/g), histopathological score and lipocalin-2 are displayed as median. To compare two groups at one time point Mann-Whitney U test was performed. For comparing two groups at several time points a One-way ANOVA Kruskal-Wallis test was performed and Dunn's multiple comparison test was done to compare selected pairs (mock vs. *M. schaedleri*). For *in vitro* assays, means are shown and One-way ANOVA with Tukey post hoc test was performed. All analysis were performed with GraphPad Prism (version 5.01 for Windows, GraphPad Software, San Diego California USA).

Diversity analysis (PCA) was performed on relative abundances from qPCR of 16S rRNA genes using the QIIME scripts (Caporaso *et al.*, 2010). Different clustering was analyzed using the quantitative Bray Curtis dissimilarity and statistical significance was determined with the nonparametric Adonis method based on the permutational multivariate ANOVA (PERMANOVA) (Anderson, 2001).

In all cases $p < 0.05$ is considered statistically significant.

4 Results

4.1 Studying the effect of *M. schaedleri* on the development of *S.* Tm induced colitis

4.1.1 *M. schaedleri* colonizes the gut of gnotobiotic mice and occupies a niche close to the epithelial border

To investigate the contribution of *M. schaedleri* on the course of *S.* Tm induced gastroenteritis, we employed two alternative gnotobiotic mouse models with a defined microbiota. First, we studied the influence of *M. schaedleri* (ASF457) on *S.* Tm colitis in ASF^{3} (3.2.13.1) mice, harboring three of the eight ASF members and secondly in OligoMM^{12} mice (3.2.13.1; (Brugiroux *et al.*, 2016)), which represent a more complex microbiota with twelve mouse-derived strains. ASF^{3} mice show reduced colonization resistance to *S*. Tm compared to OligoMM^{12} mice, as described previously (Brugiroux *et al.*, 2016).

Our data reveal that *M. schaedleri* is able to colonize in both gnotobiotic mouse models, ASF^{3} as well as OligoMM^{12}. By qPCR we could detect each individual strain in fecal samples ten days after inoculation with *M. schaedleri*, based on the 16S rRNA gene. The relative abundance of *M. schaedleri* in ASF^{3} mice ranges between 1.0 % and 15 % (Fig. 5A) whereas the relative abundance in OligoMM^{12} mice is lower, 0.1 % to 0.4 % (Fig. 5C). *M. schaedleri* was not detected in the respective control groups. To characterize the localization of *M. schaedleri* in the cecum of mice, we used a microscopy approach. With a *M. schaedleri* specific FISH probe (Loy *et al.*, 2017), we could localize this bacterium close to the epithelial border in ASF^{3} (Fig. 5B) and OligoMM^{12} mice (Fig. 5D), where it forms a mesh like structure, but was not detected in control mice.

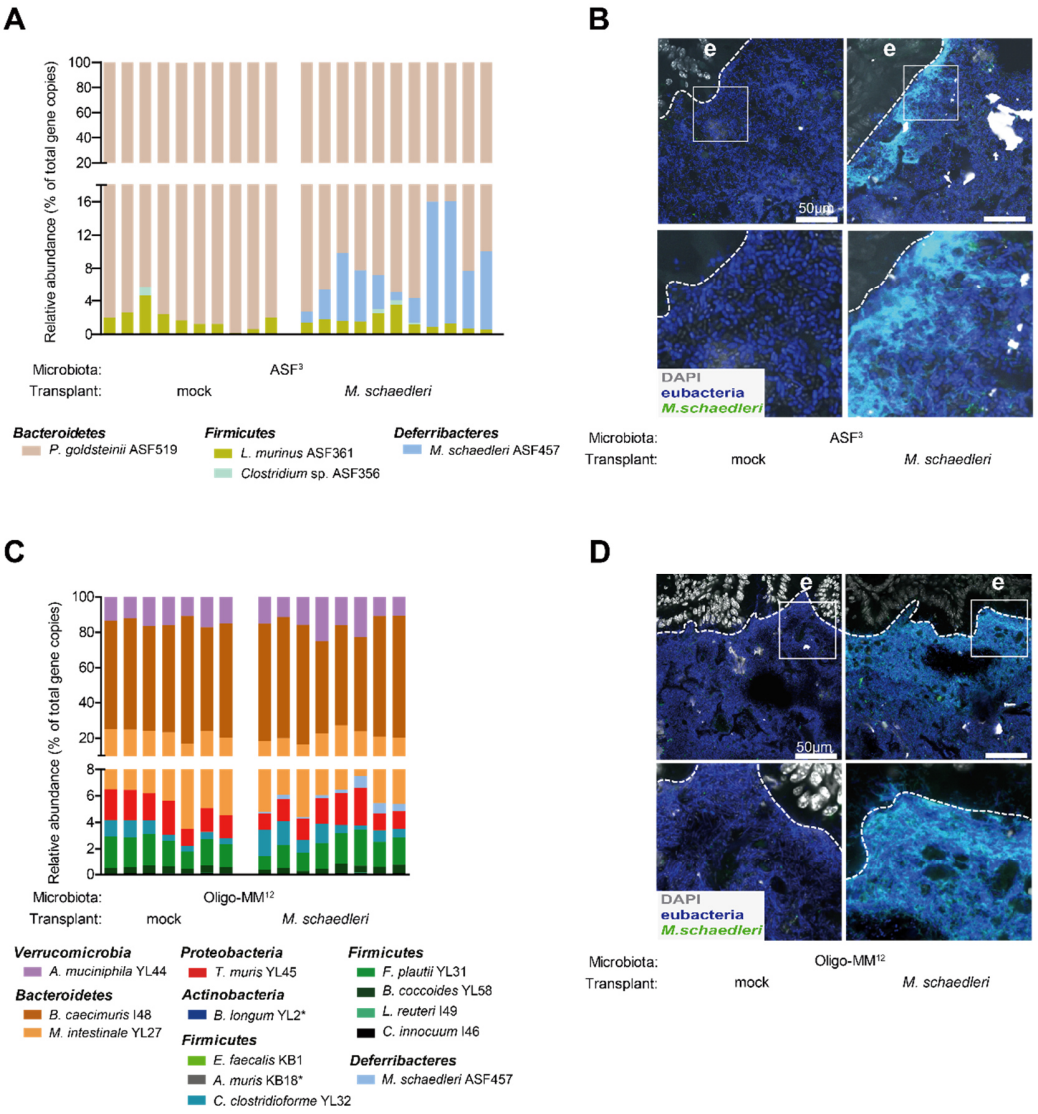

Fig. 5: *M. schaedleri* colonizes the intestine of gnotobiotic mice. Gnotobiotic ASF[3] or OligoMM[12] mice were colonized for 10 days with *M. schaedleri* by oral and rectal inoculation. **A)** Microbiota composition of fecal samples from ASF[3] mice with *M. schaedleri* or control shown as the relative abundance of each individual strain (% of all 16S rRNA gene copies). Each bar represents one mouse. * under detection limit **B)** Localization of *M. schaedleri* by FISH analysis in PFA fixed cecum of ASF[3] mice. grey, DAPI; blue, all bacteria (eub338 I:III probe); green, *M. schaedleri* (msc487_correct probe), scale bar 50 µm. White squares indicate magnified area. e, epithelium **C)** Microbiota composition of fecal samples from OligoMM[12] mice with *M. schaedleri* or control. Shown is the relative abundance of each individual strain (% of all 16S rRNA gene copies). Each bar represents one mouse. * under detection limit **D)** Localization of *M. schaedleri* by FISH analysis in PFA fixed cecum of OligoMM[12] mice. Grey, DAPI; blue, all bacteria (eub338 I:III probe); green, *M. schaedleri* (msc487_correct probe), scale bar 50 µm. White squares indicate magnified area. e, epithelium.

4.1.2 *M. schaedleri* protects gnotobiotic ASF[3] mice from *S.* Tm induced colitis

To verify the role of *M. schaedleri* during *S.* Tm induced colitis we infected ASF[3] mice pre-colonized with *M. schaedleri* or control (n= 11 / 10) with *S.* Tm[wt] (Fig. 6A). After 24 h of

infection, mice were sacrificed and *S.* Tm loads were enumerated in the cecal content by plating. No differences in *S.* Tm colonization was detected between both groups ($p > 0.05$ Mann–Whitney U test; Fig. 6B). Systemic dissemination of *S.* Tm could already be observed in mesenteric lymph nodes (Fig. 6C) but only low *S.* Tm loads in spleen (Fig. 6D) or liver (Fig. 6E). No significant differences between control and experimental group were detected ($p > 0.05$ Mann–Whitney U test). During inflammation the cecal tissue undergoes drastic pathological changes like formation of submucosal edema, loss of goblet cells, infiltration of neutrophils and epithelial damage (Stecher *et al.*, 2007). Mice pre-colonized with *M. schaedleri* show reduced inflammation assed by histology (***$p<0.001$ Mann–Whitney U test; Fig. 6F). To confirm this observation, lipocalin-2, a marker for inflammation, was measured by quantitative ELISA in cecal sample*s.* No lipocalin-2 was detected in mice pre-colonized with *M. schaedleri* compared to control group (**$p<0.001$ Mann–Whitney U test; Fig. 6G).

From this experiment we concluded that *M. schaedleri* does not confer colonization resistance but reduces *S.* Tm induced colitis in ASF[3] mice.

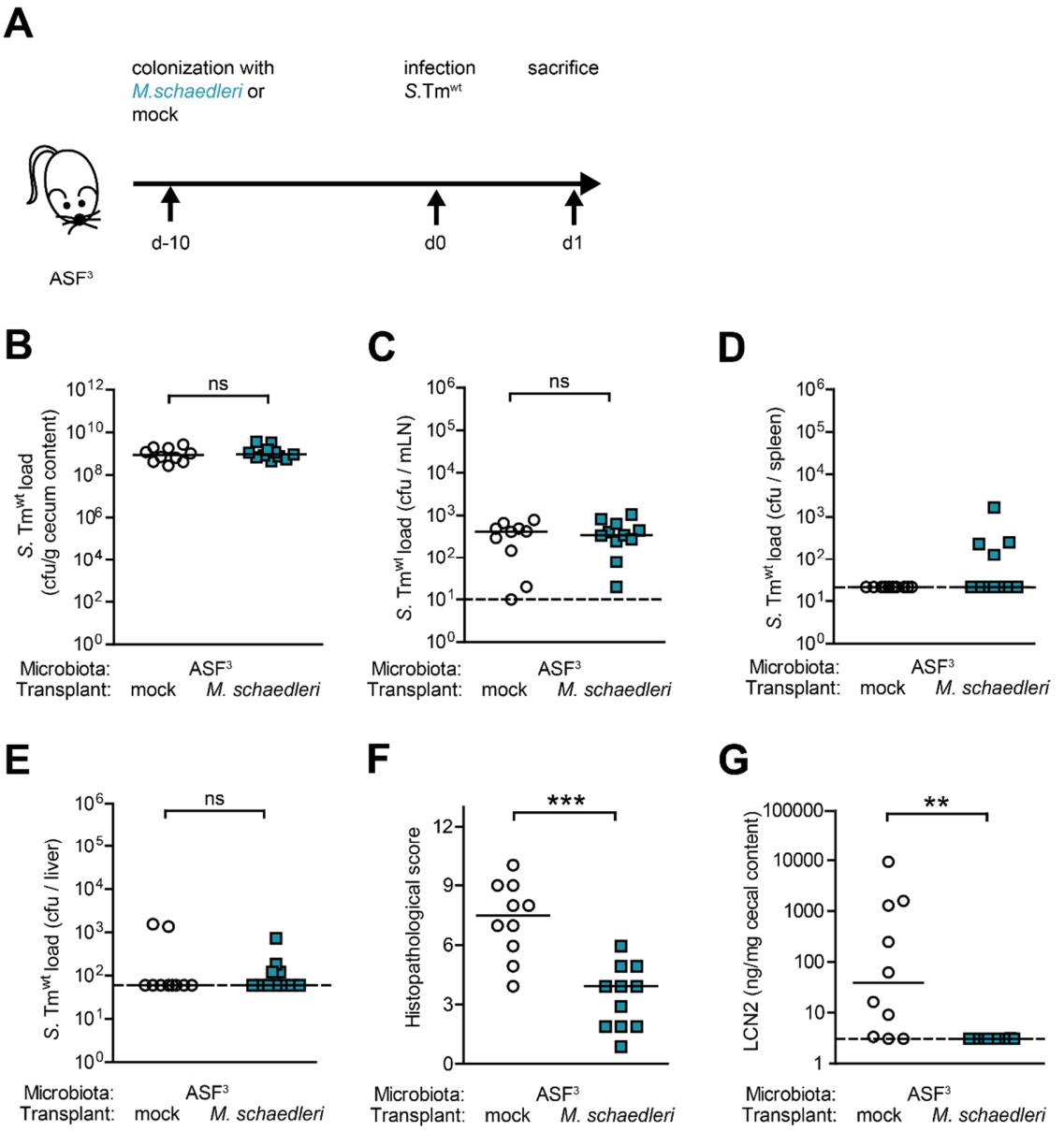

Fig. 6: *M. schaedleri* protects ASF[3] mice from *S.* Tm induced colitis. A) Experimental set up. ASF[3] mice were pre-colonized for 10 days with *M. schaedleri* or control media before infection with 10^7 cfu of *S.* Tm^{wt} and sacrificed one day post infection. **B)** *S.* Tm loads in cecal content, **C)** mesenteric lymph nodes, **D)** spleen and **E)** liver quantified by plating at day 1 p.i.. **F)** Histopathological score of cecal tissue on day 1 p. i. stained with hematoxylin and eosin. The degree of submucosal edema, neutrophil infiltration, loss of goblet cells and epithelial damage was scored in a double-blinded manner. 0-3: no pathological changes; 4-7: moderate inflammation; above 8: severe inflammation. **G)** Lipocalin-2 levels of cecal content were measured by quantitative ELISA on day 1 p.i.. Dashed line: detection limit. One dot represents one mouse. Mann–Whitney U test; ns, no significant difference $p \geq 0.05$, *$p < 0.05$, **$p < 0.01$, ***$p < 0.001$.

4.1.3 OligoMM^{12} mice are protected from *S.* Tm induced colitis by *M. schaedleri*

To further investigate, if the protective effect of *M. schaedleri* is dependent on the microbiota we performed an analogous experiment (4.1.2) in the OligoMM^{12} mice (Brugiroux *et al.*, 2016) which harbor a more complex microbiota than the ASF^{3} mice. Due to the higher complexity of the microbiota, onset of inflammation is delayed and starts at day 3 p.i. resulting in a profound colitis on day 4 p. i. (Fig. 3C) (Beutler, 2016). OligoMM^{12} mice were pre-colonized for ten days with *M. schaedleri* or control media, infected with *S.* Tm^{wt} and sacrificed at day 4 p.i. (Fig. 7A). As seen in ASF^{3} mice, *S.* Tm loads in the cecal content of OligoMM^{12} mice with and without *M. schaedleri* show no significant difference (Fig. 7B) ($p > 0.05$ Mann–Whitney U test). *S.* Tm dissemination to mesenteric lymph nodes (Fig. 7C), spleen (Fig. 7D) and liver (Fig. 7 E) was observed but no significant difference between both groups was detected ($p > 0.05$ Mann–Whitney U test). In contrast, we found a significant reduction (**$p < 0.01$) of the histopathological score (Fig. 7F) in OligoMM^{12} mice pre-colonized with *M. schaedleri* compared to control at day 4 p.i.. To verify this result we measured the lipcalin-2 levels (Fig. 7G) in the cecal content day 4 p.i. and found an app. 100 fold decrease in lipocalin-2 in mice colonized with *M. schaedleri*. Taken together, these results show a strong protective effect of *M. schaedleri* on *S.* Tm induced colitis in two gnotobiotic mouse models, with different microbiota complexity. This indicates that *M. schaedleri* protects in a microbiota independent way from *S.* Tm colitis even though it does not provide colonization resistance.

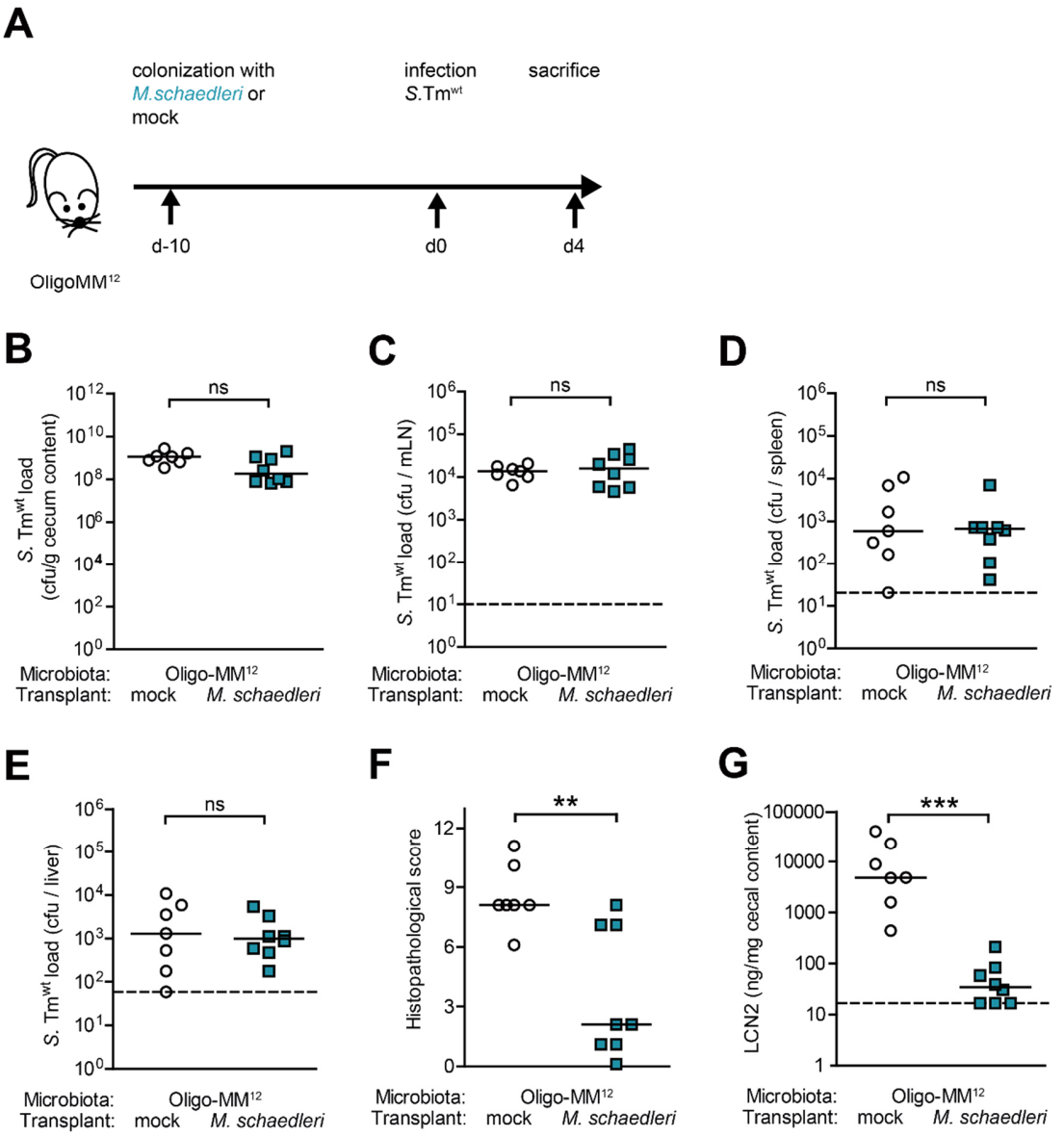

Fig. 7: *M. schaedleri* protects OligoMM^{12} mice from *S.* Tm induced colitis. A) Experimental set up. OligoMM^{12} mice were pre-colonized for 10 days with *M. schaedleri* or control media before infection with 10^7 cfu of *S.* Tm^{wt} and sacrificed four days post infection. **B)** *S.* Tm loads in cecal content, **C)** mesenteric lymph nodes, **D)** spleen and **E)** liver quantified by plating at day 4 p.i.. **F)** Histopathological score of cecal tissue on day 4 p.i. stained with hematoxylin and eosin. The degree of submucosal edema, neutrophil infiltration, loss of goblet cells and epithelial damage was scored in a double-blinded manner. 0-3: no pathological changes; 4-7: moderate inflammation; above 8: severe inflammation. **G)** Lipocalin-2 levels of cecal content were measured by quantitative ELISA on day 4 p.i.. Dashed line: detection limit. One dot represents one mouse; Mann–Whitney U test; ns, no significant difference $p \geq 0.05$, *$p < 0.05$, **$p < 0.01$, ***$p < 0.001$.

4.2 Elucidating the protective effect of *M. schaedleri*

4.2.1 *M. schaedleri* does not inhibit the replication of *S.* Tm in mice

The previous experiments left us with the question of the mechanism underlying the protective effect of *M. schaedleri*. When *S.* Tm enters the gut it is in need to multiply to enable colonization of the intestine at high numbers (≥ 10^8 cfu/g), which subsequently allows *S.* Tm shedding and transmission by the fecal oral route (Lawley *et al.*, 2008; Rivera-Chávez *et al.*, 2016). Therefore we analyzed the influence of *M. schaedleri* on the replication of *S.* Tm *in vivo*.

To measure the growth rate of *S.* Tm *in vivo*, an avirulent *S.* Tm strain harboring a temperature sensitive plasmid (pM1419, Amp^R (Stecher *et al.*, 2008)) was used. The plasmid replicates and is transferred to the daughter cell at permissive temperatures (< 30 °C), but at higher temperature (> 37 °C) replication of the plasmid is blocked and the plasmid is lost (Benjamin *et al.*, 1990; Stecher *et al.*, 2008). Therefore, during infection in mice, the fraction of bacteria harboring this plasmid will be reduced if cell division occurs. The replication rate of *S.* Tm in the uninflamed gut was calculated in $OligMM^{12}$ mice and mice pre-colonized with *M. schaedleri* but was not different between both groups after 5 h p.i. in feces or 20 h p.i. (Fig. 8B).

An analogous experiment was performed in ASF^3 mice. Streptomycin treatment in these mice is not necessary as the low complex microbiota does not confer colonization resistance to *S.* Tm (Fig. 8C). The replicative index was again assessed 5 h p.i. in feces or 20 h p.i. in cecal content in ASF^3 mice pre-colonized with *M. schaedleri* or control. No difference between both groups was observed in feces 5 h p.i.. Longer infection time (20 h p.i.) lead to a slight increased, but not significant, replication of *S.* Tm in ASF^3 mice pre-colonized with *M. schaedleri* compared to control mice.

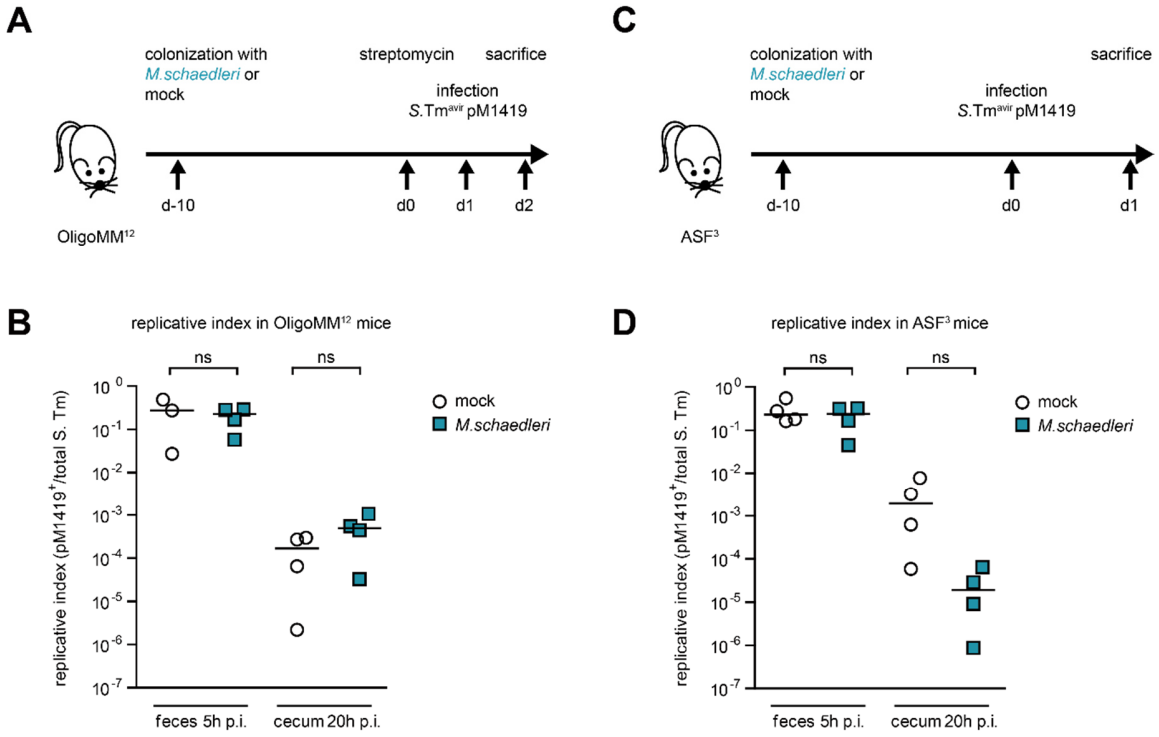

Fig. 8: *M. schaedleri* does not influence the replication rate of *S.* Tm. A) Experimental set up. OligoMM^{12} mice were colonized with *M. schaedleri* or sterile control media for 10 days before treatment with 25 mg streptomycin by oral gavage. One day later mice were infected orally with *S.* Tm^{avir}pM1419 (4 x 10^{7}cfu), feces was collected 5 h post infection and mice were sacrificed 20 h p.i.. *S.* Tm loads were quantified on selective agar plates and **B)** replicative index is displayed. **C)** Experimental set up. ASF^3 mice were colonized with *M. schaedleri* or sterile control media for 10 days. Mice were infected orally with *S.* Tm^{avir}pM1419 (2 x 10^{7}cfu), feces was collected 5 h post infection and mice were sacrificed 20 h p.i.. *S.* Tm loads were quantified on selective agar plates and **D)** replicative index is displayed. One dot represents one mouse. One-way ANOVA Kruskal-Wallis test with Dunn's multiple comparison test compare selected pairs (mock vs. *M. schaedleri*); ns, no significant difference $p \geq 0.05$, *$p < 0.05$, **$p < 0.01$, ***$p < 0.001$

4.2.2 Competition between *S.* Tm and *M. schaedleri* for hydrogen or nitrate does not play a role in the uninflamed gut of OligoMM^{12} mice

Hydrogen, generated by the microbiota is vital for growth of *S.* Tm in the gut (Maier *et al.*, 2013) and nitrate respiration plays an important role for *S.* Tm growth during colitis (Lopez *et al.*, 2015). Genome analysis and *in vitro* cultures revealed that *M. schaedleri* is able to use H_2 as electron donor and nitrate as electron acceptor under anaerobic conditions and perform full dissimilatory nitrate reduction to ammonia (DNRA) (Loy *et al.*, 2017) (Fig. 2B). Thus we hypothesize, that *M. schaedleri* competes for H_2 or NO_3 with *S.* Tm and thereby inhibits growth or virulence of the pathogen. To investigate, if the availability of hydrogen and nitrate during the early phase of infection plays a role for *S.* Tm infection we performed competitive mouse infection experiments with a *S.* Tm mutant, defective in all three hydrogenase genes (*S.* Tm$^{avir\ hyd3}$; (Maier *et al.*, 2013)) and a *S.* Tm defective in three nitrate reductase genes (*S.* Tm$^{avir\Delta nr3}$) (Table 21). First, mice were infected with a 1:1 mix of *S.* Tm$^{avir\ hyd3}$ /*S.* Tm^{avir} or *S.* Tm$^{avir\Delta nr3}$/ *S.* Tm^{avir} and *S.* Tm loads were monitored over time and the competitive index between mutant and *S.* Tm^{avir} was calculated. In the OligoMM^{12} mice *S.* Tm^{avir} does not show a growth benefit over the hydrogenase mutant *S.* Tm$^{avir\ hyd3}$, revealing that H_2 does not play a role for efficient colonization in this model. This was not altered in *M. schaedleri* pre-colonized mice or at later time points of the experiment. The *S.* Tm$^{avir\ hyd3}$ and the hydrogenase proficient *S.* Tm^{avir} colonize the gut at the same rate, resulting in a CI of 1 (Fig. 9 B).

On the other hand, co-infection with *S.* Tm$^{avir\Delta nr3}$/ *S.* Tm^{avir} gave conflicting results. Instead of attenuation the *S.* Tm$^{avir\Delta nr3}$ mutant showed a significant growth advantage in mice pre-colonized with *M. schaedleri* compared to the control group (*$p < 0.05$; One-way ANOVA Kruskal-Wallis test with Dunn's multiple comparison test compare selected pairs) which prevailed at day 3 p.i. but was reduced at day 4 p.i. in feces and cecal content (Fig. 9C).

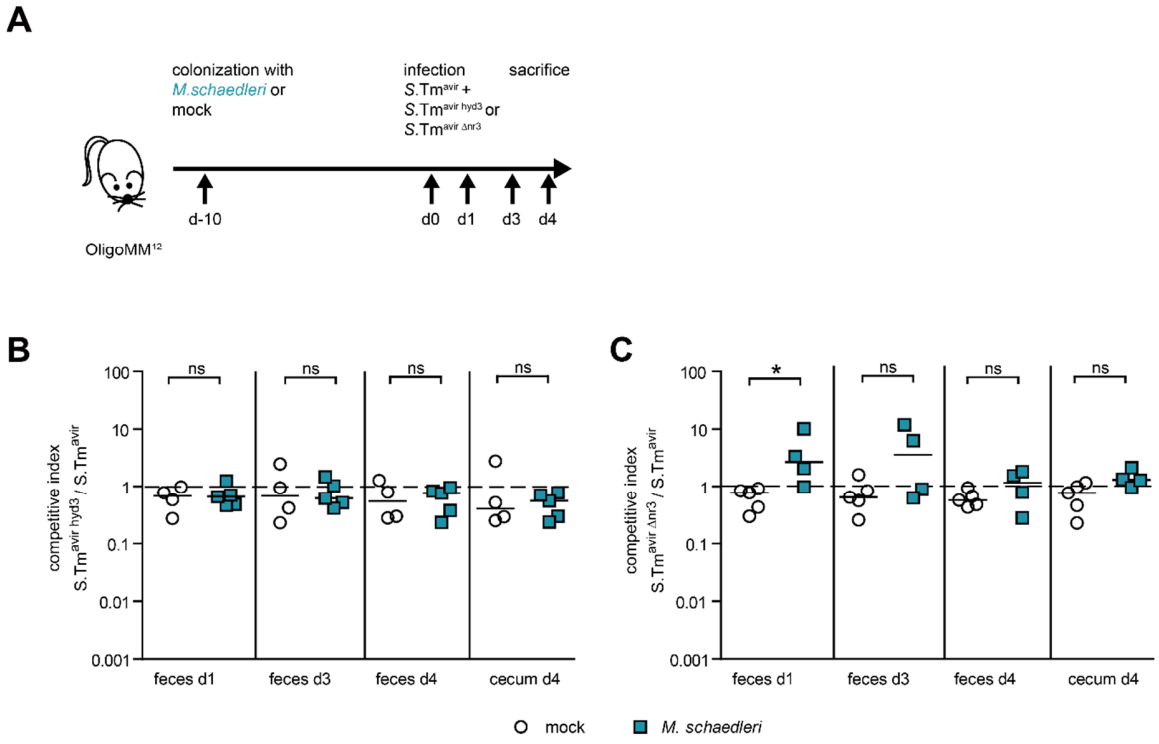

Fig. 9: Competition for hydrogen or nitrate does not play a role in the uninflamed gut of OligoMM^{12} mice. **A)** Experimental set up. OligoMM^{12} mice were colonized with *M. schaedleri* or sterile control media for ten days before oral infection with a 1:1 mix of *S.* Tm$^{avir\ hyd3}$/ *S.* Tm^{avir} or *S.* Tm$^{avir\ \Delta nr3}$/ *S.* Tm^{avir} (10^7 cfu/per strain). Feces was collected at day 1, day 3 and mice were sacrificed on day 4 post infection. Individual *S.* Tm strains were quantified on selective agar plates and competitive index was calculated. **B)** Competitive index between *S.* Tm$^{avir\ hyd3}$ and *S.* Tm^{avir}. **C)** Competitive index between *S.* Tm$^{avir\ \Delta nr3}$ and *S.* Tm^{avir}. One-way ANOVA Kruskal-Wallis test with Dunn's multiple comparison test compare selected pairs (mock vs. *M. schaedleri*); ns, no significant difference $p \geq 0.05$, *$p < 0.05$, **$p < 0.01$, ***$p < 0.001$.

4.2.3 Colonization by *M. schaedleri* reduces the expression of *S.* Tm SPI1-T3SS in the intestine of mice

For inducing gastroenteritis, *S.* Tm needs its SPI1-T3SS which translocates effector proteins into epithelial cells (Collazo & Galán, 1997), mediates pathogen invasion and triggers inflammation (Barthel *et al.*, 2003; Hapfelmeier *et al.*, 2004). We studied the expression of SPI1-T3SS using an avirulent *S.* Tm strain harboring a SPI-1 reporter plasmid (pM974; (Ackermann *et al.*, 2008)) with GFP fused to the promotor of *sicA* (*S.* Tm^{avir}p^{sicAgfp}), a chaperone of the SPI1-T3SS translocases SipB and SipC (Tucker & Galan, 2000). Mice, pre-colonized with *M. schaedleri* or control were treated with 25 mg streptomycin to allow efficient colonization of *S.* Tm in the gut which enabled us to detect *S.* Tm in high numbers by confocal microscopy. *M. schaedleri* is streptomycin resistant (Fig. 20) and therefore not affected by this antibiotic. After 24 h post infection with the reporter strain *S.* Tm^{avir}p^{sicAgfp}, the cecum was fixed in PFA and all *S.* Tm were stained with a *Salmonella* specific antiserum (Table 32). The fraction of GFP$^+$ *S.* Tm of all *S.* Tm was determined by image analysis (3.2.5). Fig. 10A shows the percentage of GFP$^+$/α-*Salmonella* double positive bacteria to all α-*Salmonella* positive bacteria per mouse. The SPI1-T3SS expression in mice pre-colonized with *M. schaedleri* was reduced about 2-fold compared to the control group (*$p < 0.05$ Mann–Whitney U test). Fig. 10B displays the percentage of each analyzed image. Similarly, the median GFP expression rate between *M. schaedleri* and control group differs significantly (***$p < 0.001$ Mann–Whitney U test). Respective images are shown in Fig. 10C.

Based on this data we conclude, that *M.schaedleri* has no impact on the replication rate of *S.* Tm nor does it compete for hydrogen or nitrate *in vivo*. Interestingly, it modulates expression of the *S.* Tm specific SPI1-T3SS which is important to drive intestinal inflammation.

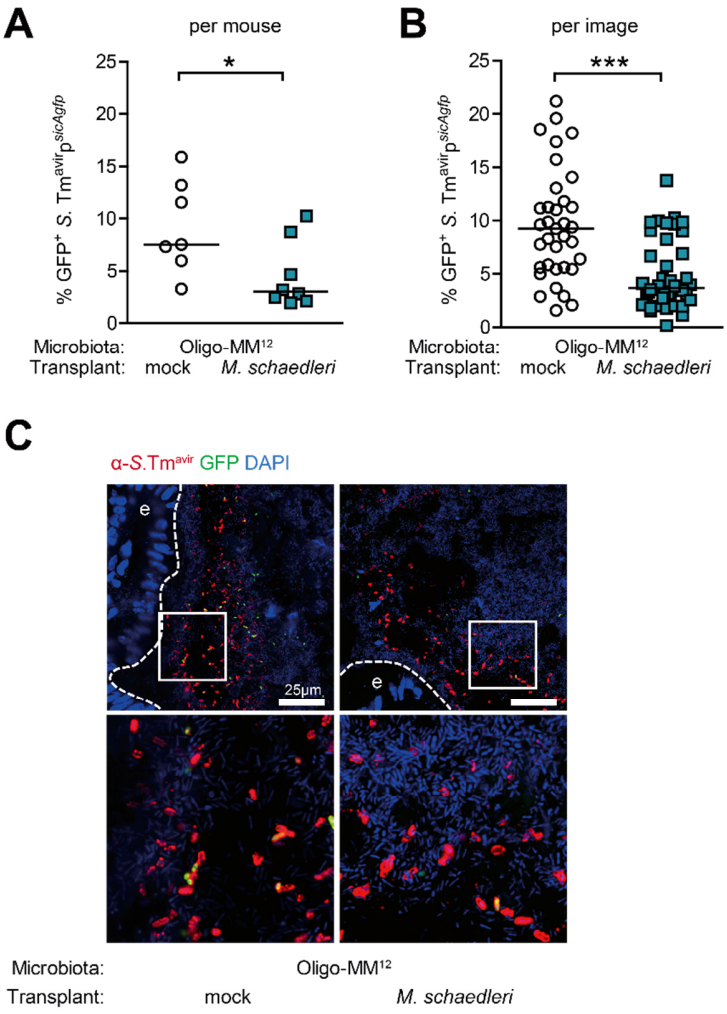

Fig. 10: *M. schaedleri* modulates *S.* Tm SPI1-T3SS expression *in vivo*. OligoMM^{12} mice were colonized with *M. schaedleri* or sterile control media for 10 days before treatment with 25 mg streptomycin. One day later mice were infected with 2 x 10^7 cfu *S.* Tm^{avir}p^{sicAgfp} and sacrificed 24 h later. Cecum was fixed in PFA and sections were stained with DAPI and primary rb-α-*Salmonella* B test serum anti-O antibody and secondary α-rabbit dyLight649. Per mouse 3 - 5 picture (2x zoom) close to the epithelial border were taken and counted. **A)** Mean fraction of GFP$^+$ and *Salmonella* B test serum$^+$ double positive bacteria of all images from each mouse is displayed. **B)** Percent of double positive bacteria (GFP$^+$ and *Salmonella* B test serum$^+$) is displayed per analyzed image. **C)** Representative images from cecal lumen of controls, mice colonized with *M. schaedleri* and infected with *S.* Tm^{avir}p^{sicAgfp}. blue, DAPI; red, α-*Salmonella*; green, GFP; e, epithelium; white boxes: sections enlarged; scale bar, 25 µm. Dashed line indicates epithelial border. Mann–Whitney U test; ns, no significant difference $p \geq 0.05$, *$p < 0.05$, **$p < 0.01$, ***$p < 0.001$

4.2.4 Transcriptome analysis of *S.* Tm *in vivo*

To analyze how *M. schaedleri* effects *S.*Tm *in vivo* we performed transcriptome analysis of total RNA extracted from cecal content of ASF[3] mice colonized with *M. schaedleri* or control media and infected with *S.* Tm^{avir}. Overall, around 100 *S.*Tm genes were differentially expressed in the presence of *M. schaedleri*. Interestingly, transcripts of genes associated with the SPI1-T3SS (*sopB, sipA, prgK* and *invF*) were downregulated in *S.*Tm in mice with *M. schaedleri* (Table 34), confirming our findings with a SPI1-T3SS reporter strain (Fig. 10). Furthermore genes involved in energy metabolism (*napA, cydA, fabI, plsX* and *accD*) and multiple translation associated transcripts were as well downregulated in the presence of *M. schaedleri*. On the other hand only one gene transcript is more abundant in *S.* Tm in the presence of *M. schaedleri* which is, *malS* an alpha-amylase. Recently, the 5'-UTR was linked to the regulation of SPI1-T3SS (Gong *et al.*, 2015).

Table 34. Differentially expressed genes of *S.* Tm between mice colonized with *M. schaedleri* vs. control mice

Annotation	logFC	logCPM	p-Value	FDR	genes
menC	-5,22	5,38	7,84E-05	1,24E-02	SALTSv1_2348
ygaP	-4,95	5,23	1,02E-04	1,41E-02	SALTSv1_2878
rhaB	-4,82	5,18	2,39E-04	2,11E-02	SALTSv1_4125
gph	-4,80	5,16	2,55E-04	2,18E-02	SALTSv1_3564
sopB	-4,72	5,12	4,95E-04	3,10E-02	SALTSv1_1052
murA	-3,67	5,63	6,68E-05	1,16E-02	SALTSv1_3394
exbD	-3,51	5,53	1,73E-04	1,89E-02	SALTSv1_3245
purF	-3,36	5,99	1,98E-04	2,05E-02	SALTSv1_2406
sipA	-3,33	5,42	7,44E-04	4,14E-02	SALTSv1_2962
yoaE	-3,30	6,61	3,57E-06	2,50E-03	SALTSv1_1800
garR	-3,12	5,81	1,36E-04	1,61E-02	SALTSv1_3334
rplW	-3,09	5,80	4,67E-04	3,03E-02	SALTSv1_3520
prgK	-3,00	6,09	7,85E-05	1,24E-02	SALTSv1_2951
lepB	-2,72	5,58	5,59E-04	3,30E-02	SALTSv1_2630
pdxY	-2,67	5,88	4,27E-04	2,92E-02	SALTSv1_1411
ycfW	-2,65	5,52	9,25E-04	4,90E-02	SALTSv1_1179

Annotation	logFC	logCPM	p-Value	FDR	genes
NA	-2,63	6,12	2,32E-04	2,11E-02	SALTSv1_miscRNA187
NA	-2,62	5,85	6,31E-04	3,64E-02	SALTSv1_1750
era	-2,62	5,84	2,69E-04	2,18E-02	SALTSv1_2628
tldD	-2,61	5,84	4,06E-04	2,85E-02	SALTSv1_3455
NA	-2,61	10,50	3,94E-10	2,05E-06	SALTSv1_miscRNA52
NA	-2,60	7,84	2,52E-05	6,89E-03	SALTSv1_miscRNA125
NA	-2,59	6,08	1,68E-04	1,89E-02	SALTSv1_tRNA79
napA	-2,59	6,32	3,08E-05	7,27E-03	SALTSv1_2299
tgt	-2,56	6,81	4,33E-06	2,50E-03	SALTSv1_0409
menD	-2,45	6,43	2,76E-04	2,21E-02	SALTSv1_2351
NA	-2,45	6,01	3,26E-04	2,48E-02	SALTSv1_1810
dnaX	-2,42	6,70	4,04E-06	2,50E-03	SALTSv1_0486
gudD	-2,40	6,57	1,75E-04	1,89E-02	SALTSv1_3044
NA	-2,39	6,37	3,33E-04	2,48E-02	SALTSv1_tRNA83
kdsA	-2,35	5,94	9,60E-04	4,98E-02	SALTSv1_1742
rplF	-2,31	7,66	4,25E-07	5,52E-04	SALTSv1_3507
NA	-2,30	7,18	2,78E-05	7,22E-03	SALTSv1_tRNA52
nusA	-2,27	8,07	3,54E-07	5,52E-04	SALTSv1_3374
yiaF	-2,26	6,61	6,06E-05	1,09E-02	SALTSv1_3733
NA	-2,20	7,29	1,28E-04	1,55E-02	SALTSv1_4534
proS	-2,15	6,37	3,99E-04	2,85E-02	SALTSv1_0246
rpsI	-2,15	8,21	7,71E-09	2,00E-05	SALTSv1_3431
melA	-2,12	7,55	7,36E-04	4,14E-02	SALTSv1_4367
glyS	-2,12	6,63	5,96E-05	1,09E-02	SALTSv1_3741
rplD	-2,11	6,84	1,66E-05	5,73E-03	SALTSv1_3521
fabI	-2,09	6,33	2,34E-04	2,11E-02	SALTSv1_1671
oxyR	-2,07	6,48	7,40E-04	4,14E-02	SALTSv1_4203
dinG	-2,04	6,30	3,34E-04	2,48E-02	SALTSv1_0815
speF	-2,02	6,44	4,52E-04	2,97E-02	SALTSv1_0699
NA	-2,01	6,42	5,75E-04	3,35E-02	SALTSv1_tRNA2
rplC	-2,00	7,69	7,72E-06	3,34E-03	SALTSv1_3522

Annotation	logFC	logCPM	p-Value	FDR	genes
infB	-1,99	7,98	2,51E-05	6,89E-03	SALTSv1_3373
iscR	-1,98	7,11	2,18E-05	6,89E-03	SALTSv1_2592
rplI	-1,97	6,94	2,36E-05	6,89E-03	SALTSv1_4463
tsf	-1,94	7,33	3,00E-05	7,27E-03	SALTSv1_0221
plsX	-1,93	6,51	5,43E-04	3,28E-02	SALTSv1_1152
rplO	-1,92	7,31	5,32E-05	1,06E-02	SALTSv1_3503
accD	-1,83	6,43	9,44E-04	4,95E-02	SALTSv1_2411
invF	-1,81	6,64	3,11E-04	2,43E-02	SALTSv1_2980
NA	-1,76	8,31	1,16E-04	1,51E-02	SALTSv1_tRNA28
rpoC	-1,76	8,87	2,58E-04	2,18E-02	SALTSv1_4222
NA	-1,75	8,65	8,53E-05	1,30E-02	SALTSv1_tRNA23
cydA	-1,75	7,36	9,67E-05	1,40E-02	SALTSv1_0737
pitA	-1,74	6,70	2,66E-04	2,18E-02	SALTSv1_3673
rpoA	-1,74	8,47	4,89E-05	1,02E-02	SALTSv1_3498
yaeT	-1,73	7,61	1,02E-05	4,09E-03	SALTSv1_0228
NA	-1,72	6,87	7,63E-04	4,17E-02	SALTSv1_miscRNA128
recA	-1,72	7,76	3,48E-04	2,55E-02	SALTSv1_2908
eno	-1,70	8,35	4,17E-04	2,88E-02	SALTSv1_3035
NA	-1,68	8,60	4,94E-04	3,10E-02	SALTSv1_tRNA62
lysS	-1,67	6,92	7,50E-04	4,14E-02	SALTSv1_3123
sspB	-1,67	6,55	5,28E-04	3,26E-02	SALTSv1_3428
pflB	-1,66	8,65	3,13E-04	2,43E-02	SALTSv1_0928
NA	-1,64	11,04	4,77E-04	3,06E-02	SALTSv1_miscRNA229
hybA	-1,64	7,80	3,41E-05	7,70E-03	SALTSv1_3236
tufB	-1,63	8,61	4,18E-05	9,05E-03	SALTSv1_3527
rpsB	-1,62	8,40	9,32E-05	1,38E-02	SALTSv1_0220
pta	-1,60	7,14	4,44E-04	2,96E-02	SALTSv1_2382
secA	-1,54	7,40	1,82E-04	1,93E-02	SALTSv1_0137
fusA	-1,52	8,97	1,28E-04	1,55E-02	SALTSv1_3528
tufB	-1,51	8,13	1,22E-06	1,27E-03	SALTSv1_4214
rplA	-1,51	8,59	5,90E-06	2,79E-03	SALTSv1_4218

Annotation	logFC	logCPM	p-Value	FDR	genes
rplE	-1,50	8,04	2,21E-04	2,09E-02	SALTSv1_3510
sspA	-1,50	7,77	1,46E-04	1,69E-02	SALTSv1_3429
cpxP	-1,48	10,70	3,13E-06	2,50E-03	SALTSv1_4138
rimM	-1,47	7,86	5,59E-05	1,07E-02	SALTSv1_2739
rplX	-1,45	7,77	2,21E-04	2,09E-02	SALTSv1_3511
rpsD	-1,43	8,08	4,01E-04	2,85E-02	SALTSv1_3499
rplN	-1,43	9,01	7,16E-05	1,20E-02	SALTSv1_3512
rpmA	-1,41	8,15	2,61E-04	2,18E-02	SALTSv1_3390
groL	-1,40	8,67	1,26E-04	1,55E-02	SALTSv1_4402
NA	-1,38	7,13	8,78E-04	4,75E-02	SALTSv1_tRNA60
lexA	-1,37	7,68	2,20E-04	2,09E-02	SALTSv1_4304
rne	-1,37	8,03	1,03E-04	1,41E-02	SALTSv1_1145
rpsA	-1,37	9,63	5,91E-06	2,79E-03	SALTSv1_0936
ftsH	-1,31	8,49	1,32E-05	4,90E-03	SALTSv1_3383
secY	-1,31	9,65	9,24E-04	4,90E-02	SALTSv1_3502
tig	-1,28	7,83	2,11E-04	2,09E-02	SALTSv1_0451
rpoB	-1,27	8,40	2,01E-04	2,05E-02	SALTSv1_4221
rpoH	-1,19	9,25	4,45E-04	2,96E-02	SALTSv1_3652
rplL	-0,95	8,88	5,35E-04	3,27E-02	SALTSv1_4220
sulII	-0,94	8,92	2,37E-04	2,11E-02	SALTSv1_p30001
NA	0,97	12,18	1,14E-04	1,51E-02	SALTSv1_16s_rRNA_2
malS	2,67	5,22	5,54E-04	3,30E-02	SALTSv1_3750

NA, not annotated; logFC, log2-transformed fold change; logCPM, average log-transformed counts per million reads; P-values were adjusted using the FalseDiscoveryRate method.

4.3 Nitrate drives expression of SPI1-T3SS *in vitro*, but is negligible for protection from colitis by *M. schaedleri in vivo*

4.3.1 Expression of SPI1-T3SS is elevated with nitrate under anaerobic conditions in an *in vitro* assay

Taken together the above mentioned results, we found that *M. schaedleri* does not compete for nitrate with *S.* Tm to promote a growth advantage. However, we hypothesized that depletion of nitrate by *M.schaedleri* by DNRA could influence expression of the SPI1-T3SS of *S.* Tm.

To test this, we first analyzed the effect of NO_3 on *S.* Tm SPI1-T3SS expression. For this we used luciferase reporter strains harboring the firefly luciferase fused to the *sicA* promoter (*S.* Tm$^{sicA\text{-}luc}$) (Häberli, 2005). In *S.* Tm$^{sicA\text{-}luc}$, light emission can be correlated with SPI1-T3SS expression. The plasmid was inserted into the *pagC* locus of the chromosome of *S.* Tm^{wt} (Häberli, 2005). By P22 transduction, the construct was transferred in recipient strains *S.* Tm^{avir} and *S.* Tm$^{avir\Delta nr3}$. Culturing the reporter strains under aerobic conditions in LB, LB supplemented with 0.3 M NaCl or different concentrations of $NaNO_3$ did not have any effect on SPI1-T3SS expression (Fig. 11A). Under microaerophilic conditions (0.8 % O_2) with high salt (0.3 M NaCl), SPI1-T3SS was significantly increased to app. 3-fold in the *S.* Tm^{avir} and *S.* Tm$^{avir\Delta nr3}$ reporter (*$p < 0.05$ One-way ANOVA with Tukey's multiple comparison test) and slightly elevated in *S.* Tm^{wt}, which was expected as high salt and low oxygen levels have been described as SPI-1 inducing (Bajaj *et al.*, 1996). No upregulation was observed when different concentrations of $NaNO_3$ were supplemented (Fig. 11A). When bacteria were cultured under anaerobic conditions we saw a strong induction (5 - 6 fold) of SPI1-T3SS in *S.* Tm^{wt} and *S.* Tm^{avir} with 10 mM and 40 mM $NaNO_3$ (***$p < 0.001$ One-way ANOVA with Tukey's multiple comparison test). This effect was absent in the nitrate reductase triple mutant *S.* Tm$^{avir\Delta nr3}$ and was not seen with lower nitrate concentrations (1 mM), as $NaNO_3$ is probably rapidly consumed by *S.* Tm under anaerobic conditions. No induction in either strain was observed with 0.3 M NaCl under anaerobic conditions. This experiment revealed, that nitrate can lead to increased SPI1-T3SS expression *in vitro* but only under anaerobic conditions.

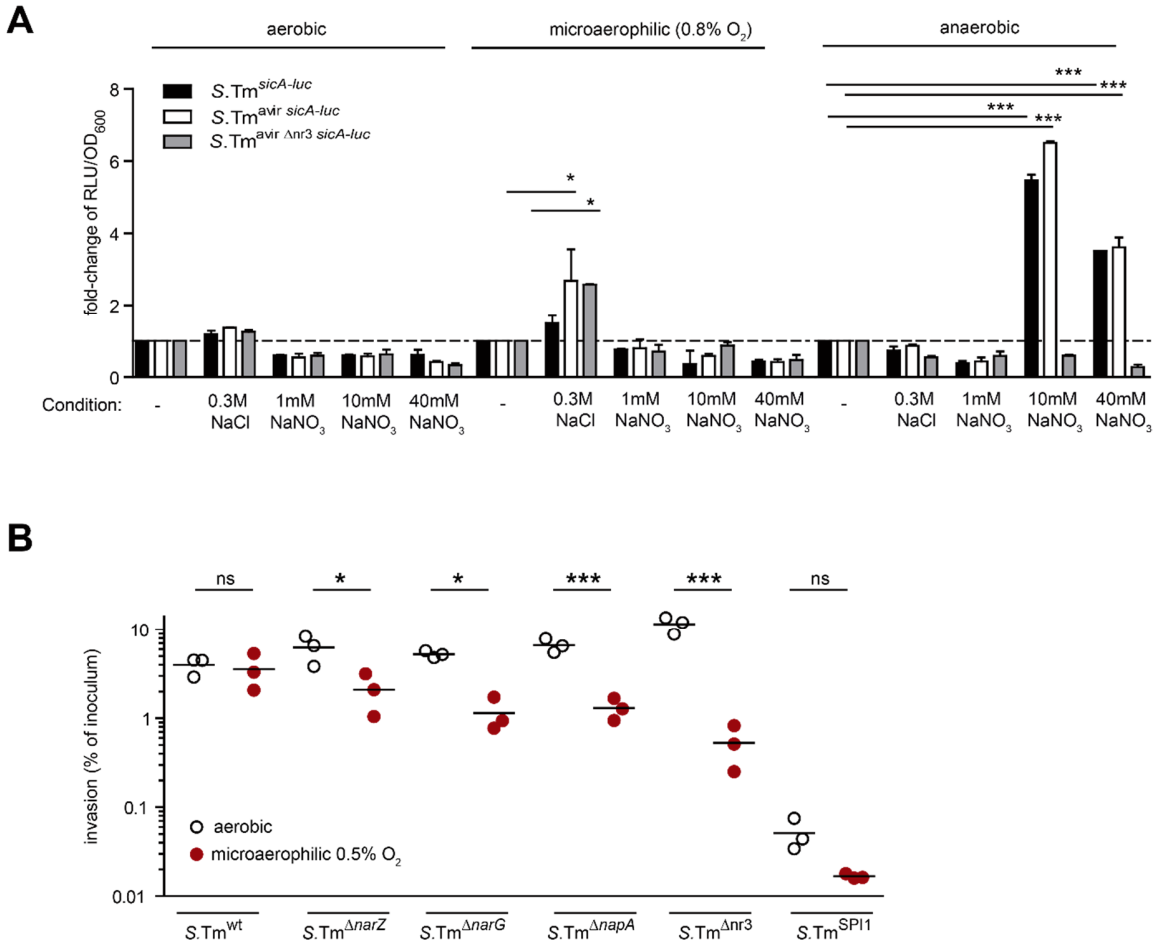

Fig. 11: The ability of nitrate respiration enhances SPI1-T3SS expression and is important for *S.* Tm to invade epithelial cells. A) Luciferase activity was measured in cell extracts of indicated *S.* Tm reporter strains grown for 4 h under aerobic, microaerophilic (0.8 % O_2) and anaerobic conditions in LB media with indicated supplements and normalized to OD_{600}. Graph shows the fold-change to cultures grown in plain LB under the indicated oxygen concentration; each bar shows the mean of two cultures and the SEM. The experiment was repeated three times and one representative experiment is displayed. One-way ANOVA with Tukey's multiple comparison test; ns, no significant difference $p \geq 0.05$; *$p < 0.05$, **$p < 0.01$, ***$p < 0.001$ **B)** Invasion of indicated *S.* Tm strains under aerobic or microaerophilic conditions in the presence of 10 mM KNO_3 into HuTu80 cells. Experiment was repeated three times (Stefanie Walter, RKI Wernigerode), each dot represents one experiment. One-way ANOVA with Tukey's multiple comparison test; ns, no significant difference $p \geq 0.05$, *$p < 0.05$, **$p < 0.01$, ***$p < 0.001$. bar: mean.

4.3.2 *S.* Tm$^{\Delta nr3}$ shows reduced invasion of HuTu80 cells under anaerobic conditions

To further investigate if nitrate respiration plays a role for invasion, we performed invasion assays in cooperation with the Robert Koch Institute in Wernigerode (Stefanie Walter). *S.* Tm^{wt} as positive control, *S.* Tm$^{\Delta narZ}$, *S.* Tm$^{\Delta narG}$, *S.* Tm$^{\Delta napA}$, the triple mutant *S.* Tm$^{\Delta nr3}$ and a SPI-1 mutant, *S.*Tm^{SPI1}, as a negative control, which is unable to invade epithelial cells, were cultured under aerobic and microaerophilic (0.5 % O_2) conditions in the presence of 10 mM $NaNO_3$ in LB. Invasion of the single nitrate reductase mutants and the triple mutant into HuTu80 cells was determined by invasion assay (3.2.9). We observed, that *S.* Tm^{wt} invades epithelial cells at the same efficiency and *S.* Tm ^{SPI1} is unable to invade under both aerobic and microaerophilic conditions ($p > 0.05$ unpaired t test; Fig. 11B). On the other hand, the single mutants *S.* Tm$^{\Delta narZ}$, *S.* Tm$^{\Delta narG}$ and *S.* Tm$^{\Delta napA}$ show decreased invasion under anaerobic condition and the triple mutant *S.* Tm$^{\Delta nr3}$ is even more inhibited (*$p < 0.05$; *$p < 0.05$; ***$p < 0.001$ and ***$p<0.001$ respectively, One-way ANOVA with Tukey's multiple comparison test). From this we conclude that under microaerophilic conditions, nitrate respiration is vital to induce the full invasive capacity of *S.* Tm.

4.3.3 *S.*Tm$^{\Delta nr3}$ shows reduced colonization in *M. schaedleri* pre-colonized OligoMM^{12} mice

With respect to the previous results, genome based predictions for DNRA in *M. schaedleri* and verification *in vitro* (Loy *et al.*, 2017) (Fig. 2), we hypothesized that *M. schaedleri*, localized close to the epithelial border (Fig. 5B & D), can limit the available nitrate in the mucus layer. This may then lead to reduced expression of *S.* Tm SPI1-T3SS and ultimately inflammation. Therefore, we designed the following experiment: if this hypothesis was true, a nitrate respiration defective *S.* Tm strain (*S.* Tm$^{\Delta nr3}$) would be attenuated in control mice and exhibit the same level of inflammation as *M. schaedleri* colonized mice. Therefore, we infected OligoMM^{12} mice colonized with *M. schaedleri* or control with the nitrate reductase triple mutant *S.* Tm$^{\Delta nr3}$ in wild type background. This time we found that *S.* Tm$^{\Delta nr3}$ has a slight but not significant growth disadvantage ($p > 0.05$ One-way ANOVA Kruskal-Wallis test with Dunn's multiple comparison test compare selected pairs) in mice pre-colonized with *M. schaedleri* compared to control mice on day 1 p.i. as well as on day 4 p.i. in feces and

cecum (Fig. 12B). Moreover, we observed a reduced inflammation in *M. schaedleri* colonized mice evaluated by cecal histology day 4 p.i. (Fig. 12F) (*$p < 0.05$ Mann–Whitney U test) and lipocalin-2 levels (Fig. 12G) in feces and cecum day 4 p.i. (*$p < 0.05$ and **$p < 0.01$ respectively; One-way ANOVA Kruskal-Wallis test with Dunn's multiple comparison test compare selected pairs). No difference was seen in the colonization of mesenteric lymph nodes (Fig. 12C), spleen (Fig. 12D), and liver (Fig. 12E) ($p > 0.05$ Mann–Whitney U test). Overall this experiment yielded inconclusive data. The protective effect may either indeed be independent of nitrate or, on the other hand, decreased inflammation could be also due to reduced colonization levels of *S.* Tm in mice pre-colonized with *M. schaedleri*. Therefore we performed an additional experiment in streptomycin treated OligoMM^{12} mice which lack colonization resistance and therefore should exhibit equal colonization of *S.* Tm in both groups.

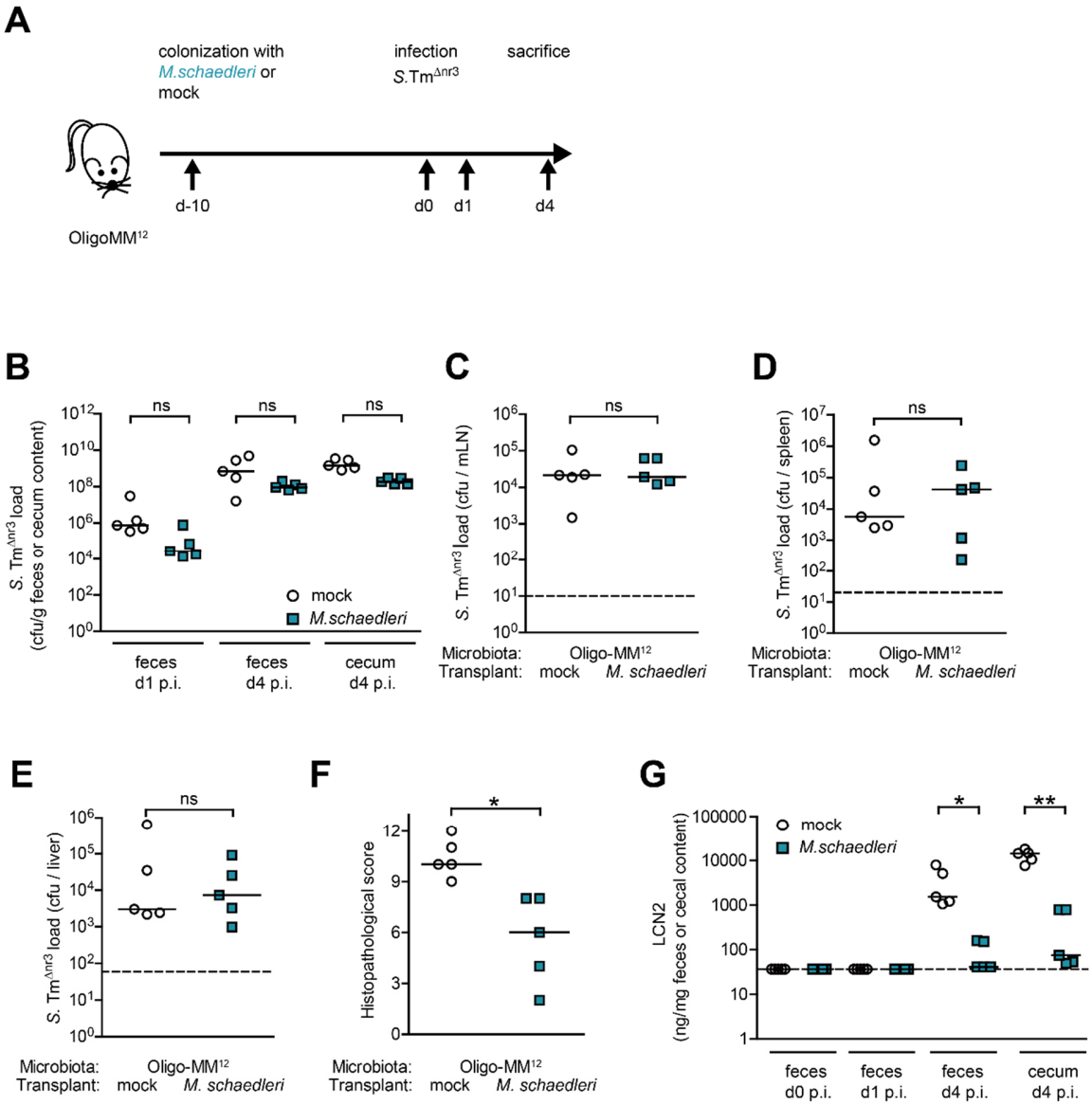

Fig. 12: *S.* Tm$^{\Delta nr3}$ colonization is reduced in *M. schaedleri* pre-colonized OligoMM^{12} mice. A) Experimental set up. OligoMM^{12} mice were pre-colonized for 10 days with *M. schaedleri* or control media before infection with 10^7 cfu of *S.* Tm$^{\Delta nr3}$ and sacrificed four days post infection. **B)** *S.* Tm loads in feces and cecal content over time of infection quantified by selective plating. *S.* Tm loads in **C)** mesenteric lymph nodes, **D)** spleen and **E)** liver at day 4 p.i.. **F)** Histopathological score of cecal tissue on day 4 p.i. stained with hematoxylin and eosin. The degree of submucosal edema, neutrophil infiltration, loss of goblet cells and epithelial damage was scored in a double-blinded manner. 0-3: no pathological changes; 4-7: moderate inflammation; above 8: severe inflammation. **G)** Lipocalin-2 levels of feces and cecal content were measured by quantitative ELISA. Dashed line: detection limit. Mann–Whitney U test; B) & G) One-way ANOVA Kruskal-Wallis test with Dunn's multiple comparison test compare selected pairs (mock vs. *M. schaedleri*); ns, no significant difference $p \geq 0.05$, *$p < 0.05$, **$p < 0.01$, ***$p < 0.001$.

4.3.4 Anaerobic electron acceptors are negligible for protection from *S.* Tm induced colitis by *M. schaedleri*

OligoMM^{12} mice were pre-colonized with *M. schaedleri* or control media and treated with a single dose of streptomycin one day prior infection with *S.* Tm$^{\Delta nr3}$ or *S.* Tm^{wt}. Equal colonization of both strains was observed at day 1 p. i. and day 2 p. i. in feces and cecal content irrespective of *M. schaedleri* (Fig. 13B). Mesenteric lymph nodes and spleen showed as well no differences in *S.* Tm loads (Fig. 13C & D). In contrast, the liver exhibited increased *S.* Tm^{wt} loads in *M. schaedleri* colonized mice (Fig. 13E) (*p < 0.05 One-way ANOVA Kruskal-Wallis test with Dunn's multiple comparison test to compare selected pairs) and also to some extend for *S.* Tm$^{\Delta nr3}$ (Fig. 13E). The histopathological score of cecal tissue on day 2 p.i. is clearly but not significantly lower in streptomycin treated mice pre-colonized with *M.schaedleri* and infected with either *S.* Tm$^{\Delta nr3}$ or *S.* Tm^{wt} (Fig. 13F) (p > 0.05 One-way ANOVA Kruskal-Wallis test with Dunn's multiple comparison test to compare selected pairs). Further, lipocalin-2 was measured over time in fecal pellets and cecal content (Fig. 13G). Mice pre-colonized with *M. schaedleri* exhibited reduced, but not significant, lipocalin-2 levels during *S.* Tm$^{\Delta nr3}$ or *S.* Tm^{wt} infection compared to control group (Fig. 13G) (p > 0.05 One-way ANOVA Kruskal-Wallis test with Dunn's multiple comparison test to compare selected pairs). With *S.* Tm^{wt} we see a 20 fold increase of lipocalin-2 in feces of control mice at day 1 p.i. which is still present in feces at day 2 p.i. but is slightly decreased in cecum at day 2 p.i. (10 fold) compared to mice associated with *M. schaedleri*. Regarding *S.* Tm$^{\Delta nr3}$ infected mice, we see a reduction in lipocalin-2 levels of app. 100 fold in feces of *M. schaedleri* pre-colonized mice at day 2 p.i. which is slightly reduced in cecum (app. 50 fold) compared to control mice.

Besides genes for DNRA, genome analysis of *M. schaedleri* ASF457 also predicted further genes involved in anaerobic respiration like a reductase system with homology to dimethyl sulfoxide (DMSO) reductase, a tetrathionate reductase and trimethylamine-N-oxide (TMAO) reductase (Loy *et al.*, 2017). The alternative electron acceptors DMSO, TMAO, tetrathionate and nitrate can also be utilized by *S.*Tm (Harel *et al.*, 2016) and are important for growth in the inflamed gut (Winter, Lopez*, et al.*, 2013). One common feature of these reductases is that they all contain a molybdopterin co-factor (Hille, 1996). By deleting *moaA,* a crucial gene in molybdopterin biosynthesis (Mehta *et al.*, 2014), anaerobic respiration is disabled in

Enterobacteriaceae (Winter, Winter*, et al.*, 2013). Besides *S.* Tm$^{\Delta nr3}$ and *S.* Tm^{wt} (as control) we additionally infected mice with *S.* Tm$^{\Delta moaA}$*.* After treatment with streptomycin, all mice (control and pre-colonized with *M. schaedleri*) show equal colonization of *S.* Tm$^{\Delta moaA}$ at all time points (feces day 1 p.i.; feces and cecum day 2 p.i.) ($p > 0.05$ One-way ANOVA Kruskal-Wallis test with Dunn's multiple comparison test) (Fig. 13B). Also no difference in colonization of mesenteric lymph nodes (Fig. 13C) and spleen was seen (Fig. 13D) ($p > 0.05$ One-way ANOVA Kruskal-Wallis test with Dunn's multiple comparison test compare selected pairs). Histopathology score at day 2 p.i. show reduced inflammation in mice pre-colonized with *M. schaedleri* and infected with *S.* Tm$^{\Delta moaA}$ compared to control mice (Fig. 13F). Though, the differences are not significant ($p > 0.05$ One-way ANOVA Kruskal-Wallis test with Dunn's multiple comparison test to compare selected pairs). Still, the protective effect is present in mice associated with *M. schaedleri*. We also monitored the lipocalin-2 levels (Fig. 13G) on day 1 and day 2 p.i.. Even though statistical analysis does not yield significant differences ($p > 0.05$ One-way ANOVA Kruskal-Wallis test with Dunn's multiple comparison test compare selected pairs) we can clearly see protection from colitis with *M. schaedleri* in the infection with *S.* Tm$^{\Delta moaA}$*.* Lipocalin-2 is decreased in mice colonized with *M. schaedleri* and infected with *S.*Tm$^{\Delta moaA}$ around 70 fold in feces day 1 p.i., 8 fold and 20 fold in feces and cecum day 2 p.i., respectively. Overall, this experiment shows that nitrate respiration and also the utilization of other sources for anaerobic respiration by *S*. Tm are likely not involved *in vivo* in *M. schaedleri* dependent reduction of *S*.Tm SPI1-T3SS expression.

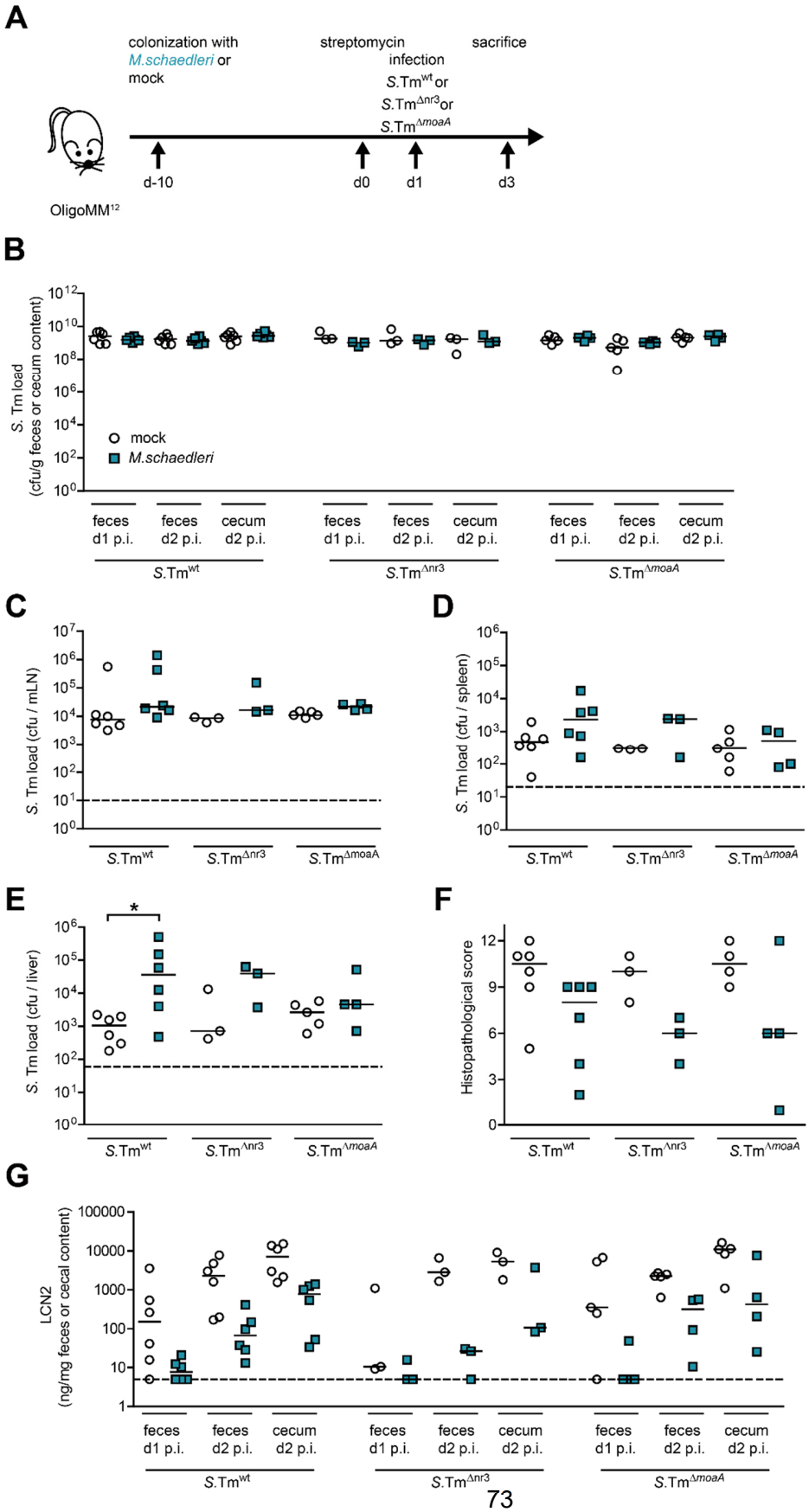
A
colonization with
M.schaedleri or
mock
streptomycin
infection
sacrifice
S.Tm^wt or
S.Tm^Δnr3 or
S.Tm^ΔmoaA
d-10
d0
d1
d3
OligoMM12
B
S. Tm load
(cfu/g feces or cecum content)
mock
M.schaedleri
feces d1 p.i.
feces d2 p.i.
cecum d2 p.i.
S.Tm^wt
S.Tm^Δnr3
S.Tm^ΔmoaA
C
S. Tm load (cfu / mLN)
D
S. Tm load (cfu / spleen)
E
S. Tm load (cfu / liver)
*
F
Histopathological score
G
LCN2
(ng/mg feces or cecal content)

Fig. 13: Competition for anaerobic electron acceptors is not responsible for protection from *S.* Tm colitis by *M. schaedleri*. A) Experimental set up. OligoMM^{12} mice were pre-colonized for 10 days with *M. schaedleri* or control media. Mice were treated with 25 mg streptomycin by oral gavage one day before infection with 10^7 cfu of *S.* Tm^{wt}, *S.* Tm$^{\Delta nr3}$ or *S.* Tm$^{\Delta moaA}$ and were sacrificed two days post infection. **B)** *S.* Tm loads in feces and cecal content were quantified by selective plating over time. *S.* Tm loads in **C)** mesenteric lymph nodes, **D)** spleen and **E)** liver were quantified at day 4 p.i.. **F)** Histopathological score of cecal tissue on day 4 p.i. stained with hematoxylin and eosin. The degree of submucosal edema, neutrophil infiltration, loss of goblet cells and epithelial damage was scored in a double-blinded manner. 0-3: no pathological changes; 4-7: moderate inflammation; above 8: severe inflammation. **G)** Lipocalin-2 levels of feces and cecal content were measured by quantitative ELISA. Dashed line: detection limit. One-way ANOVA Kruskal-Wallis test with Dunn's multiple comparison test compare selected pairs (mock vs. *M. schaedleri*); ns, no significant difference $p \geq 0.05$; *$p < 0.05$, **$p < 0.01$, ***$p < 0.001$.

4.4 Does *M. schaedleri* have a protective effect against *S.* Tm in a gnotobiotic *Agr2*$^{-/-}$/*Agr2*$^{+/-}$ mouse model?

4.4.1 *M. schaedleri* colonizes the cecum of mucus deficient *Agr2*$^{-/-}$ mice

Previous research in our lab by Dr. Sandrine Brugiroux showed that conventional streptomycin treated *Agr2*$^{-/-}$ mice (colonized with a complex microbiota) are protected from *S.* Tm colitis compared to *Agr2*$^{+/-}$ mice or ampicillin treated *Agr2*$^{-/-}$/*Agr2*$^{+/-}$ mice (Fig. 4A). Microbiome analysis showed that the abundance of *Deferribacteres* (*M. schaedleri*) was increased in these protected mice (Fig. 4B) (Brugiroux, 2016). To investigate if this protective effect is dependent on the *Agr2*$^{-/-}$ genotype we generated gnotobiotic *Agr2*$^{-/-}$ mice colonized with the defined OligoMM^{12} microbiota (Beutler, 2016). OligoMM^{12} associated *Agr2*$^{-/-}$ and *Agr2*$^{+/-}$ mice were colonized with *M. schaedleri* or control media for 10 days. By FISH analysis (Fig. 14A) we could localize *M. schaedleri* in the cecum of OligoMM^{12} *Agr2*$^{+/-}$ and OligoMM^{12} *Agr2*$^{-/-}$ mice. Interestingly, the latter does not harbor an intact mucus layer, stating that *M. schaedleri* does not require mucus for successful colonization. OligoMM^{12} composition of these mice was analyzed by quantitative PCR assay (3.2.12) (Fig. 14B). *M. schaedleri* was detected in the colonized groups but not in control mice. To get a closer look on differences between the microbiota of OligoMM^{12} *Agr2*$^{-/-}$, *Agr2*$^{+/-}$ with and without *M. schaedleri,* cluster analysis (based on Bray-Curtis distance matrices) was performed. OligoMM^{12} *Agr2*$^{-/-}$ mice colonized with *M. schaedleri* show a distinct microbiota composition compared to all other three groups (Fig. 15A; according to Adonis ***$p < 0.001$ with 35.7 % of variation explained). Only slight differences were found between genotype (*Agr2*$^{-/-}$ vs. *Agr2*$^{+/-}$ Fig. 15B; according to Adonis *$p < 0.024$ with 13.5 % of variation explained) and between colonization (*M. schaedleri* vs. mock Fig. 15C; according to Adonis **$p < 0.004$, with 20.99 % of variation explained).

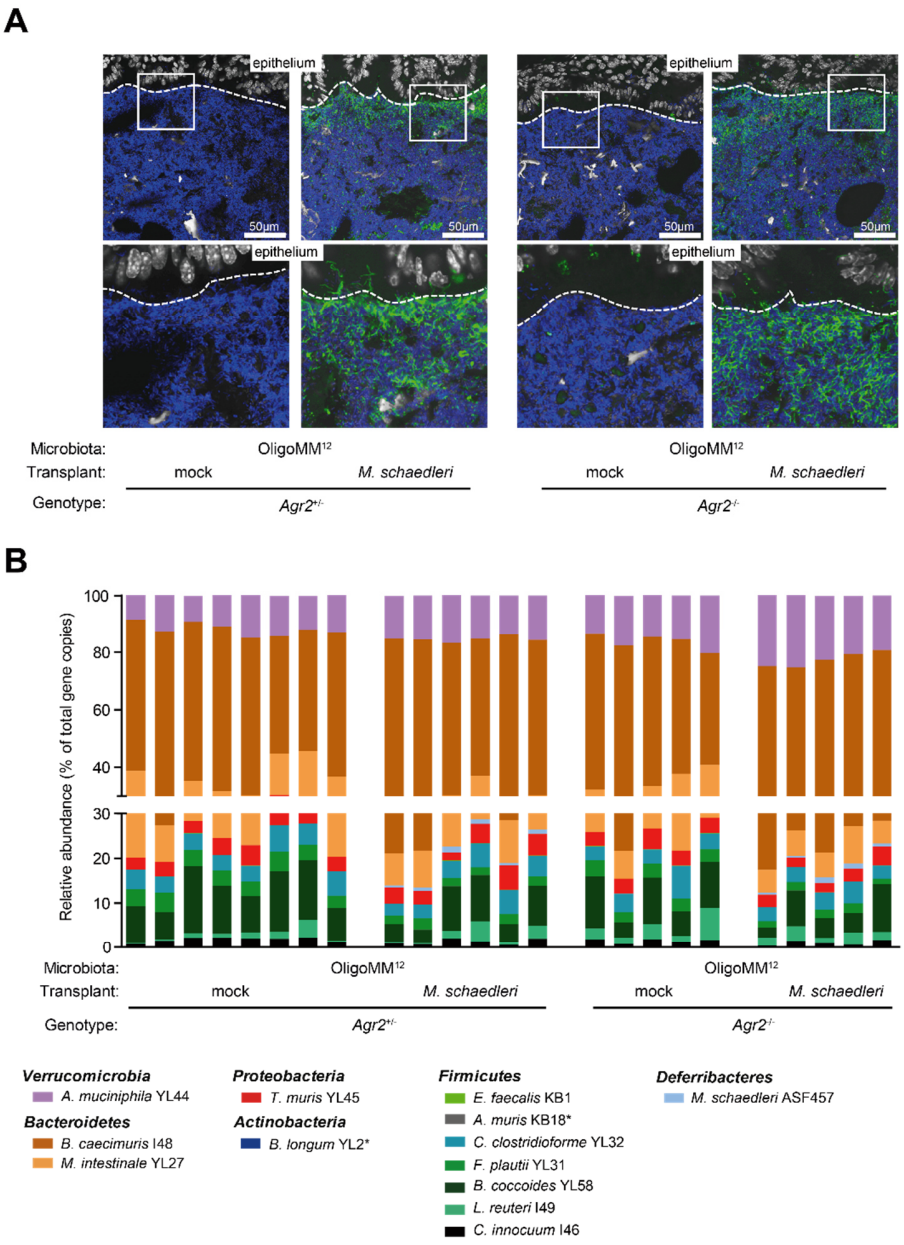

Fig. 14: *M. schaedleri* colonizes in *Agr2*$^{+/-}$ as well as in mucus deficient *Agr2*$^{-/-}$ mice. A) Localization of *M. schaedleri* by FISH analysis in PFA fixed cecum of *Agr2*$^{+/-}$ and *Agr2*$^{-/-}$ mice pre-colonized with *M. schaedleri* or control for 10 days. grey, DAPI; blue, all bacteria (eub338 I:III probe); green, *M. schaedleri* (msc487_correct probe), scale bar 50 µm. White squares indicate enlarged area. Dashed line indicates epithelial border. **B)** Microbiota composition of cecal content from *Agr2*$^{+/-}$ and *Agr2*$^{-/-}$ mice with *M. schaedleri* or control. Shown is the relative abundance of each individual strain (% of all 16S rRNA gene copies). Each bar represents one mouse. * below detection limit.

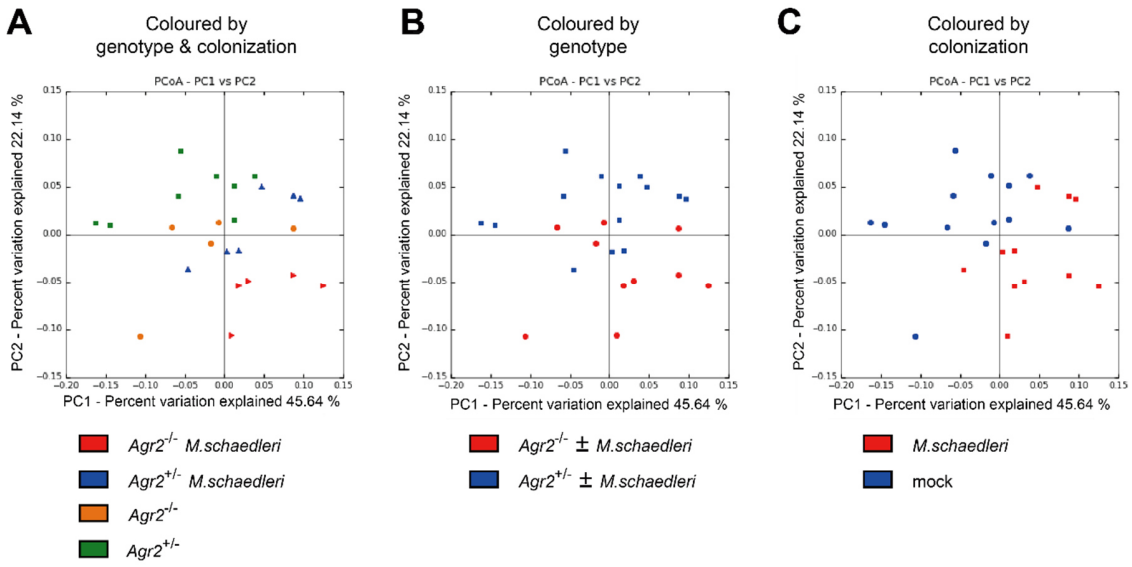

Fig. 15: Cluster analysis of OligoMM^{12} *Agr2*$^{-/-}$ and *Agr2*$^{+/-}$ mice pre-colonized with *M. schaedleri* or control. Cluster analysis is based on Bray-Curtis distance matrices and visualized as PCoA plots. **A)** 2D PCoA plot of cecal microbiota from OligoMM^{12} *Agr2*$^{-/-}$ and *Agr2*$^{+/-}$ mice pre-colonized with *M. schaedleri* or control for 10 days colored by genotype & colonization (*M. schaedleri* or control); significant for Bray-Curtis (***p < 0.001, Adonis) with 35.7 % of variation explained. **B)** Coloring by genotype (*Agr2*$^{-/-}$ vs. *Agr2*$^{+/-}$); significant for Bray-Curtis (*p < 0.024, Adonis) with 13.5 % of variation explained or **C)** colonization (*M. schaedleri* vs. mock); significant for Bray-Curtis (**p < 0.004, Adonis) with 20.99 % of variation explained.

4.4.2 Protection from *S.* Tm induced colitis by *M. schaedleri* is independent of the *Agr2* genotype

First we analyzed in uninfected mice (Fig. 14) if OligoMM^{12} *Agr2*$^{-/-}$ mice showed already signs of inflammation in cecal tissue before infection. We observed no pathological changes (Fig. 16F) and no increased lipocalin-2 levels (Fig. 16G). Therefore, OligoMM^{12} *Agr2*$^{-/-}$ and *Agr2*$^{+/-}$ littermates were colonized with *M. schaedleri* or control media for 10 days and subsequently infected with wildtype *S.*Tm. Fecal colonization of *S.* Tm was slightly but not significantly elevated (app. 2 $\log_{10}$ levels) at day 1 p.i. in *Agr2*$^{-/-}$ mice with and without *M. schaedleri* compared to *Agr2*$^{+/-}$ control groups; this difference was absent at day 3 p.i. ($p > 0.05$ One-way ANOVA Kruskal-Wallis test with Dunn's multiple comparison test compare selected pairs; Fig. 16B). No difference was seen in colonization of mesenteric lymph nodes (Fig. 16C), spleen (Fig. 16D) and liver (Fig. 16E) ($p > 0.05$ One-way ANOVA Kruskal-Wallis test with Dunn's multiple comparison test compare selected pairs). *S.* Tm infected *Agr2*$^{+/-}$ mice colonized with *M. schaedleri* show a significantly reduced cecal histopathological score (Fig. 16F) and significantly reduced lipocalin-2 levels (Fig. 16G) (**$p < 0.01$ One-way ANOVA Kruskal-Wallis test with Dunn's multiple comparison test compare selected pairs) 3 days p.i.. In the same way, *Agr2*$^{-/-}$ mice colonized with *M. schaedleri* show a reduced histopathological score (Fig. 16F) and decreased lipocalin-2 levels (Fig. 16G) ($p > 0.05$ One-way ANOVA Kruskal-Wallis test with Dunn's multiple comparison test compare selected pairs). We conclude that *M. schaedleri* protects both OligoMM^{12} *Agr2*$^{-/-}$ and *Agr2*$^{+/-}$ mice independent of the genotype in a gnotobiotic setting. Thus we conclude that the protective effect observed in conventional *Agr2*$^{-/-}$ but not *Agr2*$^{+/-}$ mice (Fig. 4A) is probably dependent on other commensal bacteria or due to the treatment with streptomycin. To investigate this further, we conducted a follow-up experiment in OligoMM^{12} *Agr2*$^{-/-}$ and *Agr2*$^{+/-}$ mice with foregoing streptomycin treatment.

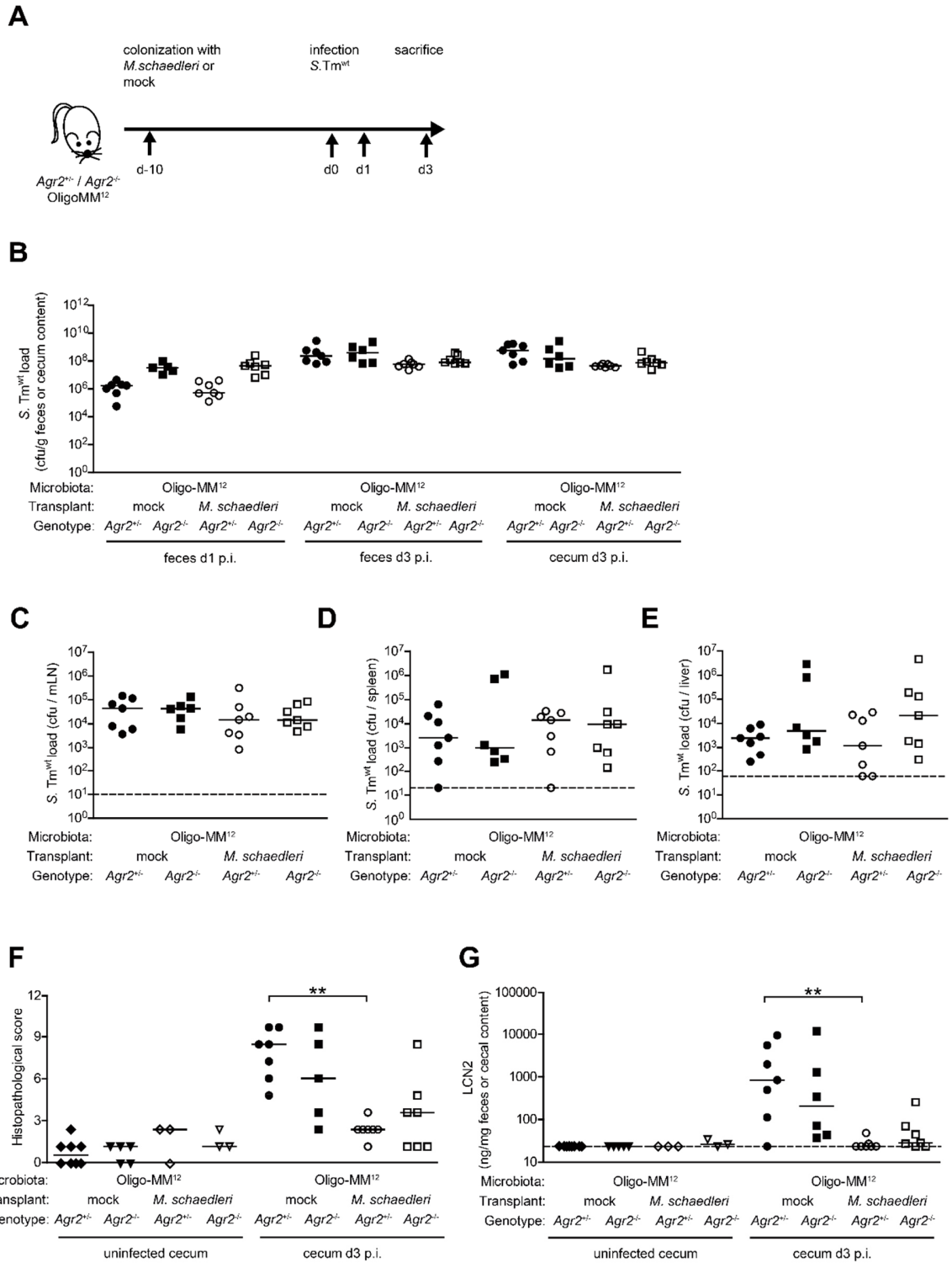

Fig. 16: *M. schaedleri* protects mice independent of the *Agr2* genotype. A) Experimental set up. *Agr2*$^{-/-}$ and *Agr2*$^{+/-}$ associated with the OligoMM^{12} microbiota were pre-colonized for 10 days with *M. schaedleri* or control media before infection with 10^7 cfu of *S.* Tm^{wt} and were sacrificed three days post infection. **B)** *S.* Tm loads in feces and cecal content were quantified over time by plating. *S.* Tm loads in **C)** mesenteric lymph nodes, **D)** spleen and **E)** liver were quantified by plating at day 3 p.i..**F)** Histopathological score of cecal tissue on day 3 p.i.

stained with hematoxylin and eosin. The degree of submucosal edema, neutrophil infiltration and epithelial damage was scored in a double-blinded manner. 0-3: no pathological changes; 4-7: moderate inflammation; above 8: severe inflammation. Pathological score is displayed without loss of goblet cells. **G)** Lipocalin-2 levels of cecal content were measured by quantitative ELISA on day 3 p.i.. Cecal content from uninfected *Agr2*$^{-/-}$ and *Agr2*$^{+/-}$ mice with and without *M. schaedleri* (**Fig. 14**) was used as negative control. Dashed line: detection limit. One dot represents one mouse. One-way ANOVA Kruskal-Wallis test with Dunn's multiple comparison test compare selected pairs (mock *Agr2*$^{+/-}$ vs. *M. schaedleri Agr2*$^{+/-}$/ mock *Agr2*$^{-/-}$ vs. *M. schaedleri Agr2*$^{-/-}$); ns, no significant difference $p \geq 0.05$; *$p < 0.05$, **$p < 0.01$, ***$p < 0.001$. From one *Agr2*$^{-/-}$ control mouse treated with *S.*Tm, histopathological analysis was not possible (F).

4.4.3 *M. schaedleri* protects streptomycin pretreated OligoMM^{12} *Agr2*$^{-/-}$/*Agr2*$^{+/-}$ mice

OligoMM^{12} *Agr2*$^{-/-}$/*Agr2*$^{+/-}$ mice were pre-colonized for 10 days with *M. schaedleri* or control media, treated with streptomycin and infected with *S.* Tm^{wt}. Colonization of *S.* Tm^{wt} in cecum (Fig. 17A), mesenteric lymph nodes (Fig. 17B), spleen (Fig. 17C) and liver (Fig. 17D) was equal between all four groups (*Agr2*$^{+/-}$/*Agr2*$^{-/-}$ +/- *M. schaedleri*) one day p.i.. As in the previous experiment, we see protection from colitis in *Agr2*$^{+/-}$ and *Agr2*$^{-/-}$ mice pre-colonized with *M. schaedleri* compared to control mice, indicated by reduced histopathological score (Fig. 17F) and lipocalin-2 levels (Fig. 17G). Microbiota analysis by a quantitative PCR assay (3.2.12) showed slight microbiota alterations in all groups one day after streptomycin treatment (Fig. 17H). *M. schaedleri* (ASF457) and *B. caecimuris* (I48) are increased in their relative abundances, whereas *M. intestinale* (YL27) and *T. muris* (YL45) are reduced (Fig. 17H). Cluster analysis (based on Bray-Curtis distance matrices) was performed and samples were grouped by genotype & colonization & streptomycin treatment (Fig. 18A; according to Adonis ***$p < 0.001$ with 65.2 % of variation explained), genotype (Fig. 18B), colonization (Fig. 18C) and streptomycin treatment (Fig. 18D) alone. No clear separation was seen for genotype (Fig. 18B according to Adonis *$p = 0.038$ with 13.2 % of variation explained) or colonization (Fig. 18C according to Adonis $p > 0.05$), but clearly all samples show a distinct pattern after streptomycin treatment, independent of their *Agr2* genotype or their colonization with or without *M. schaedleri* (Fig. 18D according to Adonis ***$p < 0.001$ with 38.8 % of variation explained).

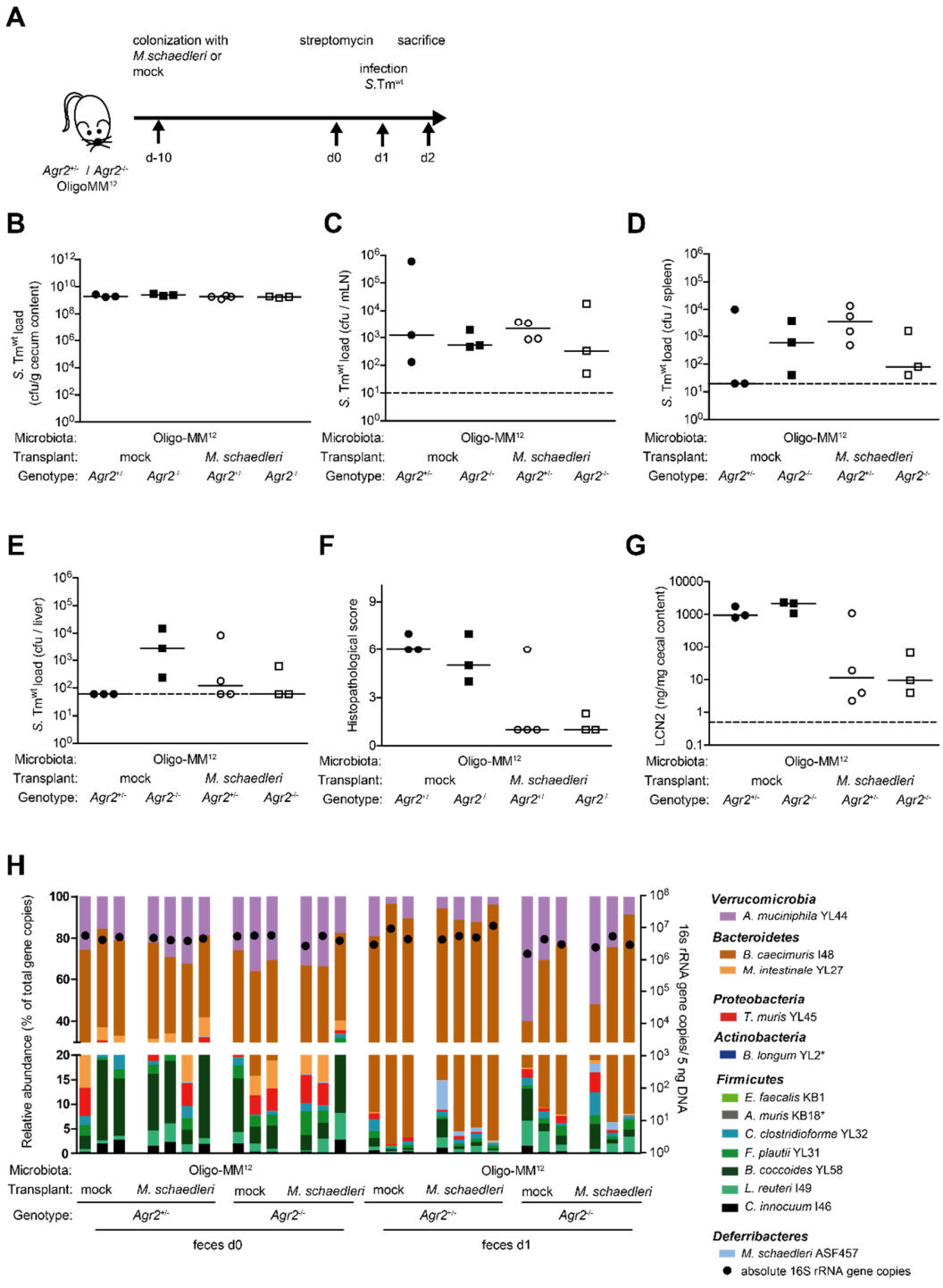

Fig. 17: Streptomycin does not influence protection by *M. schaedleri* in OligoMM^{12} *Agr2*$^{-/-}$/*Agr2*$^{+/-}$ mice. A) Experimental set up. OligoMM^{12} *Agr2*$^{+/-}$ and *Agr2*$^{-/-}$ mice were pre-colonized for 10 days with *M. schaedleri* or control media. Mice were treated with 25 mg streptomycin by oral gavage one day before infection with 10^7 cfu of *S.* Tm^{wt} and were sacrificed one day post infection. **B)** *S.* Tm loads in cecal content, **C)** mesenteric lymph nodes, **D)** spleen and **E)** liver were quantified by plating day 1 p.i.. **F)** Histopathological score of cecal tissue on day 1 p.i. stained with hematoxylin and eosin. The degree of submucosal edema, neutrophil infiltration and epithelial damage was scored in a double-blinded manner. 0-3: no pathological changes; 4-7: moderate

inflammation; above 8: severe inflammation. Pathological score is displayed without loss of goblet cells. **G)** Lipocalin-2 levels in cecal content were measured by quantitative ELISA day 1 p.i.. Dashed line: detection limit. One dot represents one mouse. One-way ANOVA Kruskal-Wallis test with Dunn's multiple comparison test compare selected pairs (mock *Agr2*$^{+/-}$ vs. *M. schaedleri Agr2*$^{+/-}$ / mock *Agr2*$^{-/-}$ vs. *M. schaedleri Agr2*$^{-/-}$); ns, no significant difference $p \geq 0.05$, *$p < 0.05$, **$p < 0.01$, ***$p < 0.001$. **H)** Microbiota composition of feces from *Agr2*$^{+/-}$ and *Agr2*$^{-/-}$ mice with *M. schaedleri* or control before and one day post streptomycin treatment. Shown is the relative abundance of each individual strain (% of all 16S rRNA gene copies). Each bar represents one mouse. On the right axis, black dots show the absolute number of 16S rRNA gene copies per 5 ng DNA quantified by a universal primer/probe combination.

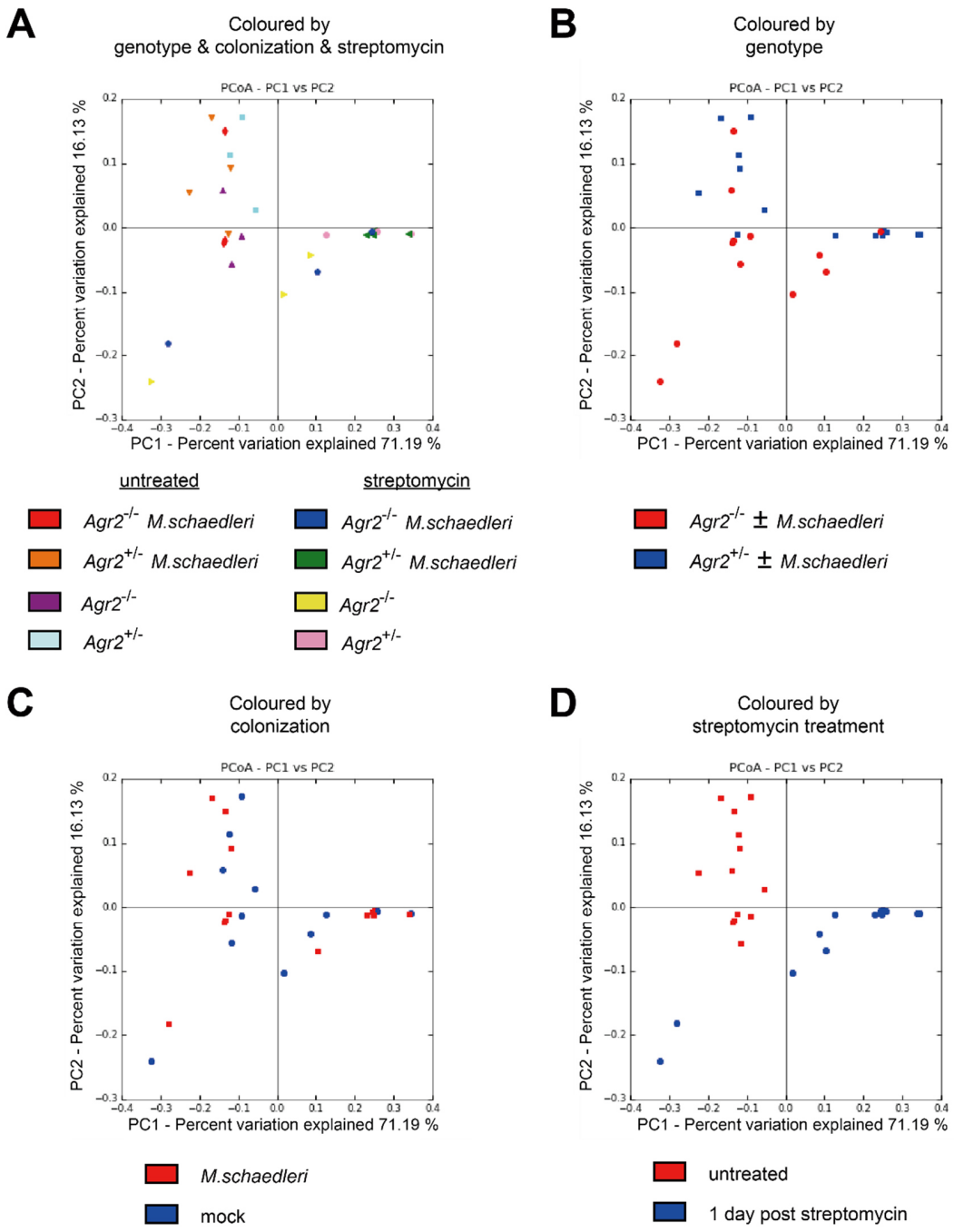

Fig. 18: Cluster analysis of streptomycin pretreated OligoMM^{12} *Agr2*$^{-/-}$ and *Agr2*$^{+/-}$ mice pre-colonized with *M. schaedleri* or control. Cluster analysis is based on Bray Curtis distance matrices and visualized as PCoA plots. **A)** 2D PCoA plot of fecal microbiota from OligoMM^{12} *Agr2*$^{-/-}$ and *Agr2*$^{+/-}$ mice pre-colonized with *M. schaedleri* or control for 10 days colored by genotype & colonization (*M. schaedleri* or control) & streptomycin treatment; significant for Bray Curtis (***$p < 0.001$, Adonis) with 65.2 % of variation explained. **B)** Coloring by genotype (*Agr2*$^{-/-}$ vs. *Agr2*$^{+/-}$); significant for Bray Curtis (*$p < 0.038$, Adonis) with 13.2 % of variation explained or **C)** colonization (*M. schaedleri* vs. mock); not significant for Bray Curtis ($p > 0.05$, Adonis) and **D)** streptomycin treatment (untreated vs. streptomycin); significant for Bray Curtis (***$p < 0.001$, Adonis) with 38.8 % of variation explained.

4.5 Influence of *M. schaedleri* on gut metabolites and pathogenicity of *C. rodentium*

4.5.1 *M. schaedleri* does not protect mice from *C. rodentium* induced intestinal inflammation and colonization

We asked whether the protective effect of *M. schaedleri* is unique to *S.* Tm infection or also applies to other pathogens. Therefore we chose *C. rodentium,* a common mouse pathogen and model for human Enteropathogenic *Escherichia coli* (EPEC) infection, to study the effect of *M. schaedleri* on colonization and colon hyperplasia in the OligoMM^{12} model. In SPF mice, *C. rodentium* induces a self-limiting disease with peak colonization at day 7 p.i. which resolves after approximately 20 days p.i.(Wiles *et al.*, 2004). Previous experiments in OligoMM^{12} mice showed, that *C. rodentium* was still detectable after 42 days of infection at 10^7 cfu/g (Beutler, 2016). We infected OligoMM^{12} mice pre-colonized with *M.schaedleri* or control for 10 days with 10^8 cfu *C. rodentium* DBS100. *C. rodentium* loads in the feces increased to mean $4*10^7$ cfu / g within 4 - 7 days and remained high for the entire duration of the experiment. *M. schaedleri* did not reduce colonization of *C. rodentium* in the feces of infected mice at the beginning nor did it facilitate clearance of the pathogen (Fig. 19B) as seen by high levels of colonization of 10^7 cfu / g until day 30 p.i. (data up to day 23 is shown as there were no further changes of *C. rodentium* loads). Furthermore, in OligoMM^{12} mice *C. rodentium* only elicits a mild inflammation, as determined by fecal lipocalin-2, starting at day 8 p.i., reaching its maximum from day 10 - 15 p.i., and then decreasing steadily until day 23 p.i. when no lipocalin-2 was detectable in the feces (Fig. 19C). No difference in lipocalin-2 between the control group and mice colonized with *M. schaedleri* was seen at any time point. We can conclude that *M. schaedleri,* while blocking *S.* Tm induced colitis, does not attenuate *C. rodentium* induced inflammation. This is in accordance with the idea that *M. schaedleri* specifically interferes with the expression of the SPI1-T3SS of *S.* Tm.

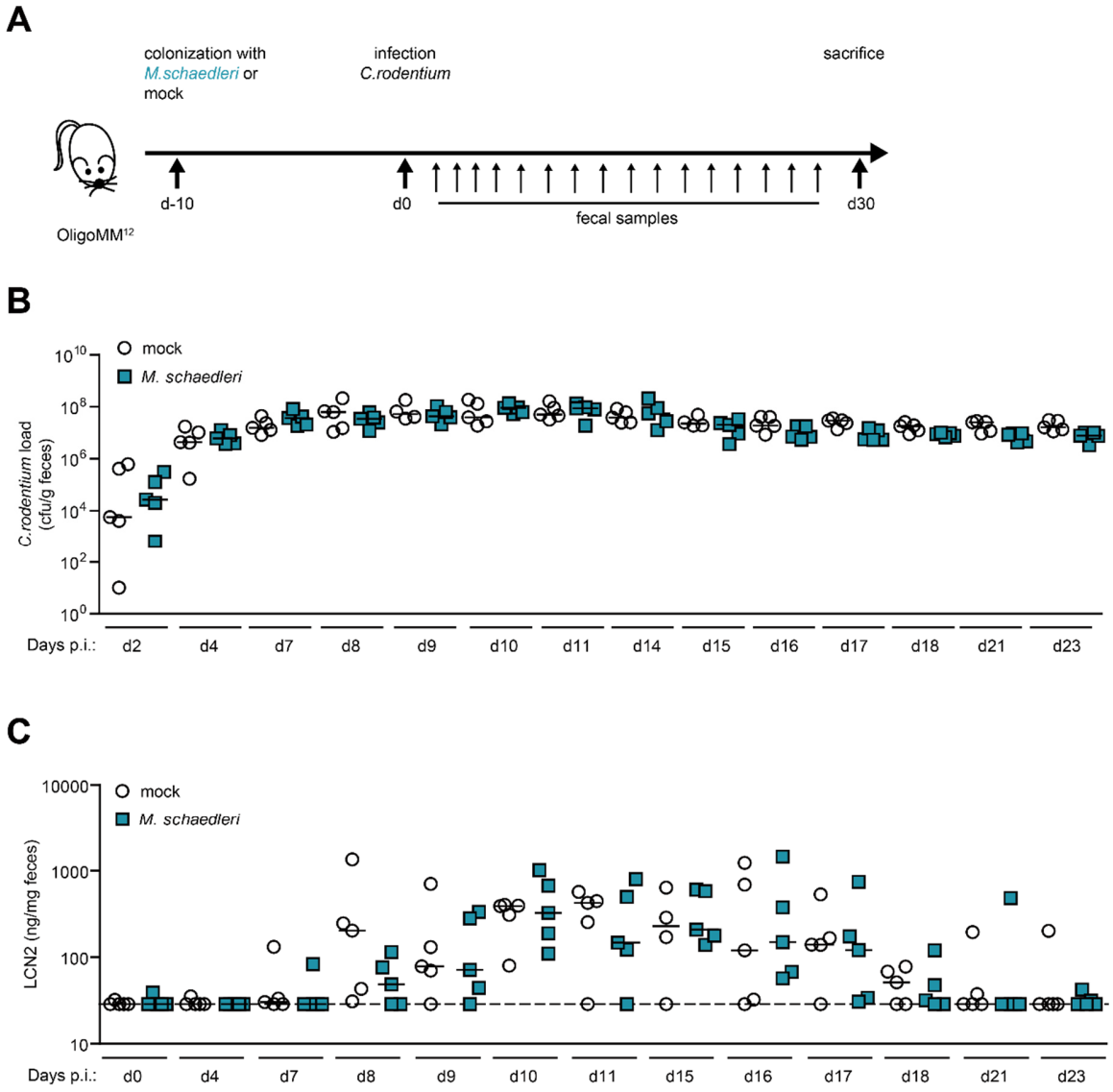

Fig. 19: The course of *C. rodentium* infection is not influenced by *M. schaedleri*. A) Experimental set up. OligoMM^{12} mice were pre-colonized with *M. schaedleri* or sterile control media 10 days prior to infection with *C. rodentium* (10^8 cfu/mouse), fecal samples were taken on a regular base day 0 until day 30 (day of termination). **B)** *C. rodentium* loads quantified over time by plating of fecal pellets. **C)** Lipocalin-2 levels in feces measured by ELISA. One dot represents one mouse, dashed line: detection limit. One-way ANOVA Kruskal-Wallis test with Dunn's multiple comparison test; ns, no significant difference $p \geq 0.05$, *$p < 0.05$, **$p < 0.01$, ***$p < 0.001$. Data points from day 23 onwards are not shown, as no further changes were observed.

4.5.2 *M. schaedleri* is streptomycin resistant but sensitive to ampicillin

As *M. schaedleri* was enriched in streptomycin treated *Agr2*$^{-/-}$ mice but not in ampicillin treated mice (Brugiroux, 2016), we tested whether *M. schaedleri* was resistant to the aminoglycoside streptomycin but not to the beta-lactam antibiotic ampicillin. Indeed, when *M. schaedleri* was cultured in the presence of standard concentrations of 100 µg/ml or 50 µg/ml of streptomycin or ampicillin, or media without antibiotic, we observed no growth of the cultures with both concentrations of ampicillin, but normal growth in the presence of streptomycin compared to control without antibiotics at 48 h and 72 h after inoculation (Two-way ANOVA with Bonferroni multiple comparison test; ***p < 0.001) (Fig. 20).

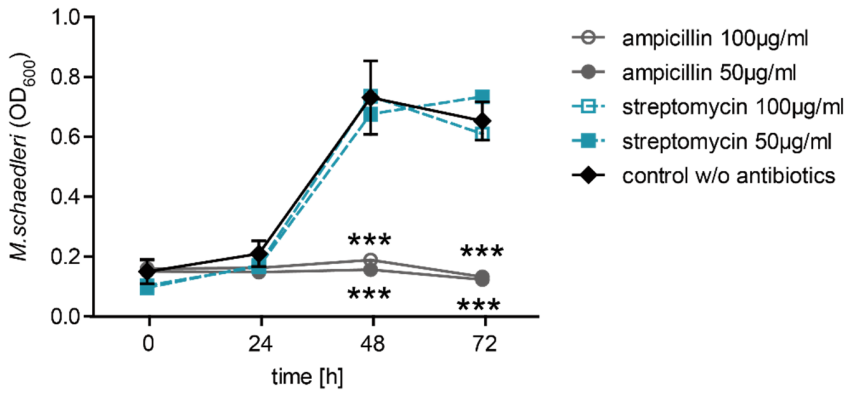

Fig. 20: *M. schaedleri* is streptomycin resistant but sensitive to ampicillin. *M. schaedleri* was grown in AAM (10 mM $NaNO_3$) in the presence of 50 or 100 µg/ml streptomycin or ampicillin or as a control without antibiotics for 72 h. OD_{600} was measured every 24 h. Displayed is the mean of three replicates and SEM. Two-way ANOVA test with Bonferroni multiple comparison test; ns, no significant difference p ≥ 0.05, *p < 0.05, **p < 0.01, ***p < 0.001.

4.5.3 *M. schaedleri* leads to alterations of the primary bile acid pool and SCFAs in the cecum of mice

Bile acids are produced in the liver and released into the intestine where they are modified by the microbiota (Wahlstrom *et al.*, 2016). A study by Prouty & Gunn showed, that SPI1-T3SS was repressed in the presence of bile acids (Prouty & Gunn, 2000). On the other hand, short-chain fatty acids (SCFAs) such as acetate, propionate and butyrate are produced by the microbiota via fermentation of dietary fibers and play an important role for gut homeostasis (e.g. as energy source for colonocytes (Donohoe *et al.*, 2011), anti-inflammatory response (Tedelind *et al.*, 2007)). An effect of butyrate and acetate on SPI1-T3SS was previously shown (Durant *et al.*, 2000; Lawhon *et al.*, 2002). Thus, we hypothesized that alterations of SCFAs or bile acids by *M. schaedleri* could lead to repression of SPI1-T3SS expression. We analyzed changes of bile acid and SCFA levels in the cecum of ASF[3] mice colonized with *M. schaedleri* or control for 10 days. Interestingly, the primary bile acids β-MCA, TCA, α-TMCA and β-TMCA were increased in mice colonized with *M. schaedleri* (Mann–Whitney U test; **p < 0.01, *p < 0.05, **p < 0.01; Fig. 21A). No secondary bile acids were detectable (data not shown). On the other hand, the SCFAs succinate, acetate, propionate and the total amount of SCFAs were slightly decreased in *M. schaedleri* colonized ASF[3] mice (Mann–Whitney U test; *p < 0.05), whereas formate, lactate and butyrate levels did not show a significant difference (Fig. 21B).

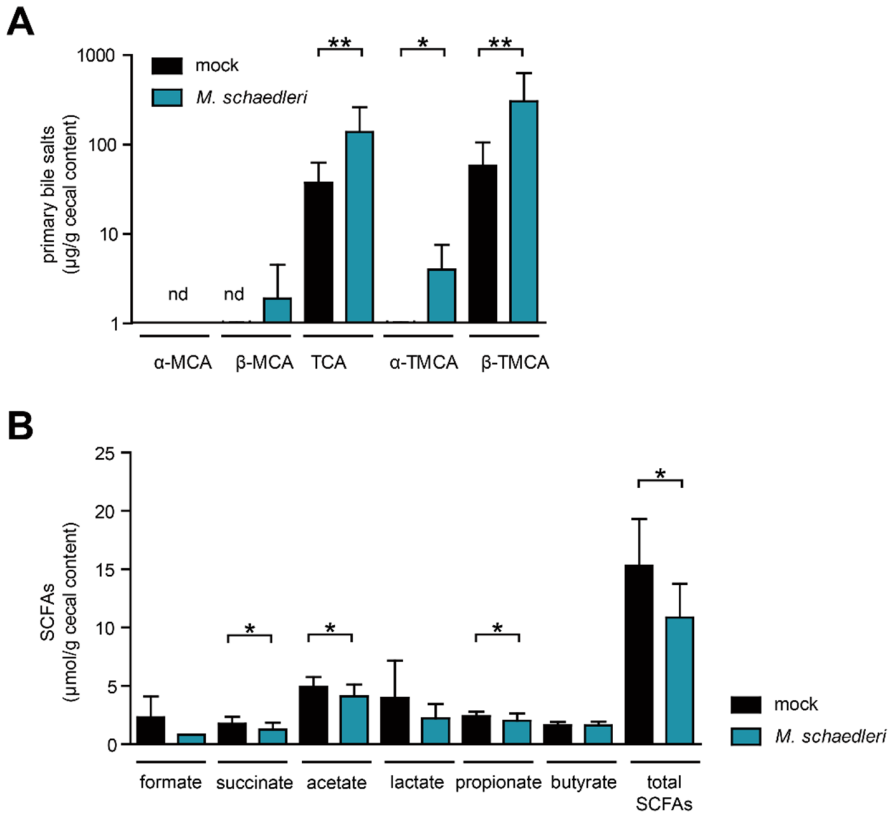

Fig. 21: *M. schaedleri* increases taurine conjugated primary bile acids and alters the SCFA pool in the cecal content of mice. A) Quantification of bile acids in cecal content by non-targeted metabolomics using UPLC-MS (Dr. Alesia Walker) from ASF[3] mice colonized for 10 days with *M. schaedleri* or mock. Secondary bile acids were not detectable (data not shown) **B)** SCFAs quantification (Dr. Buck Hanson) by capillary electrophoresis from same samples as used for bile acid quantification. Shown is the mean concentration with SD from 8 mice per group. nd, not detected; Mann–Whitney U test; ns, no significant difference $p \geq 0.05$, *$p < 0.05$, **$p < 0.01$, ***$p < 0.001$

5 Discussion

In the last few years the field of microbiome research has extremely expanded. The importance of the microbiota on the human health has been acknowledged and dysbiosis is associated to a wide range of diseases. A higher susceptibility of a disrupted microbiota to enteric pathogens is of significant importance for human health (Buffie *et al.*, 2012; Ubeda *et al.*, 2010). A small number of intestinal microbiota species were already identified which protect the host from pathogenic bacteria. Among them are *Clostridium scindens*, *Escherichia coli* Nissle 1917, *Bifidobacterium* spp. and *Ruminococcus obeum* which were shown to confer resistance to major intestinal pathogens like *Clostridium difficile*, *S*. Tm, Enterohaemorrhagic *Escherichia coli* (EHEC) O157:H7 and *Vibrio cholerae* respectively (Buffie *et al.*, 2015; Deriu *et al.*, 2013; Fukuda *et al.*, 2011; Hsiao *et al.*, 2014; Studer *et al.*, 2016). Those bacteria employ distinct mechanisms to confer colonization resistance. *C. scindens* produces secondary bile acids which prevent germination of *C. difficile* spores, whereas *E. coli* Nissle competes with *S*.Tm for iron (Buffie *et al.*, 2015; Deriu *et al.*, 2013; Studer *et al.*, 2016). Specific *Bifidobacterium* spp. are able to produce acetate which promotes an anti-inflammatory response preventing translocation of shiga toxin type 2 to the bloodstream (Fukuda *et al.*, 2011). On the other hand, *R. obeum* interferes with the *V. cholerae* quorum-sensing and therefore represses major colonization factors of *V. cholerae* (Hsiao *et al.*, 2014). To date, no bacterium has been identified which influences the expression of a major virulence factor but does not confer colonization resistance. In my thesis I was able to demonstrate a causal role of *M. schaedleri* in protection from *S.* Tm colitis by employing different gnotobiotic mouse models, *S*. Tm mutants and RNAseq. This protective effect is achieved by downregulation of the *S*.Tm SPI1-T3SS, its major virulence factor.

5.1 *M.schaedleri* delays the onset of *S*.Tm colitis in mice

S.Tm is a major cause of gastroenteritis in humans and leads to high mortality in immunocompromised people (Gordon, 2008; Uche *et al.*, 2017). Further, antibiotic-resistant strains are emerging (Okoro *et al.*, 2012). Therefore, it is necessary to develop protective strategies. One future strategy could be the precise manipulation of the microbiota ("precision editing", (Zhu *et al.*, 2018)) to increase protection against disease in high risk populations. A complex microbiota precludes the analysis of the contribution of single bacterial species to the outcome of disease. *S*.Tm infection in the mucus deficient *Agr2*$^{-/-}$

mouse model identified a potential protective role of *M. schaedleri* in *S.* Tm colitis (Fig. 4) (Brugiroux, 2016). By utilizing two distinct gnotobiotic mouse models (ASF^3 and $OligoMM^{12}$) I confirmed causality of *M. schaedleri* in protection from *S.*Tm colitis by selectively adding this species only. Due to the low complex microbiota no streptomycin pretreatment is needed to breach colonization resistance in both types of mice (Beutler, 2016; Brugiroux, 2016; Stecher *et al.*, 2010). Indeed, *M.schaedleri* reduced colitis in gnotobiotic ASF^3 and as well $OligoMM^{12}$ mice infected with wildtype *S.* Tm (Fig. 6F & G; Fig. 7F & G). In contrast, *M.schaedleri* is not able to confer colonization resistance to *S.* Tm (Fig. 6B; Fig. 7B). This observation indicates that *M.schaedleri* is a beneficial bacterium in respect to protection of mice from *S.*Tm colitis and that this effect is independent of the microbial context. The microbiota produces diverse metabolites and generates a complex environment. Recently it was shown that protection from vancomycin-resistant *Enterococcus* (VRE) in mice is mediated in a cooperative manner by four different species (Caballero *et al.*, 2017). A niche is created by members of this consortium to allow efficient colonization of the protective strain *Blautia producta* (Caballero *et al.*, 2017). Furthermore, the *E. coli* strain Mt1B1 was only able to confer colonization resistance to *S.* Tm in gnotobiotic mice colonized with the $OligoMM^{12}$ microbiota but not in the very low complex ASF mice (Brugiroux *et al.*, 2016), showing the importance of the microbiota composition on protection. Cross feeding is an important interaction between different species in the gut. *In vitro, Parabacteroides goldsteinii* ASF519 was reported to produce multiple amino acids, among them methionine, threonine and tryptophan (Biggs *et al.*, 2017) which are in contrast not synthesized by *M. schaedleri* (Loy *et al.*, 2017). Further *M. schaedleri* utilizes H_2 as electron donor to perform dissimilatory nitrate reduction to ammonia (DNRA) (Loy *et al.*, 2017). The ceca of germ-free mice are devoid of H_2 and the resident microbiota is responsible for H_2 production (Maier *et al.*, 2013). Therefore, *M. schaedleri* could rely on amino acids and H_2 produced by the intestinal microbiota. Infection experiments in germ-free mice mono-colonized with *M. schaedleri* could show if colonization of *M. schaedleri* and the protective effect is completely microbiota independent.

5.2 *S*.Tm SPI1-T3SS expression is reduced in the presence of *M.schaedleri*

Elucidating the mechanism underlying the protective effect of *M. schaedleri* in *S*. Tm colitis proofed to be rather difficult. Until now, genetic manipulation of *M. schaedleri* is not possible and therefore mutants are not available. Furthermore, *M. schaedleri* is a fastidious bacterium growing slowly in liquid culture under anaerobic conditions. It was isolated on agar plates but does not readily form single colonies (Robertson *et al.*, 2005). In our lab, we were so far unable to obtain reproducible growth on agar plates which would be a prerequisite for *in vitro* studies. Therefore we relied so far on *S*.Tm reporter and *S*.Tm mutant strains as well as transcriptome analysis to identify the mechanism of protection indirectly.

The SPI1-T3SS is the major virulence factor of *S*.Tm which is employed to invade intestinal epithelial cells and trigger inflammation (Barthel *et al.*, 2003). *S*.Tm colitis is drastically reduced by *M. schaedleri* in gnotobiotic mice and invasion of *S*.Tm into the cecal tissue of protected streptomycin treated *Agr2*$^{-/-}$ mice was reduced (Brugiroux, 2016). Therefore, we analyzed SPI1-T3SS expression *in vivo* using an avirulent *S*.Tm harboring a SPI1 reporter plasmid (Ackermann *et al.*, 2008). In control mice, approximately 8 % of the *S*.Tm population expresses SPI1-T3SS. This is significantly reduced about 2-fold to approximately 4 % in the presence of *M.schaedleri* (Fig. 10). SPI1-T3SS was shown to be expressed in a bistable manner (Ackermann *et al.*, 2008). It was stated that only approximately 15 % of the total *S*.Tm population express SPI1-T3SS (Ackermann *et al.*, 2008). Those SPI1^{+} bacteria can invade the tissue and trigger inflammation. In contrast, SPI1^{-} bacteria can benefit of the inflammatory milieu in the gut and acquire nutrients released by the inflamed mucosa and expand in the gut (Ackermann *et al.*, 2008; Diard *et al.*, 2013). This strategy is known as phenotypic heterogeneity (Ackermann *et al.*, 2008; Diard *et al.*, 2013). Further, it was reported that inflammation is enhanced proportional to increasing numbers of SPI1^{+} bacteria (Ackermann *et al.*, 2008). Therefore, a reduction of about half of SPI1^{+} bacteria seen in mice colonized with *M. schaedleri* will have a strong impact on inflammation.

RNAseq data from *S*.Tm infection *in vivo* confirmed the downregulation of SPI1-T3SS in the presence of *M. schaedleri* (Table 34). InvF, a main positive regulator of SPI1-T3SS effector protein genes, is ~ 2-fold downregulated. Further, SPI1-T3SS genes like *sipA* and *prgK* are also downregulated 3 - 5-fold. SipA effects the rearrangement of actin filaments and

mediates the uptake of *S.*Tm in host cells (Galkin *et al.*, 2002) whereas PrgK forms together with PrgH the inner ring of the SPI1-T3SS apparatus (Bergeron *et al.*, 2015). In addition the expression of the effector protein SopB is also negatively influenced by the presence of *M. schaedleri*. SopB is not encoded on the SPI-1 locus but is translocated via the SPI1-T3SS and leads to disruption of the tight junctions of epithelial cells (Boyle *et al.*, 2006). This argues that the expression of the entire *S*.Tm SPI1-T3SS and some effector proteins is seriously affected by *M. schaedleri* and therefore SPI1-T3SS mediated invasion and induction of inflammation is severly reduced. Utilizing two distinct methods, a *gfp*-reporter strain and RNAseq, I could confirm that *M. schaedleri* influences the expression of *S*.Tm SPI1-T3SS which results in a significantly decreased *S*.Tm colitis *in vivo.*

On the other hand, *M.schaedleri* does not confer protection to mice against infection with the common mouse pathogen *Citrobacter rodentium* (Fig. 19B&C). This bacterium is used as a model for human Enteropathogenic *Escherichia coli* infection (EPEC) (Wiles *et al.*, 2004). *C. rodentium* elicits a milder inflammation compared to *S*.Tm which sets in 6-10 days post infection and is usually cleared from the intestine 20 days post infection (Wiles *et al.*, 2004). In OligoMM^{12} mice *C. rodentium* colonizes the gut for at least 42 days (Beutler, 2016). Mice pre-colonized with *M. schaedleri* show a slight but not significant reduction of *C. rodentium* loads (Fig. 19BC). This could indicate that *M. schaedleri* contributes to some extend to the clearance of *C. rodentium* in OligoMM^{12} mice. Like *S*. Tm, *C. rodentium* harbors a T3SS encoded on the locus of enterocyte effacement (LEE) (Jarvis *et al.*, 1995). Expression of LEE is tightly regulated by environmental factors like fucose, butyrate, pH, NO, epinephrine/norepinephrine and bacterially derived auto-inducer 3 signaling molecule (AI-3) or acyl-homoserine lactones (Branchu *et al.*, 2014; Connolly *et al.*, 2015; Hughes *et al.*, 2010; Kanamaru *et al.*, 2000; Nakanishi *et al.*, 2009; Pacheco *et al.*, 2012; Walters & Sperandio, 2006). It is essential for injection of effector proteins which lead to cytoskeletal rearrangement and inflammation (Hueck, 1998; Kaper *et al.*, 2004). We suppose that the inhibition of virulence of *S*.Tm by *M.schaedleri* is specific for *S*.Tm and not the T3SS. Experiments with other pathogens harboring a T3SS like *Shigella flexneri* or *Yersinia enterocolitica* (Notti & Stebbins, 2016) will help further to analyze this aspect.

5.3 Nitrate induces *S*.Tm SPI1-T3SS expression under anaerobic conditions *in vitro*

The SPI1-T3SS system is controlled by a complex regulatory network. Little is known on the environmental cues stimulating SPI1-T3SS expression. During inflammation the environment of the gut changes dramatically. Cells of the innate immune response release ROS as a first line of defense against invading pathogens and thereby creating a hostile environment (Rivera-Chavez & Baumler, 2015). On the other hand, growth of *S*. Tm is promoted in the presence of alternative electron acceptors (Price-Carter *et al.*, 2001; Unden & Dunnwald, 2008). For *S*.Tm, nitrate is the most preferred alternative electron acceptor directly after oxygen (Unden & Dunnwald, 2008). Nitrate concentrations are low (0.03 mM) in the uninflamed gut but increase during inflammation (0.3 mM) in the cecal mucus layer (Lopez *et al.*, 2015). It was shown that the periplasmic nitrate reductase plays an important role for *S*.Tm colonization in the gut, highlighting its importance in *S*.Tm infection (Lopez *et al.*, 2015). *M. schaedleri* performs full dissimilatory nitrate reduction to ammonia (DNRA) and could therefore limit available nitrate in the gut and compete with *S*. Tm (Fig. 2B) (Loy *et al.*, 2017). Data from an *in vitro* SPI1-luciferase reporter assay show that under anaerobic conditions in the presence of nitrate (10 mM or 40 mM) SPI1-T3SS expression is enhanced app. 5-fold (Fig. 11A). This stimulatory effect is abolished in a nitrate respiration deficient *S*.Tm mutant (*S*.Tm$^{\Delta nr3}$) (Fig. 11A), suggesting that functional nitrate respiration is needed for SPI1-T3SS induction under anaerobic conditions. Further, published SPI1-T3SS inducing factors like microaerobic conditions and high osmolarity (Lee & Falkow, 1990; Song *et al.*, 2004) were also able to enhance SPI1-T3SS in our assay (Fig. 11A). Nitrate dependent induction of SPI1-T3SS was only observed under anaerobic conditions (Fig. 11A). Further, induction was not observed with low nitrate concentrations (1 mM). The three different nitrate reductases are induced under different nitrate concentrations. The high affinity periplasmic nitrate reductase NapABCGH is induced at low nitrate concentrations (1 mM) whereas the low affinity NarGHI is maximally synthesized at nitrate concentrations of 10 mM (Wang *et al.*, 1999). Nitrate is consumed rapidly by *S*. Tm during anaerobic growth, therefore high concentrations of nitrate (> 10 mM) are needed to sustain constant supply of nitrate over the 4 h growth period (DeMoss & Hsu, 1991). It would be of interest to analyze the minimal nitrate concentration needed to induce *S*. Tm SPI1-T3SS *in vitro* and whether this concentration is comparable to conditions found *in vivo*. Therefore, growth in a

chemostat with constant supply of nitrate would be mandatory. An invasion assay confirmed that under low oxygen conditions (0.5 %) functional nitrate respiration is needed to enable full invasion into HuTu80 cells (Fig. 11B). In conclusion, I identified nitrate as a new inducer of SPI1-T3SS under anaerobic conditions which could play an important role *in vivo* for *S*.Tm invasion into epithelial cells. Other alternative electron acceptors (DMSO, TMAO) were also tested using the SPI1-luciferase reporter assay. Both, DMSO and TMAO respiration induce SPI1-T3SS under anaerobic conditions (unpublished, Master Thesis R. Götz). Those alternative electron acceptors are as well metabolized by *M.schaedleri* as predicted by genome analysis (Loy *et al.*, 2017) and first *in vitro* culture experiments (preliminary data, not shown).

5.4 How does *M.schaedleri* influence the regulation of *S*.Tm SPI1-T3SS *in vivo*?

In vitro, nitrate was found to be a potent *S.* Tm SPI1-T3SS inducer. We hypothesized that *M. schaedleri* limits available nitrate in the gut by performing dissimilatory nitrate reduction to ammonia (DNRA) (Loy *et al.*, 2017). Therefore, SPI1-T3SS expression should be reduced and hence inflammation dampened. Due to the lack of a genetic system for *M. schaedleri* I employed a *S*. Tm mutant defective in nitrate respiration (*S*.Tm$^{\Delta nr3}$) for infection experiments. Assuming that *M. schaedleri* limits nitrate, control mice without *M. schaedleri* should exhibit higher intestinal nitrate concentrations. If nitrate plays a role as SPI1-T3SS inducer *in vivo,* a *S*.Tm$^{\Delta nr3}$ mutant unable to utilize nitrate should induce less inflammation in control mice even if nitrate is present. The inflammation should be as low as in mice colonized with *M. schaedleri* and infected with wildtype *S*.Tm or *S*.Tm$^{\Delta nr3}$.

In contrast to our expectations, *S*.Tm$^{\Delta nr3}$ still elicits a profound inflammation in control mice, comparable to wildtype *S*.Tm infection (Fig. 13F & G). Mice colonized with *M. schaedleri* are still protected from colitis during *S*.Tm$^{\Delta nr3}$ infection (Fig. 13F & G). This indicates that nitrate is negligible *in vivo* for protection from *S*.Tm colitis by *M. schaedleri*.

During inflammation in the intestine, an altered environmental condition is established that boost growth of enteric pathogens (Winter, Lopez*, et al.*, 2013). However, also other metabolites besides nitrate like TMAO, DMSO and tetrathionate are released which can be used as alternative electron acceptors by *S*.Tm under anaerobic conditions (Unden & Dunnwald, 2008). This leads to a growth advantage of *S*.Tm over the resident microbiota in

the intestine (Winter, Lopez*, et al.*, 2013; Winter *et al.*, 2010). Infection experiments with *S*.Tm$^{\Delta moaA}$, a mutant unable to utilize nitrate, TMAO, DMSO, tetrathionate and fumarate, showed that this mutant still elicits profound inflammation in control mice, resembling wildtype *S*.Tm infection.

These results show that the protective effect of *M.schaedleri* is not dependent on the alternative electron acceptors nitrate, DMSO, TMAO, tetrathionate and fumarate. Both mutants, *S*.Tm$^{\Delta nr3}$ and *S*.Tm$^{\Delta moaA}$, could still acquire nitrite and convert nitrite to ammonia by its nitrite reductases (NirBD, NrfA) (Einsle, 2011; Einsle *et al.*, 1999; Gilberthorpe & Poole, 2008; Rycovska-Blume *et al.*, 2015). Further, three nitrite transporters (NarK, NarU and NirC) are described to import environmental nitrite into *S*.Tm (Jia *et al.*, 2009; Rycovska *et al.*, 2012). Nitrite is an intermediate in nitrate reduction and is the most preferred anaerobic electron acceptor after nitrate under anoxic conditions (Unden & Dunnwald, 2008). The SPI1-T3SS inducing effect observed *in vitro* could be accounted to nitrite respiration rather than nitrate respiration. If this is the case, SPI1-T3SS should be inducible by nitrite in *S*.Tm$^{\Delta nr3}$, *S*.Tm$^{\Delta moaA}$ and wildtype *S*.Tm but not in a nitrite reductase mutant *S*.Tm$^{\Delta nrfA\Delta nirB}$. This can be analyzed by an *in vitro* luciferase-assay. Further the nitrite respiration mutant *S*.Tm$^{\Delta nrfA\Delta nirB}$ and a *S*.Tm mutant completely unable of anaerobic respiration *S*.Tm$^{\Delta moaA\Delta nrfA\Delta nirB}$ could be used for infection experiments in OligoMM^{12} mice colonized with *M. schaedleri* or control to study the effect *in vivo*. Complete abrogation of anaerobic respiration could lead to a severe growth defect of *S*.Tm in the gut, especially as *nrfA* plays as well a role in detoxification of NO (Mills *et al.*, 2008). This has to be experimentally tested. *S*.Tm$^{\Delta nirC}$, defective in a nitrite transporter, showed reduced dissemination into the spleen of mice (Das *et al.*, 2009) indicating a role in *S*.Tm pathogenesis.

Measurement of nitrate and nitrite concentrations in the intestinal mucus would give important information about environmental available nitrate / nitrite and changes in the presence of *M.schaedleri*. Due to inhibitors and probably low amounts of nitrate / nitrite in mucus scrapings a colorimetric assay (Lopez *et al.*, 2015) and a commercial fluorometric nitric oxide kit failed to measure accurate nitrate concentrations.

A second important factor is the presence of oxygen in the usually hypoxic intestine. In the *in vitro* luciferase assay we showed that oxygen is a potent inducer of *S*. Tm SPI1-T3SS which was already described (Ibarra *et al.*, 2010; Lee & Falkow, 1990). Further, oxygen induces the T3SS of the pathogen *Shigella flexneri* (Marteyn *et al.*, 2010). Therefore oxygen,

present at the epithelial border could influence the expression of SPI1-T3SS *in vivo*. Streptomycin treatment disturbs the resident microbiota and depletes especially members of the *Clostridia* (Rivera-Chávez *et al.*, 2016). This leads to an increase of available oxygen which is readily consumed by facultative anaerobic bacteria like *S*.Tm and results in expansion of *S*.Tm (Rivera-Chávez *et al.*, 2016). It was shown that the post-antibiotic expansion of *S*.Tm relies on its cytochrome *bd*-II oxidase (CyxA) (Rivera-Chávez *et al.*, 2016). Therefore, a *S*.Tm$^{\Delta cyxA}$ mutant could contribute to understand the potential role of oxygen for the protective effect of *M.schaedleri*. The protective effect of *M. schaedleri* was also observed in the unperturbed gut of OligoMM^{12} and ASF^{3} mice (Fig. 6 & Fig. 7). Due to the low complexity of the microbiota and under – representation of butyrate producing *Clostridia* it could be possible that oxygen is present at low levels in the gut. *M. schaedleri* could compete with *S*.Tm for oxygen using a cytochrome c oxidase (Loy *et al.*, 2017) and thereby decrease SPI1-T3SS in *S*.Tm. Intestinal oxygen quantification is a challenging task. Several techniques are published but are not easy to perform (Espey, 2013). In contrast, O_2 microsensors were recently used in cockroaches and honeybees to measure O_2 concentrations in the gut (Tegtmeier *et al.*, 2016; Zheng *et al.*, 2017). To the best of my knowledge there are so far no studies in the mouse gut. If this method is applicable to mice has to be shown. Further, hypoxia staining with pimonidazol was recently used to visualize hypoxia of the intestinal epithelium (Byndloss *et al.*, 2017; Rivera-Chávez *et al.*, 2016). However, as preliminary experiments suggested this method is not sensitive enough for our needs.

Transcriptome analysis revealed that in the presence of *M. schaedleri S*. Tm downregulates the genes for the periplasmic nitrate reductase *napA*, hydrogenases as well as cytochrome d oxidase subunit I *cydA* (Table 34). This points at efficient competition for nitrate, hydrogen and oxygen of *M. schaedleri* with *S*. Tm. Competition for nutrients was already shown to be an essential mechanism in conferring colonization resistance to *S*. Tm (Deriu *et al.*, 2013). It was also demonstrated that commensal *E. coli* reduces colonization of pathogenic *E. coli* probably by competing for the same nutrients (Leatham *et al.*, 2009). H_2 and nitrate are known to be factors important for *S*. Tm colonization of the mouse intestine (Lopez *et al.*, 2015; Maier *et al.*, 2013). Initial competition experiments indicate that in the OligoMM^{12} mice H_2 as well as nitrate utilization are negligible for efficient colonization (Fig. 9). The impact of available oxygen has to be evaluated as discussed above.

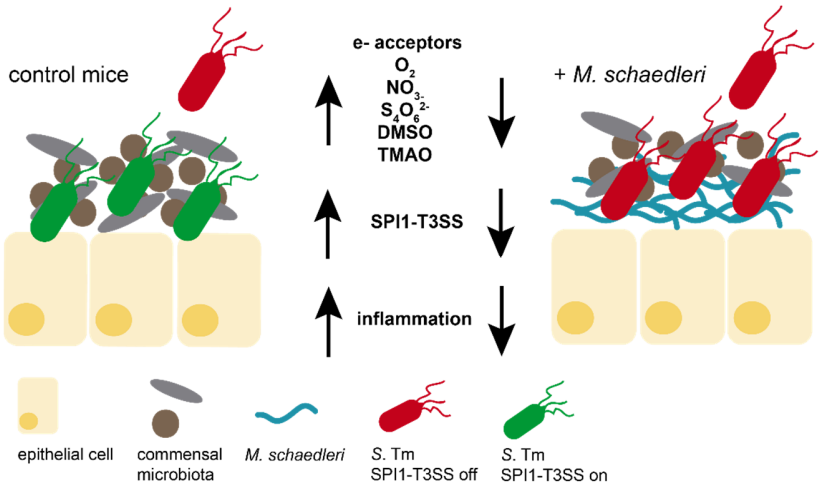

Fig. 22. Hypothetical mechanism of protection by *M. schaedleri* from *S*.Tm colitis. During inflammation several eletron acceptors become available, especially in close proximity of the epithelial border. Those can be sensed by *S*. Tm and used as signal for SPI1-T3SS expression which leads to cell invasion and triggering of the innate immune response (left). *M. schaedleri* has the capacity to utilize those electron acceptors as well, suggesting competition between *M. schaedleri* and *S*. Tm. By depletion of the complex pool of electron acceptors by *M. schaedleri S*. Tm respiration and SPI1-T3SS expression is reduced which leads to decreased epithelial cell invasion and subsequently to lower inflammation.

Further, transcriptome data showed that several genes involved in translation are as well downregulated implying reduced growth of *S*.Tm in the presence of *M.schaedleri* (Klumpp *et al.*, 2013; Zhu *et al.*, 2016). This could not be substantiated by experiments where we measured the replication rate of *S*. Tm harboring a temperature sensitive plasmid (Stecher *et al.*, 2008) (Fig. 8). In ASF^{3} mice colonized with *M.schaedleri* we actually observed a higher replication rate (Fig. 8B). On the other side, in $OligoMM^{12}$ mice we rather saw a slightly reduced growth rate with *M.schaedleri* which would be in line with the transcriptome data. This discrepancy has to be addressed further.

A genetic system for *M. schaedleri* would be highly useful to further entangle the mechanistic details underlying *S*. Tm antagonism. *M.schaedleri* is a vastly unexplored bacterium. This is also due to its fastidious lifestyle and its inability to form single colonies on agar plates (Robertson *et al.*, 2005). So far reproducible growth is only obtained in liquid culture. We suppose that *M. schaedleri* has even more requirements for growth on solid media and the media have to be adjusted. The genome analysis revealed that *M.schaedleri* is unable to synthesize several amino acids like methionine and tryptophan (Loy *et al.*, 2017), therefore supplementation of these could yield in growth. Recently it was reported that fastidious bacteria were able to grow in the presence of another bacterium, a so called helper strain. Those helper strains produce nutrients vital for recipient strains (Fenn *et al.*, 2017; Nichols

et al., 2008; Ohno *et al.*, 1999). Growth in the presence of *E.coli*, the OligoMM^{12} or ASF strains will be tested.

In respect to *S*.Tm colitis *M.schaedleri* fulfills definitely a protective role. On the other hand it was indicated as a potential pathobiont (Loy *et al.*, 2017). It is increased in its abundance in the context of inflammation in several studies performed in mice (Berry *et al.*, 2012; Rooks *et al.*, 2014; Selvanantham *et al.*, 2016; Song *et al.*, 2018). Further it is also elevated in obese mice where a dysbiotic microbiota changed the intestinal environment (Ravussin *et al.*, 2012; Serino *et al.*, 2012). During inflammation, alternative electron acceptors like DMSO, TMAO, nitrate, tetrathionate and oxygen become available (Rivera-Chavez & Baumler, 2015). *M. schaedleri* can perform full DNRA and possesses genes for potential DMSO, TMAO and tetrathionate reductases (Loy *et al.*, 2017). Therefore it is not surprising that *M. schaedleri* is increased in experimental colitis models (Berry *et al.*, 2012; Rooks *et al.*, 2014; Selvanantham *et al.*, 2016; Song *et al.*, 2018; Vereecke *et al.*, 2014). Further, the presence of genes encoding cytochrome c oxidase, catalase, superoxide reductase, cytochrome c peroxidase and rubrerythrin allows it to withstand efficiently neutrophil oxidative burst (Loy *et al.*, 2017). If *M.schaedleri* is a true pathobiont and actually promotes colitis or just benefits from released nutrients has to be experimentally tested in the future using gnotobiotic mice.

5.5 *M. schaedleri* is a natural member of the murine microbiota

M. schaedleri is part of the minimal consortium Altered Schaedler Flora (ASF) (Orcutt *et al.*, 1987). It was isolated from mice and is predominant in wild living mice (Linnenbrink *et al.*, 2013; Robertson *et al.*, 2005; Rosshart *et al.*, 2017). Records of *M. schaedleri* in human are scarce and it is so far only detected in samples from colonic biopsies at low levels (Bik *et al.*, 2006; Harrell *et al.*, 2012; Rausch *et al.*, 2011). It was stated that *Mucispirillum* is an exclusive genus in mice compared to human (Krych *et al.*, 2013). Limiting sequencing depth, the low abundance of *M. schaedleri* even in mice and its localization at the epithelial border could account for its rare detection in human. Further, *M. schaedleri* is not present in each laboratory mouse strain. In mice from Taconic and Charles River, *M. schaedleri* is highly abundant, whereas it is not detected in mice from Jackson (Rosshart *et al.*, 2017). In the context of the protective effect of *M. schaedleri* on *S*.Tm infection found in this study the choice of vendor should be carefully reconsidered in future experiments when using mice for infection studies.

M. schaedleri inhabits a distinct niche close to the epithelium, which was shown by FISH analysis in gnotobiotic ASF[3] and OligoMM[12] mice (Fig. 5B & D) (Loy *et al.*, 2017). Genome analysis of *M.schaedleri* predicts a cytochrome c oxidase, catalase, superoxide reductase, cytochrome c peroxidase and rubrerythrin to fend off oxidative stress which is likely encountered in close proximity to the epithelial border (Fig. 2A) (Loy *et al.*, 2017). This is also in accordance with observations in our lab which showed that *M. schaedleri* is oxygen tolerant. *M.schaedleri* is described as a mucus dwelling bacterium (Loy *et al.*, 2017; Robertson *et al.*, 2005). Surprisingly, *M. schaedleri* is also abundant in MUC2 deficient OligoMM[12] *Agr2*$^{-/-}$ mice and is localized close to the epithelial border (Fig. 14A). Together with the genome prediction of Loy *et al.* which found no evidence for mucus degrading enzymes we can conclude that MUC2 is dispensable for successful *M. schaedleri* colonization in mice (Loy *et al.*, 2017). At the epithelial border, *M.schaedleri* forms a dense, mesh like biofilm (Fig. 5B & D; Fig. 14A) (Loy *et al.*, 2017). In combination with its oxygen detoxifying enzymes, *M. schaedleri* could contribute to the anoxic conditions found in the intestinal lumen. *M. schaedleri* is fully adapted to its life close at the epithelial border, where it is exposed to harsh environmental conditions.

5.6 *M. schaedleri* changes the intestinal metabolome

SCFAs and bile acids were shown to be important environmental cues for SPI1-T3SS expression as their concentrations and compositions differ along the gastrointestinal tract (Durant *et al.*, 2000; Eade *et al.*, 2016; Lawhon *et al.*, 2002; Prouty & Gunn, 2000). SCFAs play a pivotal role in gut homeostasis and are mainly produced by the microbiota (den Besten *et al.*, 2013; Donohoe *et al.*, 2011; Furusawa *et al.*, 2013; Macfarlane *et al.*, 1998).The ileum exhibits high concentrations of acetate which induce SPI1-T3SS *in vitro* (Lawhon *et al.*, 2002). In contrast, the cecum and colon are rich in butyrate and propionate which were shown to have an inhibitory effect on SPI1-T3SS (Lawhon *et al.*, 2002). *M.schaedleri* slightly alters SCFA concentrations in the cecum of mice (Fig. 21B). The differences observed are only subtle and an effect on *S.* Tm SPI1-T3SS expression is unclear. *M. schaedleri* does not only colonize the cecum of mice but is distributed along the whole gastrointestinal tract (Sarma-Rupavtarm *et al.*, 2004). The distal ileum was reported to be the preferred site of *S.* Tm invasion (Carter & Collins, 1974). Therefore *M. schaedleri* could change the SCFA composition in the ileum rather than the cecum. This has to be

followed up by analyzing the SCFAs in the ileum of mice colonized with *M. schaedleri* or control.

Primary bile acids are produced by the host and metabolized by the gut microbiota (de Aguiar Vallim *et al.*, 2013; Sayin *et al.*, 2013). Only few intestinal bacteria like *Clostridium scindens* and *Clostridium hylemonae* are capable to produce secondary bile acids (Ridlon *et al.*, 2016; Ridlon *et al.*, 2006). As none of these bacteria are a member of the ASF[3] consortium it is not surprising that ASF[3] mice lack secondary bile acids (Fig. 21A). Additionally, we can conclude that *M.schaedleri* is not a secondary bile acid producer. Further, taurine-conjugated primary bile acids are decreased by bile salt hydrolase (BSH) activity of taurine deconjugating bacteria (Sayin *et al.*, 2013). Interestingly, taurine conjugated bile acids like TCA, α-TMCA and β-TMCA are increased in the cecal content of ASF[3] mice with *M. schaedleri* compared to control (Fig. 21A). BSH are widely distributed among bacteria and are required for taurine deconjugation (Begley *et al.*, 2006; Jones *et al.*, 2008; Tanaka *et al.*, 1999). We suspect that *M. schaedleri* may inhibit the BSHs of *L. murinus* (ASF361) and *P. goldsteinii* (ASF519) which could explain the increased concentrations of TCA, α-TMCA and β-TMCA.

5.7 *Agr2*$^{-/-}$ and *Agr2*$^{+/-}$ mice are protected by *M. schaedleri* independent of their genotype or streptomycin treatment

The intestinal mucus layer protects the host from invading pathogens and serves as a nutrient source for the microbiota (Derrien *et al.*, 2004; Johansson *et al.*, 2008; Sonnenburg *et al.*, 2005). The mucus layer is intensely studied and it was shown that mucus deficient (*Agr2*$^{-/-}$) mice are more susceptible to chemically induced DSS colitis (Park *et al.*, 2009). Recently, its role in *S.* Tm infection was addressed. Interestingly, *Agr2*$^{-/-}$ mice pretreated with streptomycin were resistant to *S.* Tm colitis at day one post infection (Fig. 4A) (Brugiroux, 2016). In contrast, littermate control *Agr2*$^{+/-}$ mice and ampicillin pretreated *Agr2*$^{+/-}$ and *Agr2*$^{-/-}$ mice developed severe colitis (Fig. 4A) (Brugiroux, 2016). A microbiota mediated effect was assumed and 16S rRNA gene sequencing combined with indicator taxa analysis revealed that *M.schaedleri* is highly enriched in protected *Agr2*$^{-/-}$ mice (Fig. 4B) (Brugiroux, 2016). In this respect, resistance of *M. schaedleri* ASF457 to the aminoglycoside streptomycin and beta-lactam ampicillin was tested in an *in vitro* culture assay (Fig. 20). Indeed, *M. schaedleri* is resistant to streptomycin but sensitive to ampicillin. This explains

the observation that protection from *S*.Tm colitis in streptomycin treated *Agr2*$^{-/-}$ mice is lost in ampicillin pretreated *Agr2*$^{-/-}$ mice (Fig. 4A) (Brugiroux, 2016). To investigate the impact of the microbiota composition on protection of *Agr2*$^{-/-}$ mice, germ-free *Agr2*$^{-/-}$ mice were associated with the defined OligoMM^{12} consortium (Beutler, 2016). Those mice were used to investigate the role of *M. schaedleri* on *S*. Tm colitis in the mucus deficient *Agr2*$^{-/-}$ model. The benefit of a low complex microbiota is that antibiotic treatment is dispensable to elicit *S*.Tm colitis in mice. Both OligoMM^{12} *Agr2*$^{-/-}$ and OligoMM^{12} *Agr2*$^{+/-}$ mice developed colitis 3 days p. i. with *S*.Tm (Fig. 16F & G). On the other hand, OligoMM^{12} *Agr2*$^{-/-}$ and OligoMM^{12} *Agr2*$^{+/-}$ pre-colonized with *M. schaedleri* were both protected from colitis (Fig. 16F & G). This is in contrast to the observations in conventional *Agr2*$^{-/-}$ mice (Fig. 4) (Brugiroux, 2016) and shows that *M. schaedleri* confers protection independent of the host genotype. OligoMM^{12} *Agr2*$^{-/-}$ mice with and without *M. schaedleri* show higher *S*. Tm loads on day 1 p. i. in feces of app. 2 $\log_{10}$ levels compared to OligoMM^{12} *Agr2*$^{+/-}$ mice (Fig. 16B). This could indicate a potential role of the mucus layer in colonization resistance to *S*.Tm. Furthermore, *Agr2*$^{-/-}$ mice exhibit low-grade inflammation in the distal part of the intestine as LCN2 levels in feces of untreated mice were elevated compared to *Agr2*$^{+/-}$ (data not shown) but not in cecal content (Fig. 16). Inflammation can promote *S*. Tm growth in the lower intestine which could explain the increased *S*. Tm loads in feces day 1 p. i.. The microbiota composition of untreated OligoMM^{12} *Agr2*$^{-/-}$ and OligoMM^{12} *Agr2*$^{+/-}$ with and without *M.schaedleri* was analyzed. Cluster analysis based on Bray-Curtis distance matrices revealed only minor differences in microbiota composition (Fig. 15). OligoMM^{12} *Agr2*$^{-/-}$ mice with *M.schaedleri* show a distinct microbiota composition compared to all the three other groups (Fig. 15 A). Conventional *Agr2*$^{-/-}$ and *Agr2*$^{+/-}$ mice harbor a divergent microbial composition of the cecum (Brugiroux, 2016). Therefore, in the case of protected conventional *Agr2*$^{-/-}$ mice, the microbiota could mediate a context dependent effect where *M. schaedleri* is repressed by the community or that *M. schaedleri* is dependent on other bacteria present only in *Agr2*$^{-/-}$ mice.

Besides the defined microbiota composition, streptomycin treatment should be taken into account. Streptomycin dramatically changes the composition and complexity of the gut microbiota of conventional mice (Lichtman *et al.*, 2016; Sekirov *et al.*, 2008). The cecal tissue of streptomycin treated mice reveals no histopathological changes compared to mock treated mice, which excludes obvious adverse effects on cecal tissue (Barthel *et al.*, 2003). However, the cecum itself is increased in size in streptomycin treated mice, probably due to

water influx and osmoregulation (Barthel *et al.*, 2003; Savage & Dubos, 1968). *M. schaedleri* is still able to protect both OligoMM^{12} *Agr2*$^{-/-}$ and *Agr2*$^{+/-}$ mice from *S*.Tm colitis even if they are pretreated with streptomycin (Fig. 17F & G). Streptomycin has an immense impact on the microbiota composition independent of *M.schaedleri* colonization or host genotype (Fig. 17H & Fig. 18). Especially *M. schaedleri* and *B. caecimuris* are increased whereas *T. muris* and *M. intestinale* are reduced by streptomycin. The increase of *M. schaedleri* after streptomycin treatment is not surprising as it is resistant to streptomycin (Fig. 20). Further it can probably benefit from the changed environment in regard to available nutrients and oxygen (Rivera-Chávez *et al.*, 2016). Until now it was not possible to unravel the discrepancy observed between conventional and gnotobiotic OligoMM^{12} *Agr2*$^{+/-}$ and *Agr2*$^{-/-}$ mice in *S*.Tm colitis.

Conventional *Agr2*$^{-/-}$ mice where described to exhibit normal growth and body weight up to four month after birth (Park *et al.*, 2009). In contrast, germ-free and OligoMM^{12} *Agr2*$^{-/-}$ mice show already from 5 weeks on tremendous growth defects compared to littermate controls (data not shown) but no spontaneous inflammation was observed in the cecum of mice (Fig. 16F & G). This indicates that a complex microbiota sustains a healthy environment which is needed in the *Agr2*$^{-/-}$ mice. The OligoMM^{12} microbiota is not able to provide this benefit.

5.8 Can *M. schaedleri* be used as a probiotic to prevent *S*.Tm colitis?

In order to answer this question, more research has to be conducted. First of all it has to be confirmed that *M. schaedleri* is able to colonize the human intestine. As discussed above (5.5) observations of *M. schaedleri* in human samples are scarce and only reported in samples obtained by colonoscopy (Harrell *et al.*, 2012; Rausch *et al.*, 2011). Therefore deep sequencing of colonic samples could reveal if *M. schaedleri* is commonly distributed among the population. If one can proof that *M. schaedleri* is a common member of the human microbiota, further studies have to be performed to rule out negative health effects of *M. schaedleri* on humans. Recently, *M. schaedleri* was implicated in the development of arteriosclerosis in mice (Qiu *et al.*, 2018). Further, we need to investigate its impact on chronic inflammatory diseases like Chron's disease and ulcerative colitis where it was found to be an indicator species for colitis mouse models (Berry *et al.*, 2015; Rooks *et al.*, 2014). We need to reveal if it is a true pathobiont promoting colitis or only benefits from the changed intestinal environment. In addition we have to address if *M. schaedleri* ameliorates the

outcome of infections with other intestinal pathogens like *Clostridium difficile*, *Vibrio cholerae, Shigella flexneri* or vancomycin resistant *Enterococcus* or in contrast leads to deterioration. Eventually, we need to establish a genetic system for *M. schaedleri.* We hope to be able to perform site directed mutagenesis in *M. schaedleri* and utilize transposon mutagenesis to unravel the mechanism behind the protection from *S*. Tm colitis in the near future.

In conclusion, I was able to proof that *M.schaedleri*, a low abundant member of the gut microbiota, delays significantly the onset of *S*.Tm colitis. This was reproducible in two gnotobiotic mouse models with distinct defined microbiota (ASF[3] and OligoMM[12]). Further I could show that protection of *Agr2*$^{-/-}$ mice in *S*.Tm colitis is microbiota dependent by using gnotobiotic OligoMM[12] *Agr2*$^{-/-}$ mice. Expression of SPI1-T3SS, the major virulent factor of *S*. Tm, is markedly reduced in the presence of *M.schaedleri*, shown by RNAseq data and infection experiments with a SPI1-T3SS *gfp*-reporter strain. This is probably achieved by changing the intestinal environment and availability of nutrients (Fig. 22). I could show a strong inducing effect of nitrate on SPI1-T3SS under anaerobic conditions *in vitro* which contributes for the further understanding of the SPI1 regulation *in vivo*. Overall this suggests, although not formally confirmed, that *M. schaedleri* inhibits *S*.Tm virulence by competition for respiratory electron acceptors (Fig. 22).

6 References

Ackermann, M., Stecher, B., Freed, N. E., Songhet, P., Hardt, W. D., & Doebeli, M. (2008). Self-destructive cooperation mediated by phenotypic noise. *Nature, 454*(7207), 987-990. doi:10.1038/nature07067

Albenberg, L., Esipova, T. V., Judge, C. P., Bittinger, K., Chen, J., Laughlin, A., Grunberg, S., Baldassano, R. N., Lewis, J. D., Li, H., Thom, S. R., Bushman, F. D., Vinogradov, S. A., & Wu, G. D. (2014). Correlation Between Intraluminal Oxygen Gradient and Radial Partitioning of Intestinal Microbiota in Humans and Mice. *Gastroenterology, 147*(5), 1055-1063.e1058. doi:10.1053/j.gastro.2014.07.020

Amann, R. I., Binder, B. J., Olson, R. J., Chisholm, S. W., Devereux, R., & Stahl, D. A. (1990). Combination of 16S rRNA-targeted oligonucleotide probes with flow cytometry for analyzing mixed microbial populations. *Appl Environ Microbiol, 56*(6), 1919-1925.

Anderson, M. (2001). A new method for non-parametric multivariate analysis of variance. *Austral Ecology, 26*, 32-46. doi:citeulike-article-id:1349561

Arike, L., & Hansson, G. C. (2016). The Densely O-glycosylated MUC2 Mucin Protects the Intestine and Provides Food for the Commensal Bacteria. *Journal of Molecular Biology, 428*(16), 3221-3229. doi:10.1016/j.jmb.2016.02.010

Aviello, G., & Knaus, U. G. (2017). ROS in gastrointestinal inflammation: Rescue Or Sabotage? *Br J Pharmacol, 174*(12), 1704-1718. doi:10.1111/bph.13428

Backhed, F., Ley, R. E., Sonnenburg, J. L., Peterson, D. A., & Gordon, J. I. (2005). Host-bacterial mutualism in the human intestine. *Science, 307*(5717), 1915-1920. doi:10.1126/science.1104816

Bajaj, V., Lucas, R. L., Hwang, C., & Lee, C. A. (1996). Co-ordinate regulation of Salmonella typhimurium invasion genes by environmental and regulatory factors is mediated by control of hilA expression. *Mol Microbiol, 22*(4), 703-714.

Barrow, P. A., Berchieri, A., Freitas Neto, O. C. d., & Lovell, M. (2015). The contribution of aerobic and anaerobic respiration to intestinal colonization and virulence for Salmonella typhimurium in the chicken. *Avian Pathology, 44*(5), 401-407. doi:10.1080/03079457.2015.1062841

Barthel, M., Hapfelmeier, S., Quintanilla-Martinez, L., Kremer, M., Rohde, M., Hogardt, M., Pfeffer, K., Russmann, H., & Hardt, W. D. (2003). Pretreatment of mice with streptomycin provides a Salmonella enterica serovar Typhimurium colitis model that allows analysis of both pathogen and host. *Infect Immun, 71*(5), 2839-2858.

Begley, M., Gahan, C. G., & Hill, C. (2005). The interaction between bacteria and bile. *FEMS Microbiol Rev, 29*(4), 625-651. doi:10.1016/j.femsre.2004.09.003

Begley, M., Hill, C., & Gahan, C. G. M. (2006). Bile Salt Hydrolase Activity in Probiotics. *Applied and Environmental Microbiology, 72*(3), 1729-1738. doi:10.1128/AEM.72.3.1729-1738.2006

Belzer, C., Chia, L. W., Aalvink, S., Chamlagain, B., Piironen, V., Knol, J., & de Vos, W. M. (2017). Microbial Metabolic Networks at the Mucus Layer Lead to Diet-Independent Butyrate and Vitamin B12 Production by Intestinal Symbionts. *mBio, 8*(5). doi:10.1128/mBio.00770-17

Benjamin, W. H., Jr., Hall, P., Roberts, S. J., & Briles, D. E. (1990). The primary effect of the Ity locus is on the rate of growth of Salmonella typhimurium that are relatively protected from killing. *J Immunol, 144*(8), 3143-3151.

Bergeron, Julien R. C., Worrall, Liam J., De, S., Sgourakis, Nikolaos G., Cheung, Adrienne H., Lameignere, E., Okon, M., Wasney, Gregory A., Baker, D., McIntosh, Lawrence P., & Strynadka, Natalie C. J. (2015). The Modular Structure of the Inner-

Membrane Ring Component PrgK Facilitates Assembly of the Type III Secretion System Basal Body. *Structure, 23*(1), 161-172. doi:10.1016/j.str.2014.10.021

Bergström, J. H., Berg, K. A., Rodríguez-Piñeiro, A. M., Stecher, B., Johansson, M. E. V., & Hansson, G. C. (2014). AGR2, an Endoplasmic Reticulum Protein, Is Secreted into the Gastrointestinal Mucus. *PLoS ONE, 9*(8), e104186. doi:10.1371/journal.pone.0104186

Berry, D., Kuzyk, O., Rauch, I., Heider, S., Schwab, C., Hainzl, E., Decker, T., Müller, M., Strobl, B., Schleper, C., Urich, T., Wagner, M., Kenner, L., & Loy, A. (2015). Intestinal Microbiota Signatures Associated with Inflammation History in Mice Experiencing Recurring Colitis. *Frontiers in Microbiology, 6*, 1408. doi:10.3389/fmicb.2015.01408

Berry, D., Schwab, C., Milinovich, G., Reichert, J., Ben Mahfoudh, K., Decker, T., Engel, M., Hai, B., Hainzl, E., Heider, S., Kenner, L., Muller, M., Rauch, I., Strobl, B., Wagner, M., Schleper, C., Urich, T., & Loy, A. (2012). Phylotype-level 16S rRNA analysis reveals new bacterial indicators of health state in acute murine colitis. *ISME J, 6*(11), 2091-2106. doi:10.1038/ismej.2012.39

Beutler, M. (2016). *Elucidating the mechanisms of dysbiosis and inflammation-induced 'blooms' of Salmonella enterica serovar Typhimurium and other enteric pathogens using a novel gnotobiotic mouse model.* (Dissertation), Ludwig-Maximilians-Universität München.

Biggs, M. B., Medlock, G. L., Moutinho, T. J., Lees, H. J., Swann, J. R., Kolling, G. L., & Papin, J. A. (2017). Systems-level metabolism of the altered Schaedler flora, a complete gut microbiota. *ISME J, 11*(2), 426-438. doi:10.1038/ismej.2016.130

Bik, E. M., Eckburg, P. B., Gill, S. R., Nelson, K. E., Purdom, E. A., Francois, F., Perez-Perez, G., Blaser, M. J., & Relman, D. A. (2006). Molecular analysis of the bacterial microbiota in the human stomach. *Proc Natl Acad Sci U S A, 103*(3), 732-737. doi:10.1073/pnas.0506655103

Bolger, A. M., Lohse, M., & Usadel, B. (2014). Trimmomatic: a flexible trimmer for Illumina sequence data. *Bioinformatics, 30*(15), 2114-2120. doi:10.1093/bioinformatics/btu170

Boyle, E. C., Brown, N. F., & Finlay, B. B. (2006). Salmonella enterica serovar Typhimurium effectors SopB, SopE, SopE2 and SipA disrupt tight junction structure and function. *Cell Microbiol, 8*(12), 1946-1957. doi:10.1111/j.1462-5822.2006.00762.x

Branchu, P., Matrat, S., Vareille, M., Garrivier, A., Durand, A., Crepin, S., Harel, J., Jubelin, G., & Gobert, A. P. (2014). NsrR, GadE, and GadX interplay in repressing expression of the Escherichia coli O157:H7 LEE pathogenicity island in response to nitric oxide. *PLoS Pathog, 10*(1), e1003874. doi:10.1371/journal.ppat.1003874

Brugiroux, S. (2016). *Establishment of a gnotobiotic mouse model to investigate the mechanisms of colonization resistance against Salmonella enterica serovar Typhimurium (S. Tm) and study of the protective role of the intestinal mucus layer during S. Tm infection.* (Dissertation), Ludwig-Maximilians-Uiversität München.

Brugiroux, S., Beutler, M., Pfann, C., Garzetti, D., Ruscheweyh, H. J., Ring, D., Diehl, M., Herp, S., Lotscher, Y., Hussain, S., Bunk, B., Pukall, R., Huson, D. H., Munch, P. C., McHardy, A. C., McCoy, K. D., Macpherson, A. J., Loy, A., Clavel, T., Berry, D., & Stecher, B. (2016). Genome-guided design of a defined mouse microbiota that confers colonization resistance against Salmonella enterica serovar Typhimurium. *Nat Microbiol, 2*, 16215. doi:10.1038/nmicrobiol.2016.215

Buckley, A. M., Webber, M. A., Cooles, S., Randall, L. P., La Ragione, R. M., Woodward, M. J., & Piddock, L. J. (2006). The AcrAB-TolC efflux system of Salmonella enterica serovar Typhimurium plays a role in pathogenesis. *Cell Microbiol, 8*(5), 847-856. doi:10.1111/j.1462-5822.2005.00671.x

Buffie, C. G., Bucci, V., Stein, R. R., McKenney, P. T., Ling, L., Gobourne, A., No, D., Liu, H., Kinnebrew, M., Viale, A., Littmann, E., van den Brink, M. R., Jenq, R. R., Taur,

Y., Sander, C., Cross, J. R., Toussaint, N. C., Xavier, J. B., & Pamer, E. G. (2015). Precision microbiome reconstitution restores bile acid mediated resistance to Clostridium difficile. *Nature, 517*(7533), 205-208. doi:10.1038/nature13828

Buffie, C. G., Jarchum, I., Equinda, M., Lipuma, L., Gobourne, A., Viale, A., Ubeda, C., Xavier, J., & Pamer, E. G. (2012). Profound Alterations of Intestinal Microbiota following a Single Dose of Clindamycin Results in Sustained Susceptibility to Clostridium difficile-Induced Colitis. *Infection and Immunity, 80*(1), 62-73. doi:10.1128/IAI.05496-11

Buffie, C. G., & Pamer, E. G. (2013). Microbiota-mediated colonization resistance against intestinal pathogens. *Nature reviews. Immunology, 13*(11), 790-801. doi:10.1038/nri3535

Burkinshaw, B. J., & Strynadka, N. C. J. (2014). Assembly and structure of the T3SS. *Biochimica et Biophysica Acta (BBA) - Molecular Cell Research, 1843*(8), 1649-1663. doi:https://doi.org/10.1016/j.bbamcr.2014.01.035

Byndloss, M. X., Olsan, E. E., Rivera-Chávez, F., Tiffany, C. R., Cevallos, S. A., Lokken, K. L., Torres, T. P., Byndloss, A. J., Faber, F., Gao, Y., Litvak, Y., Lopez, C. A., Xu, G., Napoli, E., Giulivi, C., Tsolis, R. M., Revzin, A., Lebrilla, C. B., & Bäumler, A. J. (2017). Microbiota-activated PPAR-γ signaling inhibits dysbiotic Enterobacteriaceae expansion. *Science, 357*(6351), 570-575. doi:10.1126/science.aam9949

Caballero, S., Kim, S., Carter, R. A., Leiner, I. M., Sušac, B., Miller, L., Kim, G. J., Ling, L., & Pamer, E. G. (2017). Cooperating Commensals Restore Colonization Resistance to Vancomycin-Resistant Enterococcus faecium. *Cell Host & Microbe, 21*(5), 592-602.e594. doi:https://doi.org/10.1016/j.chom.2017.04.002

Calo, J. R., Park, S. H., Baker, C. A., & Ricke, S. C. (2015). Specificity of Salmonella Typhimurium strain (ATCC 14028) growth responses to Salmonella serovar-generated spent media. *J Environ Sci Health B, 50*(6), 422-429. doi:10.1080/03601234.2015.1011962

Caporaso, J. G., Kuczynski, J., Stombaugh, J., Bittinger, K., Bushman, F. D., Costello, E. K., Fierer, N., Pena, A. G., Goodrich, J. K., Gordon, J. I., Huttley, G. A., Kelley, S. T., Knights, D., Koenig, J. E., Ley, R. E., Lozupone, C. A., McDonald, D., Muegge, B. D., Pirrung, M., Reeder, J., Sevinsky, J. R., Turnbaugh, P. J., Walters, W. A., Widmann, J., Yatsunenko, T., Zaneveld, J., & Knight, R. (2010). QIIME allows analysis of high-throughput community sequencing data. *Nat Methods, 7*(5), 335-336. doi:10.1038/nmeth.f.303

Carter, P. B., & Collins, F. M. (1974). THE ROUTE OF ENTERIC INFECTION IN NORMAL MICE. *J Exp Med, 139*(5), 1189-1203. doi:10.1084/jem.139.5.1189

Cash, H. L., Whitham, C. V., Behrendt, C. L., & Hooper, L. V. (2006). Symbiotic bacteria direct expression of an intestinal bactericidal lectin. *Science, 313*(5790), 1126-1130. doi:10.1126/science.1127119

Chand, D., Avinash, V. S., Yadav, Y., Pundle, A. V., Suresh, C. G., & Ramasamy, S. (2017). Molecular features of bile salt hydrolases and relevance in human health. *Biochimica et Biophysica Acta (BBA) - General Subjects, 1861*(1, Part A), 2981-2991. doi:https://doi.org/10.1016/j.bbagen.2016.09.024

Cherepanov, P. P., & Wackernagel, W. (1995). Gene disruption in Escherichia coli: Tc R and Km R cassettes with the option of Flp-catalyzed excision of the antibiotic-resistance determinant. *Gene, 158*(1), 9-14.

Coburn, B., Grassl Guntram, A., & Finlay, B. B. (2006). Salmonella, the host and disease: a brief review. *Immunology and Cell Biology, 85*(2), 112-118. doi:10.1038/sj.icb.7100007

Collazo, C. M., & Galán, J. E. (1997). The invasion-associated type-III protein secretion system inSalmonella – a review1Presented at the Workshop on `Type-4 Pili – Biogenesis, Adhesins, Protein Export, and DNA Import', Schloss Ringberg,

Germany, 26–29 November 1995.1. *Gene, 192*(1), 51-59. doi:https://doi.org/10.1016/S0378-1119(96)00825-6

Connolly, J. P., Finlay, B. B., & Roe, A. J. (2015). From ingestion to colonization: the influence of the host environment on regulation of the LEE encoded type III secretion system in enterohaemorrhagic Escherichia coli. *Front Microbiol, 6*, 568. doi:10.3389/fmicb.2015.00568

Corr, S. C., Li, Y., Riedel, C. U., Toole, P. W., Hill, C., & Gahan, C. G. M. (2007). Bacteriocin production as a mechanism for the antiinfective activity of Lactobacillus salivarius UCC118. *Proceedings of the National Academy of Sciences, 104*(18), 7617.

Daims, H., Bruhl, A., Amann, R., Schleifer, K. H., & Wagner, M. (1999). The domain-specific probe EUB338 is insufficient for the detection of all Bacteria: development and evaluation of a more comprehensive probe set. *Syst Appl Microbiol, 22*(3), 434-444. doi:10.1016/s0723-2020(99)80053-8

Das, P., Lahiri, A., Lahiri, A., & Chakravortty, D. (2009). Novel role of the nitrite transporter NirC in Salmonella pathogenesis: SPI2-dependent suppression of inducible nitric oxide synthase in activated macrophages. *Microbiology, 155*(8), 2476-2489. doi:doi:10.1099/mic.0.029611-0

Datsenko, K. A., & Wanner, B. L. (2000). One-step inactivation of chromosomal genes in Escherichia coli K-12 using PCR products. *Proc Natl Acad Sci U S A, 97*(12), 6640-6645. doi:10.1073/pnas.120163297

Day D, W., Mandal B, K., & Morson B, C. (1978). The rectal biopsy appearances in Salmonella colitis. *Histopathology, 2*(2), 117-131. doi:10.1111/j.1365-2559.1978.tb01700.x

de Aguiar Vallim, T. Q., Tarling, E. J., & Edwards, P. A. (2013). Pleiotropic roles of bile acids in metabolism. *Cell Metab, 17*(5), 657-669. doi:10.1016/j.cmet.2013.03.013

DeMoss, J. A., & Hsu, P. Y. (1991). NarK enhances nitrate uptake and nitrite excretion in Escherichia coli. *Journal of Bacteriology, 173*(11), 3303-3310.

den Besten, G., van Eunen, K., Groen, A. K., Venema, K., Reijngoud, D.-J., & Bakker, B. M. (2013). The role of short-chain fatty acids in the interplay between diet, gut microbiota, and host energy metabolism. *Journal of Lipid Research, 54*(9), 2325-2340. doi:10.1194/jlr.R036012

Deriu, E., Liu, Janet Z., Pezeshki, M., Edwards, Robert A., Ochoa, Roxanna J., Contreras, H., Libby, Stephen J., Fang, Ferric C., & Raffatellu, M. (2013). Probiotic Bacteria Reduce Salmonella Typhimurium Intestinal Colonization by Competing for Iron. *Cell Host & Microbe, 14*(1), 26-37. doi:https://doi.org/10.1016/j.chom.2013.06.007

Derrien, M., Vaughan, E. E., Plugge, C. M., & de Vos, W. M. (2004). Akkermansia muciniphila gen. nov., sp. nov., a human intestinal mucin-degrading bacterium. *Int J Syst Evol Microbiol, 54*(Pt 5), 1469-1476. doi:10.1099/ijs.0.02873-0

Devlin, A. S., & Fischbach, M. A. (2015). A biosynthetic pathway for a prominent class of microbiota-derived bile acids. *Nat Chem Biol, 11*(9), 685-690. doi:10.1038/nchembio.1864

Dewhirst, F. E., Chien, C. C., Paster, B. J., Ericson, R. L., Orcutt, R. P., Schauer, D. B., & Fox, J. G. (1999). Phylogeny of the defined murine microbiota: altered Schaedler flora. *Appl Environ Microbiol, 65*(8), 3287-3292.

Diard, M., Garcia, V., Maier, L., Remus-Emsermann, M. N., Regoes, R. R., Ackermann, M., & Hardt, W. D. (2013). Stabilization of cooperative virulence by the expression of an avirulent phenotype. *Nature, 494*(7437), 353-356. doi:10.1038/nature11913

Donohoe, D. R., Garge, N., Zhang, X., Sun, W., O'Connell, T. M., Bunger, M. K., & Bultman, S. J. (2011). The Microbiome and Butyrate Regulate Energy Metabolism and Autophagy in the Mammalian Colon. *Cell metabolism, 13*(5), 517-526. doi:10.1016/j.cmet.2011.02.018

Durant, J. A., Corrier, D. E., & Ricke, S. C. (2000). Short-chain volatile fatty acids modulate the expression of the hilA and invF genes of Salmonella typhimurium. *J Food Prot, 63*(5), 573-578.

Eade, C. R., Hung, C.-C., Bullard, B., Gonzalez-Escobedo, G., Gunn, J. S., & Altier, C. (2016). Bile Acids Function Synergistically To Repress Invasion Gene Expression in Salmonella by Destabilizing the Invasion Regulator HilD. *Infection and Immunity, 84*(8), 2198-2208. doi:10.1128/IAI.00177-16

Einsle, O. (2011). Chapter Sixteen - Structure and Function of Formate-Dependent Cytochrome c Nitrite Reductase, NrfA. In M. G. Klotz & L. Y. Stein (Eds.), *Methods in Enzymology* (Vol. 496, pp. 399-422): Academic Press.

Einsle, O., Messerschmidt, A., Stach, P., Bourenkov, G. P., Bartunik, H. D., Huber, R., & Kroneck, P. M. H. (1999). Structure of cytochrome c nitrite reductase. *Nature, 400*, 476. doi:10.1038/22802

Espey, M. G. (2013). Role of oxygen gradients in shaping redox relationships between the human intestine and its microbiota. *Free Radical Biology and Medicine, 55*, 130-140. doi:https://doi.org/10.1016/j.freeradbiomed.2012.10.554

Evans, M. R., Fink, R. C., Vazquez-Torres, A., Porwollik, S., Jones-Carson, J., McClelland, M., & Hassan, H. M. (2011). Analysis of the ArcA regulon in anaerobically grown Salmonella enterica sv. Typhimurium. *BMC Microbiol, 11*, 58. doi:10.1186/1471-2180-11-58

Falany, C. N., Johnson, M. R., Barnes, S., & Diasio, R. B. (1994). Glycine and taurine conjugation of bile acids by a single enzyme. Molecular cloning and expression of human liver bile acid CoA:amino acid N-acyltransferase. *J Biol Chem, 269*(30), 19375-19379.

Fenn, K., Strandwitz, P., Stewart, E. J., Dimise, E., Rubin, S., Gurubacharya, S., Clardy, J., & Lewis, K. (2017). Quinones are growth factors for the human gut microbiota. *Microbiome, 5*(1), 161. doi:10.1186/s40168-017-0380-5

Fink, R. C., Evans, M. R., Porwollik, S., Vazquez-Torres, A., Jones-Carson, J., Troxell, B., Libby, S. J., McClelland, M., & Hassan, H. M. (2007). FNR is a global regulator of virulence and anaerobic metabolism in Salmonella enterica serovar Typhimurium (ATCC 14028s). *J Bacteriol, 189*(6), 2262-2273. doi:10.1128/jb.00726-06

Fukuda, S., Toh, H., Hase, K., Oshima, K., Nakanishi, Y., Yoshimura, K., Tobe, T., Clarke, J. M., Topping, D. L., Suzuki, T., Taylor, T. D., Itoh, K., Kikuchi, J., Morita, H., Hattori, M., & Ohno, H. (2011). Bifidobacteria can protect from enteropathogenic infection through production of acetate. *Nature, 469*(7331), 543-547. doi:10.1038/nature09646

Furusawa, Y., Obata, Y., Fukuda, S., Endo, T. A., Nakato, G., Takahashi, D., Nakanishi, Y., Uetake, C., Kato, K., Kato, T., Takahashi, M., Fukuda, N. N., Murakami, S., Miyauchi, E., Hino, S., Atarashi, K., Onawa, S., Fujimura, Y., Lockett, T., Clarke, J. M., Topping, D. L., Tomita, M., Hori, S., Ohara, O., Morita, T., Koseki, H., Kikuchi, J., Honda, K., Hase, K., & Ohno, H. (2013). Commensal microbe-derived butyrate induces the differentiation of colonic regulatory T cells. *Nature, 504*(7480), 446-450. doi:10.1038/nature12721

Galan, J. E., & Curtiss, R., 3rd. (1990). Expression of Salmonella typhimurium genes required for invasion is regulated by changes in DNA supercoiling. *Infect Immun, 58*(6), 1879-1885.

Galkin, V. E., Orlova, A., VanLoock, M. S., Zhou, D., Galán, J. E., & Egelman, E. H. (2002). The bacterial protein SipA polymerizes G-actin and mimics muscle nebulin. *Nature Structural Biology, 9*, 518. doi:10.1038/nsb811

Gao, L., Li, J. Q., Zhou, Y. Z., Huang, X., Qin, X. M., & Du, G. H. (2018). The effects of baicalein on cortical pro-inflammatory cytokines and the intestinal microbiome in

senescence accelerated mouse prone 8. *ACS Chem Neurosci*. doi:10.1021/acschemneuro.8b00074

Gerlach, R. G., Jackel, D., Stecher, B., Wagner, C., Lupas, A., Hardt, W. D., & Hensel, M. (2007). Salmonella Pathogenicity Island 4 encodes a giant non-fimbrial adhesin and the cognate type 1 secretion system. *Cell Microbiol, 9*(7), 1834-1850. doi:10.1111/j.1462-5822.2007.00919.x

Gilberthorpe, N. J., & Poole, R. K. (2008). Nitric oxide homeostasis in Salmonella typhimurium: roles of respiratory nitrate reductase and flavohemoglobin. *J Biol Chem, 283*(17), 11146-11154. doi:10.1074/jbc.M708019200

Gong, M., Xu, S., Jin, Y., Zhang, Y., Dadzie, I., Zhang, X., Wang, Z., Zhu, Y., Ni, B., Sheng, X., & Huang, X. (2015). 5'-UTR of malS increases the invasive capacity of Salmonella enterica serovar Typhi by influencing the expression of bax. *Future Microbiol, 10*(6), 941-954. doi:10.2217/fmb.15.12

Gordon, M. A. (2008). Salmonella infections in immunocompromised adults. *J Infect, 56*(6), 413-422. doi:10.1016/j.jinf.2008.03.012

Gunsalus, R. P., & Park, S. J. (1994). Aerobic-anaerobic gene regulation in Escherichia coli: control by the ArcAB and Fnr regulons. *Res Microbiol, 145*(5-6), 437-450.

Häberli, L. (2005). *Funktion und Expression von Salmonella Typhimurium Virulenzgenen im Maus-Kolitis Modell.* (Diplomarbeit), Eidgenössischen Technischen Hochschule Zürich.

Hapfelmeier, S., Ehrbar, K., Stecher, B., Barthel, M., Kremer, M., & Hardt, W. D. (2004). Role of the Salmonella pathogenicity island 1 effector proteins SipA, SopB, SopE, and SopE2 in Salmonella enterica subspecies 1 serovar Typhimurium colitis in streptomycin-pretreated mice. *Infect Immun, 72*(2), 795-809.

Hapfelmeier, S., Stecher, B., Barthel, M., Kremer, M., Muller, A. J., Heikenwalder, M., Stallmach, T., Hensel, M., Pfeffer, K., Akira, S., & Hardt, W. D. (2005). The Salmonella pathogenicity island (SPI)-2 and SPI-1 type III secretion systems allow Salmonella serovar typhimurium to trigger colitis via MyD88-dependent and MyD88-independent mechanisms. *J Immunol, 174*(3), 1675-1685.

Harel, A., Haggblom, M. M., Falkowski, P. G., & Yee, N. (2016). Evolution of prokaryotic respiratory molybdoenzymes and the frequency of their genomic co-occurrence. *FEMS Microbiol Ecol, 92*(12). doi:10.1093/femsec/fiw187

Harrell, L., Wang, Y., Antonopoulos, D., Young, V., Lichtenstein, L., Huang, Y., Hanauer, S., & Chang, E. (2012). Standard Colonic Lavage Alters the Natural State of Mucosal-Associated Microbiota in the Human Colon. *PLoS ONE, 7*(2), e32545. doi:10.1371/journal.pone.0032545

He, M., Fang, S., Huang, X., Zhao, Y., Ke, S., Yang, H., Li, Z., Gao, J., Chen, C., & Huang, L. (2016). Evaluating the Contribution of Gut Microbiota to the Variation of Porcine Fatness with the Cecum and Fecal Samples. *Frontiers in Microbiology, 7*, 2108. doi:10.3389/fmicb.2016.02108

Hecht, A. L., Casterline, B. W., Earley, Z. M., Goo, Y. A., Goodlett, D. R., & Bubeck Wardenburg, J. (2016). Strain competition restricts colonization of an enteric pathogen and prevents colitis. *EMBO reports, 17*(9), 1281.

Hensel, M., Shea, J. E., Waterman, S. R., Mundy, R., Nikolaus, T., Banks, G., Vazquez-Torres, A., Gleeson, C., Fang, F. C., & Holden, D. W. (1998). Genes encoding putative effector proteins of the type III secretion system of Salmonella pathogenicity island 2 are required for bacterial virulence and proliferation in macrophages. *Mol Microbiol, 30*(1), 163-174.

Hille, R. (1996). The Mononuclear Molybdenum Enzymes. *Chemical Reviews, 96*(7), 2757-2816. doi:10.1021/cr950061t

Hoiseth, S. K., & Stocker, B. A. (1981). Aromatic-dependent Salmonella typhimurium are non-virulent and effective as live vaccines. *Nature, 291*(5812), 238-239.

Hsiao, A., Shamsir Ahmed, A. M., Subramanian, S., Griffin, N. W., Drewry, L. L., Petri, W. A., Haque, R., Ahmed, T., & Gordon, J. I. (2014). Members of the human gut microbiota involved in recovery from Vibrio cholerae infection. *Nature, 515*(7527), 423-426. doi:10.1038/nature13738

Hueck, C. J. (1998). Type III Protein Secretion Systems in Bacterial Pathogens of Animals and Plants. *Microbiology and Molecular Biology Reviews, 62*(2), 379-433.

Hughes, D. T., Terekhova, D. A., Liou, L., Hovde, C. J., Sahl, J. W., Patankar, A. V., Gonzalez, J. E., Edrington, T. S., Rasko, D. A., & Sperandio, V. (2010). Chemical sensing in mammalian host-bacterial commensal associations. *Proc Natl Acad Sci U S A, 107*(21), 9831-9836. doi:10.1073/pnas.1002551107

Ibarra, J. A., Knodler, L. A., Sturdevant, D. E., Virtaneva, K., Carmody, A. B., Fischer, E. R., Porcella, S. F., & Steele-Mortimer, O. (2010). Induction of Salmonella pathogenicity island 1 under different growth conditions can affect Salmonella–host cell interactions in vitro. *Microbiology, 156*(Pt 4), 1120-1133. doi:10.1099/mic.0.032896-0

Jarvis, K. G., Giron, J. A., Jerse, A. E., McDaniel, T. K., Donnenberg, M. S., & Kaper, J. B. (1995). Enteropathogenic Escherichia coli contains a putative type III secretion system necessary for the export of proteins involved in attaching and effacing lesion formation. *Proc Natl Acad Sci U S A, 92*(17), 7996-8000.

Jia, W., Tovell, N., Clegg, S., Trimmer, M., & Cole, J. (2009). A single channel for nitrate uptake, nitrite export and nitrite uptake by Escherichia coli NarU and a role for NirC in nitrite export and uptake. *Biochem J, 417*(1), 297-304. doi:10.1042/bj20080746

Johansson, M. E., Phillipson, M., Petersson, J., Velcich, A., Holm, L., & Hansson, G. C. (2008). The inner of the two Muc2 mucin-dependent mucus layers in colon is devoid of bacteria. *Proc Natl Acad Sci U S A, 105*(39), 15064-15069. doi:10.1073/pnas.0803124105

Jones, B. V., Begley, M., Hill, C., Gahan, C. G. M., & Marchesi, J. R. (2008). Functional and comparative metagenomic analysis of bile salt hydrolase activity in the human gut microbiome. *Proceedings of the National Academy of Sciences, 105*(36), 13580-13585. doi:10.1073/pnas.0804437105

Kanamaru, K., Kanamaru, K., Tatsuno, I., Tobe, T., & Sasakawa, C. (2000). SdiA, an Escherichia coli homologue of quorum-sensing regulators, controls the expression of virulence factors in enterohaemorrhagic Escherichia coli O157:H7. *Mol Microbiol, 38*(4), 805-816.

Kaniga, K., Bossio, J. C., & Galan, J. E. (1994). The Salmonella typhimurium invasion genes invF and invG encode homologues of the AraC and PulD family of proteins. *Mol Microbiol, 13*(4), 555-568.

Kaper, J. B., Nataro, J. P., & Mobley, H. L. T. (2004). Pathogenic Escherichia coli. *Nature Reviews Microbiology, 2*, 123. doi:10.1038/nrmicro818

Kim, S., Covington, A., & Pamer, E. G. (2017). The intestinal microbiota: Antibiotics, colonization resistance, and enteric pathogens. *Immunol Rev, 279*(1), 90-105. doi:10.1111/imr.12563

Klumpp, S., Scott, M., Pedersen, S., & Hwa, T. (2013). Molecular crowding limits translation and cell growth. *Proc Natl Acad Sci U S A, 110*(42), 16754-16759. doi:10.1073/pnas.1310377110

Koch, H., Lucker, S., Albertsen, M., Kitzinger, K., Herbold, C., Spieck, E., Nielsen, P. H., Wagner, M., & Daims, H. (2015). Expanded metabolic versatility of ubiquitous nitrite-oxidizing bacteria from the genus Nitrospira. *Proc Natl Acad Sci U S A, 112*(36), 11371-11376. doi:10.1073/pnas.1506533112

Krych, L., Hansen, C. H. F., Hansen, A. K., van den Berg, F. W. J., & Nielsen, D. S. (2013). Quantitatively Different, yet Qualitatively Alike: A Meta-Analysis of the Mouse Core

Gut Microbiome with a View towards the Human Gut Microbiome. *PLoS ONE, 8*(5), e62578. doi:10.1371/journal.pone.0062578

Laughlin, R. C., Knodler, L. A., Barhoumi, R., Payne, H. R., Wu, J., Gomez, G., Pugh, R., Lawhon, S. D., Bäumler, A. J., Steele-Mortimer, O., & Adams, L. G. (2014). Spatial Segregation of Virulence Gene Expression during Acute Enteric Infection with Salmonella enterica serovar Typhimurium. *mBio, 5*(1), e00946-00913. doi:10.1128/mBio.00946-13

Lawhon, S. D., Maurer, R., Suyemoto, M., & Altier, C. (2002). Intestinal short-chain fatty acids alter Salmonella typhimurium invasion gene expression and virulence through BarA/SirA. *Mol Microbiol, 46*(5), 1451-1464.

Lawley, T. D., Bouley, D. M., Hoy, Y. E., Gerke, C., Relman, D. A., & Monack, D. M. (2008). Host transmission of Salmonella enterica serovar Typhimurium is controlled by virulence factors and indigenous intestinal microbiota. *Infect Immun, 76*(1), 403-416. doi:10.1128/iai.01189-07

Lazazzera, B. A., Beinert, H., Khoroshilova, N., Kennedy, M. C., & Kiley, P. J. (1996). DNA binding and dimerization of the Fe− S-containing FNR protein from Escherichia coli are regulated by oxygen. *Journal of Biological Chemistry, 271*(5), 2762-2768.

Leatham, M. P., Banerjee, S., Autieri, S. M., Mercado-Lubo, R., Conway, T., & Cohen, P. S. (2009). Precolonized human commensal Escherichia coli strains serve as a barrier to E. coli O157:H7 growth in the streptomycin-treated mouse intestine. *Infect Immun, 77*(7), 2876-2886. doi:10.1128/iai.00059-09

Lee, C. A., & Falkow, S. (1990). The ability of Salmonella to enter mammalian cells is affected by bacterial growth state. *Proceedings of the National Academy of Sciences, 87*(11), 4304.

Li, H., & Durbin, R. (2009). Fast and accurate short read alignment with Burrows-Wheeler transform. *Bioinformatics, 25*(14), 1754-1760. doi:10.1093/bioinformatics/btp324

Lichtman, J. S., Ferreyra, J. A., Ng, K. M., Smits, S. A., Sonnenburg, J. L., & Elias, J. E. (2016). Host-Microbiota Interactions in the Pathogenesis of Antibiotic-Associated Diseases. *Cell Reports, 14*(5), 1049-1061. doi:10.1016/j.celrep.2016.01.009

Linnenbrink, M., Wang, J., Hardouin, E. A., Kunzel, S., Metzler, D., & Baines, J. F. (2013). The role of biogeography in shaping diversity of the intestinal microbiota in house mice. *Mol Ecol, 22*(7), 1904-1916. doi:10.1111/mec.12206

Lopez, C. A., Rivera-Chávez, F., Byndloss, M. X., & Bäumler, A. J. (2015). The Periplasmic Nitrate Reductase NapABC Supports Luminal Growth of Salmonella enterica Serovar Typhimurium during Colitis. *Infection and Immunity, 83*(9), 3470-3478. doi:10.1128/IAI.00351-15

Lorkowski, M., Felipe-López, A., Danzer, C. A., Hansmeier, N., & Hensel, M. (2014). Salmonella enterica Invasion of Polarized Epithelial Cells Is a Highly Cooperative Effort. *Infection and Immunity, 82*(6), 2657-2667. doi:10.1128/IAI.00023-14

Loy, A., Pfann, C., Steinberger, M., Hanson, B., Herp, S., Brugiroux, S., Gomes Neto, J. C., Boekschoten, M. V., Schwab, C., Urich, T., Ramer-Tait, A. E., Rattei, T., Stecher, B., & Berry, D. (2017). Lifestyle and Horizontal Gene Transfer-Mediated Evolution of Mucispirillum schaedleri, a Core Member of the Murine Gut Microbiota. *mSystems, 2*(1). doi:10.1128/mSystems.00171-16

Macfarlane, S., & Macfarlane, G. T. (2003). Regulation of short-chain fatty acid production. *Proceedings of the Nutrition Society, 62*(1), 67-72. doi:10.1079/PNS2002207

Macfarlane, S., Quigley, M. E., Hopkins, M. J., Newton, D. F., & Macfarlane, G. T. (1998). Polysaccharide degradation by human intestinal bacteria during growth under multi-substrate limiting conditions in a three-stage continuous culture system. *FEMS Microbiol Ecol, 26*(3), 231-243. doi:10.1111/j.1574-6941.1998.tb00508.x

Maier, L., Diard, M., Sellin, M. E., Chouffane, E. S., Trautwein-Weidner, K., Periaswamy, B., Slack, E., Dolowschiak, T., Stecher, B., Loverdo, C., Regoes, R. R., & Hardt, W. D.

(2014). Granulocytes impose a tight bottleneck upon the gut luminal pathogen population during Salmonella typhimurium colitis. *PLoS Pathog, 10*(12), e1004557. doi:10.1371/journal.ppat.1004557

Maier, L., Vyas, R., Cordova, Carmen D., Lindsay, H., Schmidt, Thomas Sebastian B., Brugiroux, S., Periaswamy, B., Bauer, R., Sturm, A., Schreiber, F., von Mering, C., Robinson, Mark D., Stecher, B., & Hardt, W.-D. (2013). Microbiota-Derived Hydrogen Fuels Salmonella Typhimurium Invasion of the Gut Ecosystem. *Cell Host & Microbe, 14*(6), 641-651. doi:http://dx.doi.org/10.1016/j.chom.2013.11.002

Marteyn, B., West, N. P., Browning, D. F., Cole, J. A., Shaw, J. G., Palm, F., Mounier, J., Prevost, M. C., Sansonetti, P., & Tang, C. M. (2010). Modulation of Shigella virulence in response to available oxygen in vivo. *Nature, 465*(7296), 355-358. doi:10.1038/nature08970

Mehta, A. P., Abdelwahed, S. H., Xu, H., & Begley, T. P. (2014). Molybdopterin biosynthesis: trapping of intermediates for the MoaA-catalyzed reaction using 2'-deoxyGTP and 2'-chloroGTP as substrate analogues. *J Am Chem Soc, 136*(30), 10609-10614. doi:10.1021/ja502663k

Merritt, M. E., & Donaldson, J. R. (2009). Effect of bile salts on the DNA and membrane integrity of enteric bacteria. *J Med Microbiol, 58*(Pt 12), 1533-1541. doi:10.1099/jmm.0.014092-0

Miller, T. L., & Wolin, M. J. (1996). Pathways of acetate, propionate, and butyrate formation by the human fecal microbial flora. *Appl Environ Microbiol, 62*(5), 1589-1592.

Mills, P. C., Rowley, G., Spiro, S., Hinton, J. C. D., & Richardson, D. J. (2008). A combination of cytochrome c nitrite reductase (NrfA) and flavorubredoxin (NorV) protects Salmonella enterica serovar Typhimurium against killing by NO in anoxic environments. *Microbiology, 154*(4), 1218-1228. doi:doi:10.1099/mic.0.2007/014290-0

Moser, S. A., & Savage, D. C. (2001). Bile Salt Hydrolase Activity and Resistance to Toxicity of Conjugated Bile Salts Are Unrelated Properties in Lactobacilli. *Applied and Environmental Microbiology, 67*(8), 3476-3480. doi:10.1128/AEM.67.8.3476-3480.2001

Muller, A. A., Dolowschiak, T., Sellin, M. E., Felmy, B., Verbree, C., Gadient, S., Westermann, A. J., Vogel, J., LeibundGut-Landmann, S., & Hardt, W. D. (2016). An NK Cell Perforin Response Elicited via IL-18 Controls Mucosal Inflammation Kinetics during Salmonella Gut Infection. *PLoS Pathog, 12*(6), e1005723. doi:10.1371/journal.ppat.1005723

Nakanishi, N., Tashiro, K., Kuhara, S., Hayashi, T., Sugimoto, N., & Tobe, T. (2009). Regulation of virulence by butyrate sensing in enterohaemorrhagic Escherichia coli. *Microbiology, 155*(Pt 2), 521-530. doi:10.1099/mic.0.023499-0

Nedialkova, L. P. (2014). *Investigation of competition and release mechanism of colicin Ib in Salmonella enterica serovar Typhimurium.* (Dissertation), Ludwig-Maximilians-Universität München.

Nichols, D., Lewis, K., Orjala, J., Mo, S., Ortenberg, R., O'Connor, P., Zhao, C., Vouros, P., Kaeberlein, T., & Epstein, S. S. (2008). Short Peptide Induces an “Uncultivable” Microorganism To Grow In Vitro. *Applied and Environmental Microbiology, 74*(15), 4889-4897. doi:10.1128/AEM.00393-08

Nishino, K., Latifi, T., & Groisman, E. A. (2006). Virulence and drug resistance roles of multidrug efflux systems of Salmonella enterica serovar Typhimurium. *Mol Microbiol, 59*(1), 126-141. doi:10.1111/j.1365-2958.2005.04940.x

Notti, R. Q., & Stebbins, C. E. (2016). The Structure and Function of Type III Secretion Systems. *Microbiology spectrum, 4*(1), 10.1128/microbiolspec.VMBF-0004-2015. doi:10.1128/microbiolspec.VMBF-0004-2015

Ochman, H., Soncini, F. C., Solomon, F., & Groisman, E. A. (1996). Identification of a pathogenicity island required for Salmonella survival in host cells. *Proceedings of the National Academy of Sciences, 93*(15), 7800-7804.

Ohno, M., Okano, I., Watsuji, T., Kakinuma, T., Ueda, K., & Beppu, T. (1999). Establishing the independent culture of a strictly symbiotic bacterium Symbiobacterium thermophilum from its supporting Bacillus strain. *Biosci Biotechnol Biochem, 63*(6), 1083-1090. doi:10.1271/bbb.63.1083

Okoro, C. K., Kingsley, R. A., Connor, T. R., Harris, S. R., Parry, C. M., Al-Mashhadani, M. N., Kariuki, S., Msefula, C. L., Gordon, M. A., de Pinna, E., Wain, J., Heyderman, R. S., Obaro, S., Alonso, P. L., Mandomando, I., MacLennan, C. A., Tapia, M. D., Levine, M. M., Tennant, S. M., Parkhill, J., & Dougan, G. (2012). Intracontinental spread of human invasive Salmonella Typhimurium pathovariants in sub-Saharan Africa. *Nat Genet, 44*(11), 1215-1221. doi:10.1038/ng.2423

Orcutt, R., Gianni, F., & Judge, R. (1987). Development of an “Altered Schaedler Flora” for NCI gnotobiotic rodents. *Microecol. Ther, 17*, 59.

Pacheco, A. R., Curtis, M. M., Ritchie, J. M., Munera, D., Waldor, M. K., Moreira, C. G., & Sperandio, V. (2012). Fucose sensing regulates bacterial intestinal colonization. *Nature, 492*(7427), 113-117. doi:10.1038/nature11623

Park, S. W., Zhen, G., Verhaeghe, C., Nakagami, Y., Nguyenvu, L. T., Barczak, A. J., Killeen, N., & Erle, D. J. (2009). The protein disulfide isomerase AGR2 is essential for production of intestinal mucus. *Proc Natl Acad Sci U S A, 106*(17), 6950-6955. doi:10.1073/pnas.0808722106

Peng, L., Li, Z. R., Green, R. S., Holzman, I. R., & Lin, J. (2009). Butyrate enhances the intestinal barrier by facilitating tight junction assembly via activation of AMP-activated protein kinase in Caco-2 cell monolayers. *J Nutr, 139*(9), 1619-1625. doi:10.3945/jn.109.104638

Price-Carter, M., Tingey, J., Bobik, T. A., & Roth, J. R. (2001). The alternative electron acceptor tetrathionate supports B12-dependent anaerobic growth of Salmonella enterica serovar typhimurium on ethanolamine or 1,2-propanediol. *J Bacteriol, 183*(8), 2463-2475. doi:10.1128/jb.183.8.2463-2475.2001

Prieto, A. I., Ramos-Morales, F., & Casadesus, J. (2004). Bile-induced DNA damage in Salmonella enterica. *Genetics, 168*(4), 1787-1794. doi:10.1534/genetics.104.031062

Prouty, A. M., Brodsky, I. E., Manos, J., Belas, R., Falkow, S., & Gunn, J. S. (2004). Transcriptional regulation of Salmonella enterica serovar Typhimurium genes by bile. *FEMS Immunol Med Microbiol, 41*(2), 177-185. doi:10.1016/j.femsim.2004.03.002

Prouty, A. M., & Gunn, J. S. (2000). Salmonella enterica Serovar Typhimurium Invasion Is Repressed in the Presence of Bile. *Infection and Immunity, 68*(12), 6763-6769.

Qiu, L., Tao, X., Xiong, H., Yu, J., & Wei, H. (2018). Lactobacillus plantarum ZDY04 exhibits a strain-specific property of lowering TMAO via the modulation of gut microbiota in mice. *Food Funct*. doi:10.1039/c8fo00349a

Rakoff-Nahoum, S., Paglino, J., Eslami-Varzaneh, F., Edberg, S., & Medzhitov, R. (2004). Recognition of Commensal Microflora by Toll-Like Receptors Is Required for Intestinal Homeostasis. *Cell, 118*(2), 229-241. doi:10.1016/j.cell.2004.07.002

Rausch, P., Rehman, A., Künzel, S., Häsler, R., Ott, S. J., Schreiber, S., Rosenstiel, P., Franke, A., & Baines, J. F. (2011). Colonic mucosa-associated microbiota is influenced by an interaction of Crohn disease and FUT2 (Secretor) genotype. *Proceedings of the National Academy of Sciences, 108*(47), 19030-19035. doi:10.1073/pnas.1106408108

Ravussin, Y., Koren, O., Spor, A., LeDuc, C., Gutman, R., Stombaugh, J., Knight, R., Ley, R. E., & Leibel, R. L. (2012). Responses of gut microbiota to diet composition and

weight loss in lean and obese mice. *Obesity (Silver Spring), 20*(4), 738-747. doi:10.1038/oby.2011.111

Ridlon, J. M., Harris, S. C., Bhowmik, S., Kang, D.-J., & Hylemon, P. B. (2016). Consequences of bile salt biotransformations by intestinal bacteria. *Gut Microbes, 7*(1), 22-39. doi:10.1080/19490976.2015.1127483

Ridlon, J. M., Kang, D.-J., & Hylemon, P. B. (2006). Bile salt biotransformations by human intestinal bacteria. *Journal of Lipid Research, 47*(2), 241-259. doi:10.1194/jlr.R500013-JLR200

Rivera-Chavez, F., & Baumler, A. J. (2015). The Pyromaniac Inside You: Salmonella Metabolism in the Host Gut. *Annu Rev Microbiol, 69*, 31-48. doi:10.1146/annurev-micro-091014-104108

Rivera-Chavez, F., Winter, S. E., Lopez, C. A., Xavier, M. N., Winter, M. G., Nuccio, S. P., Russell, J. M., Laughlin, R. C., Lawhon, S. D., Sterzenbach, T., Bevins, C. L., Tsolis, R. M., Harshey, R., Adams, L. G., & Baumler, A. J. (2013). Salmonella uses energy taxis to benefit from intestinal inflammation. *PLoS Pathog, 9*(4), e1003267. doi:10.1371/journal.ppat.1003267

Rivera-Chávez, F., Zhang, Lillian F., Faber, F., Lopez, Christopher A., Byndloss, Mariana X., Olsan, Erin E., Xu, G., Velazquez, Eric M., Lebrilla, Carlito B., Winter, Sebastian E., & Bäumler, Andreas J. (2016). Depletion of Butyrate-Producing Clostridia from the Gut Microbiota Drives an Aerobic Luminal Expansion of Salmonella. *Cell Host & Microbe, 19*(4), 443-454. doi:10.1016/j.chom.2016.03.004

Robertson, B. R., O'Rourke, J. L., Neilan, B. A., Vandamme, P., On, S. L. W., Fox, J. G., & Lee, A. (2005). Mucispirillum schaedleri gen. nov., sp. nov., a spiral-shaped bacterium colonizing the mucus layer of the gastrointestinal tract of laboratory rodents. *International Journal of Systematic and Evolutionary Microbiology, 55*(3), 1199-1204. doi:10.1099/ijs.0.63472-0

Robinson, M. D., McCarthy, D. J., & Smyth, G. K. (2010). edgeR: a Bioconductor package for differential expression analysis of digital gene expression data. *Bioinformatics, 26*(1), 139-140. doi:10.1093/bioinformatics/btp616

Rooks, M. G., Veiga, P., Wardwell-Scott, L. H., Tickle, T., Segata, N., Michaud, M., Gallini, C. A., Beal, C., van Hylckama-Vlieg, J. E., & Ballal, S. A. (2014). Gut microbiome composition and function in experimental colitis during active disease and treatment-induced remission. *ISME J, 8*(7), 1403.

Rosshart, S. P., Vassallo, B. G., Angeletti, D., Hutchinson, D. S., Morgan, A. P., Takeda, K., Hickman, H. D., McCulloch, J. A., Badger, J. H., Ajami, N. J., Trinchieri, G., Pardo-Manuel de Villena, F., Yewdell, J. W., & Rehermann, B. (2017). Wild Mouse Gut Microbiota Promotes Host Fitness and Improves Disease Resistance. *Cell, 171*(5), 1015-1028.e1013. doi:10.1016/j.cell.2017.09.016

Rycovska-Blume, A., Lü, W., Andrade, S., Fendler, K., & Einsle, O. (2015). Chapter Twenty-Two - Structural and Functional Studies of NirC from Salmonella typhimurium. In A. K. Shukla (Ed.), *Methods in Enzymology* (Vol. 556, pp. 475-497): Academic Press.

Rycovska, A., Hatahet, L., Fendler, K., & Michel, H. (2012). The nitrite transport protein NirC from Salmonella typhimurium is a nitrite/proton antiporter. *Biochimica et Biophysica Acta (BBA) - Biomembranes, 1818*(5), 1342-1350. doi:https://doi.org/10.1016/j.bbamem.2012.02.004

Santos, R. L., Zhang, S., Tsolis, R. M., Kingsley, R. A., Garry Adams, L., & Bäumler, A. J. (2001). Animal models of Salmonella infections: enteritis versus typhoid fever. *Microbes and Infection, 3*(14), 1335-1344. doi:https://doi.org/10.1016/S1286-4579(01)01495-2

Sarma-Rupavtarm, R. B., Ge, Z., Schauer, D. B., Fox, J. G., & Polz, M. F. (2004). Spatial Distribution and Stability of the Eight Microbial Species of the Altered Schaedler

Flora in the Mouse Gastrointestinal Tract. *Applied and Environmental Microbiology, 70*(5), 2791-2800. doi:10.1128/aem.70.5.2791-2800.2004

Sassone-Corsi, M., Nuccio, S.-P., Liu, H., Hernandez, D., Vu, C. T., Takahashi, A. A., Edwards, R. A., & Raffatellu, M. (2016). Microcins mediate competition among Enterobacteriaceae in the inflamed gut. *Nature, 540*(7632), 280-283. doi:10.1038/nature20557

Savage, D. C., & Dubos, R. (1968). ALTERATIONS IN THE MOUSE CECUM AND ITS FLORA PRODUCED BY ANTIBACTERIAL DRUGS. *J Exp Med, 128*(1), 97-110.

Sayin, S. I., Wahlstrom, A., Felin, J., Jantti, S., Marschall, H. U., Bamberg, K., Angelin, B., Hyotylainen, T., Oresic, M., & Backhed, F. (2013). Gut microbiota regulates bile acid metabolism by reducing the levels of tauro-beta-muricholic acid, a naturally occurring FXR antagonist. *Cell Metab, 17*(2), 225-235. doi:10.1016/j.cmet.2013.01.003

Schaedler, R. W., Dubos, R., & Costello, R. (1965). ASSOCIATION OF GERMFREE MICE WITH BACTERIA ISOLATED FROM NORMAL MICE. *J Exp Med, 122*(1), 77-82. doi:10.1084/jem.122.1.77

Schauer, D. B., & Falkow, S. (1993). Attaching and effacing locus of a Citrobacter freundii biotype that causes transmissible murine colonic hyperplasia. *Infect Immun, 61*(6), 2486-2492.

Scupham, A. J., Patton, T. G., Bent, E., & Bayles, D. O. (2008). Comparison of the cecal microbiota of domestic and wild turkeys. *Microb Ecol, 56*(2), 322-331. doi:10.1007/s00248-007-9349-4

Segata, N., Izard, J., Waldron, L., Gevers, D., Miropolsky, L., Garrett, W. S., & Huttenhower, C. (2011). Metagenomic biomarker discovery and explanation. *Genome Biology, 12*(6), R60-R60. doi:10.1186/gb-2011-12-6-r60

Sekirov, I., Tam, N. M., Jogova, M., Robertson, M. L., Li, Y., Lupp, C., & Finlay, B. B. (2008). Antibiotic-induced perturbations of the intestinal microbiota alter host susceptibility to enteric infection. *Infect Immun, 76*(10), 4726-4736. doi:10.1128/iai.00319-08

Sellin, M. E., Muller, A. A., Felmy, B., Dolowschiak, T., Diard, M., Tardivel, A., Maslowski, K. M., & Hardt, W. D. (2014). Epithelium-intrinsic NAIP/NLRC4 inflammasome drives infected enterocyte expulsion to restrict Salmonella replication in the intestinal mucosa. *Cell Host Microbe, 16*(2), 237-248. doi:10.1016/j.chom.2014.07.001

Selvanantham, T., Lin, Q., Guo, C. X., Surendra, A., Fieve, S., Escalante, N. K., Guttman, D. S., Streutker, C. J., Robertson, S. J., Philpott, D. J., & Mallevaey, T. (2016). NKT Cell–Deficient Mice Harbor an Altered Microbiota That Fuels Intestinal Inflammation during Chemically Induced Colitis. *The Journal of Immunology, 197*(11), 4464.

Serino, M., Luche, E., Gres, S., Baylac, A., Bergé, M., Cenac, C., Waget, A., Klopp, P., Iacovoni, J., Klopp, C., Mariette, J., Bouchez, O., Lluch, J., Ouarné, F., Monsan, P., Valet, P., Roques, C., Amar, J., Bouloumié, A., Théodorou, V., & Burcelin, R. (2012). Metabolic adaptation to a high-fat diet is associated with a change in the gut microbiota. *Gut, 61*(4), 543-553. doi:10.1136/gutjnl-2011-301012

Sistrunk, J. R., Nickerson, K. P., Chanin, R. B., Rasko, D. A., & Faherty, C. S. (2016). Survival of the Fittest: How Bacterial Pathogens Utilize Bile To Enhance Infection. *Clin Microbiol Rev, 29*(4), 819-836. doi:10.1128/cmr.00031-16

Song, H., Wang, W., Shen, B., Jia, H., Hou, Z., Chen, P., & Sun, Y. (2018). Pretreatment with probiotic Bifico ameliorates colitis-associated cancer in mice: Transcriptome and gut flora profiling. *Cancer Sci, 109*(3), 666-677. doi:10.1111/cas.13497

Song, M., Kim, H. J., Kim, E. Y., Shin, M., Lee, H. C., Hong, Y., Rhee, J. H., Yoon, H., Ryu, S., Lim, S., & Choy, H. E. (2004). ppGpp-dependent stationary phase induction of genes on Salmonella pathogenicity island 1. *J Biol Chem, 279*(33), 34183-34190. doi:10.1074/jbc.M313491200

Sonnenburg, J. L., Xu, J., Leip, D. D., Chen, C. H., Westover, B. P., Weatherford, J., Buhler, J. D., & Gordon, J. I. (2005). Glycan foraging in vivo by an intestine-adapted bacterial symbiont. *Science, 307*(5717), 1955-1959. doi:10.1126/science.1109051

Stecher, B., Barthel, M., Schlumberger, M. C., Haberli, L., Rabsch, W., Kremer, M., & Hardt, W. D. (2008). Motility allows S. Typhimurium to benefit from the mucosal defence. *Cell Microbiol, 10*(5), 1166-1180. doi:10.1111/j.1462-5822.2008.01118.x

Stecher, B., Berry, D., & Loy, A. (2013). Colonization resistance and microbial ecophysiology: using gnotobiotic mouse models and single-cell technology to explore the intestinal jungle. *FEMS Microbiol Rev, 37*(5), 793-829. doi:10.1111/1574-6976.12024

Stecher, B., Chaffron, S., Käppeli, R., Hapfelmeier, S., Freedrich, S., Weber, T. C., Kirundi, J., Suar, M., McCoy, K. D., von Mering, C., Macpherson, A. J., & Hardt, W.-D. (2010). Like Will to Like: Abundances of Closely Related Species Can Predict Susceptibility to Intestinal Colonization by Pathogenic and Commensal Bacteria. *PLoS Pathog, 6*(1), e1000711. doi:10.1371/journal.ppat.1000711

Stecher, B., Robbiani, R., Walker, A. W., Westendorf, A. M., Barthel, M., Kremer, M., Chaffron, S., Macpherson, A. J., Buer, J., Parkhill, J., Dougan, G., von Mering, C., & Hardt, W. D. (2007). Salmonella enterica serovar typhimurium exploits inflammation to compete with the intestinal microbiota. *PLoS Biol, 5*(10), 2177-2189. doi:10.1371/journal.pbio.0050244

Steele-Mortimer, O., Meresse, S., Gorvel, J. P., Toh, B. H., & Finlay, B. B. (1999). Biogenesis of Salmonella typhimurium-containing vacuoles in epithelial cells involves interactions with the early endocytic pathway. *Cell Microbiol, 1*(1), 33-49.

Studer, N., Desharnais, L., Beutler, M., Brugiroux, S., Terrazos, M. A., Menin, L., Schurch, C. M., McCoy, K. D., Kuehne, S. A., Minton, N. P., Stecher, B., Bernier-Latmani, R., & Hapfelmeier, S. (2016). Functional Intestinal Bile Acid 7alpha-Dehydroxylation by Clostridium scindens Associated with Protection from Clostridium difficile Infection in a Gnotobiotic Mouse Model. *Front Cell Infect Microbiol, 6*, 191. doi:10.3389/fcimb.2016.00191

Sung, J. Y., Shaffer, E. A., & Costerton, J. W. (1993). Antibacterial activity of bile salts against common biliary pathogens. Effects of hydrophobicity of the molecule and in the presence of phospholipids. *Dig Dis Sci, 38*(11), 2104-2112.

Tanaka, H., Doesburg, K., Iwasaki, T., & Mierau, I. (1999). Screening of Lactic Acid Bacteria for Bile Salt Hydrolase Activity. *Journal of Dairy Science, 82*(12), 2530-2535. doi:https://doi.org/10.3168/jds.S0022-0302(99)75506-2

Tartera, C., & Metcalf, E. S. (1993). Osmolarity and growth phase overlap in regulation of Salmonella typhi adherence to and invasion of human intestinal cells. *Infection and Immunity, 61*(7), 3084-3089.

Tedelind, S., Westberg, F., Kjerrulf, M., & Vidal, A. (2007). Anti-inflammatory properties of the short-chain fatty acids acetate and propionate: a study with relevance to inflammatory bowel disease. *World J Gastroenterol, 13*(20), 2826-2832.

Tegtmeier, D., Thompson, C. L., Schauer, C., & Brune, A. (2016). Oxygen Affects Gut Bacterial Colonization and Metabolic Activities in a Gnotobiotic Cockroach Model. *Applied and Environmental Microbiology, 82*(4), 1080-1089. doi:10.1128/aem.03130-15

Tharmalingam, S., Alhasawi, A., Appanna, V. P., Lemire, J., & Appanna, V. D. (2017). Reactive nitrogen species (RNS)-resistant microbes: adaptation and medical implications. *Biol Chem, 398*(11), 1193-1208. doi:10.1515/hsz-2017-0152

Trompette, A., Gollwitzer, E. S., Yadava, K., Sichelstiel, A. K., Sprenger, N., Ngom-Bru, C., Blanchard, C., Junt, T., Nicod, L. P., Harris, N. L., & Marsland, B. J. (2014). Gut microbiota metabolism of dietary fiber influences allergic airway disease and hematopoiesis. *Nat Med, 20*(2), 159-166. doi:10.1038/nm.3444

Tucker, S. C., & Galan, J. E. (2000). Complex function for SicA, a Salmonella enterica serovar typhimurium type III secretion-associated chaperone. *J Bacteriol, 182*(8), 2262-2268.

Turnbaugh, P. J., Hamady, M., Yatsunenko, T., Cantarel, B. L., Duncan, A., Ley, R. E., Sogin, M. L., Jones, W. J., Roe, B. A., Affourtit, J. P., Egholm, M., Henrissat, B., Heath, A. C., Knight, R., & Gordon, J. I. (2009). A core gut microbiome in obese and lean twins. *Nature, 457*(7228), 480-484. doi:10.1038/nature07540

Ubeda, C., Lipuma, L., Gobourne, A., Viale, A., Leiner, I., Equinda, M., Khanin, R., & Pamer, E. G. (2012). Familial transmission rather than defective innate immunity shapes the distinct intestinal microbiota of TLR-deficient mice. *J Exp Med, 209*(8), 1445-1456. doi:10.1084/jem.20120504

Ubeda, C., Taur, Y., Jenq, R. R., Equinda, M. J., Son, T., Samstein, M., Viale, A., Socci, N. D., van den Brink, M. R. M., Kamboj, M., & Pamer, E. G. (2010). Vancomycin-resistant Enterococcus domination of intestinal microbiota is enabled by antibiotic treatment in mice and precedes bloodstream invasion in humans. *J Clin Invest, 120*(12), 4332-4341. doi:10.1172/JCI43918

Uche, I. V., MacLennan, C. A., & Saul, A. (2017). A Systematic Review of the Incidence, Risk Factors and Case Fatality Rates of Invasive Nontyphoidal Salmonella (iNTS) Disease in Africa (1966 to 2014). *PLoS Negl Trop Dis, 11*(1), e0005118. doi:10.1371/journal.pntd.0005118

Unden, G., & Dunnwald, P. (2008). The Aerobic and Anaerobic Respiratory Chain of Escherichia coli and Salmonella enterica: Enzymes and Energetics. *EcoSal Plus, 3*(1). doi:10.1128/ecosalplus.3.2.2

Vereecke, L., Vieira-Silva, S., Billiet, T., van Es, J. H., Mc Guire, C., Slowicka, K., Sze, M., van den Born, M., De Hertogh, G., Clevers, H., Raes, J., Rutgeerts, P., Vermeire, S., Beyaert, R., & van Loo, G. (2014). A20 controls intestinal homeostasis through cell-specific activities. *Nat Commun, 5*, 5103. doi:10.1038/ncomms6103

Vessey, D. A. (1978). The biochemical basis for the conjugation of bile acids with either glycine or taurine. *Biochem J, 174*(2), 621-626.

Wahlstrom, A., Sayin, S. I., Marschall, H. U., & Backhed, F. (2016). Intestinal Crosstalk between Bile Acids and Microbiota and Its Impact on Host Metabolism. *Cell Metab, 24*(1), 41-50. doi:10.1016/j.cmet.2016.05.005

Wallace, N., Zani, A., Abrams, E., & Sun, Y. (2016). The Impact of Oxygen on Bacterial Enteric Pathogens. *Adv Appl Microbiol, 95*, 179-204. doi:10.1016/bs.aambs.2016.04.002

Walters, M., & Sperandio, V. (2006). Autoinducer 3 and epinephrine signaling in the kinetics of locus of enterocyte effacement gene expression in enterohemorrhagic Escherichia coli. *Infect Immun, 74*(10), 5445-5455. doi:10.1128/iai.00099-06

Wang, H., Tseng, C.-P., & Gunsalus, R. P. (1999). The napF and narG Nitrate Reductase Operons in Escherichia coli Are Differentially Expressed in Response to Submicromolar Concentrations of Nitrate but Not Nitrite. *Journal of Bacteriology, 181*(17), 5303-5308.

Weisburg, W. G., Barns, S. M., Pelletier, D. A., & Lane, D. J. (1991). 16S ribosomal DNA amplification for phylogenetic study. *Journal of bacteriology, 173*(2), 697-703.

WHO. (2018, 20.02.2018). Retrieved from http://www.who.int/en/news-room/fact-sheets/detail/salmonella-(non-typhoidal)

Wiles, S., Clare, S., Harker, J., Huett, A., Young, D., Dougan, G., & Frankel, G. (2004). Organ specificity, colonization and clearance dynamics in vivo following oral challenges with the murine pathogen Citrobacter rodentium. *Cell Microbiol, 6*(10), 963-972. doi:10.1111/j.1462-5822.2004.00414.x

Winter, S. E., Lopez, C. A., & Bäumler, A. J. (2013). The dynamics of gut-associated microbial communities during inflammation. *EMBO reports, 14*(4), 319-327. doi:10.1038/embor.2013.27

Winter, S. E., Thiennimitr, P., Winter, M. G., Butler, B. P., Huseby, D. L., Crawford, R. W., Russell, J. M., Bevins, C. L., Adams, L. G., Tsolis, R. M., Roth, J. R., & Baumler, A. J. (2010). Gut inflammation provides a respiratory electron acceptor for Salmonella. *Nature, 467*(7314), 426-429. doi:10.1038/nature09415

Winter, S. E., Winter, M. G., Xavier, M. N., Thiennimitr, P., Poon, V., Keestra, A. M., Laughlin, R. C., Gomez, G., Wu, J., Lawhon, S. D., Popova, I. E., Parikh, S. J., Adams, L. G., Tsolis, R. M., Stewart, V. J., & Bäumler, A. J. (2013). Host-Derived Nitrate Boosts Growth of E. coli in the Inflamed Gut. *Science, 339*(6120), 708-711. doi:10.1126/science.1232467

Winterbourn, C. C., Kettle, A. J., & Hampton, M. B. (2016). Reactive Oxygen Species and Neutrophil Function. *Annu Rev Biochem, 85*, 765-792. doi:10.1146/annurev-biochem-060815-014442

Wohlgemuth, S., Keller, S., Kertscher, R., Stadion, M., Haller, D., Kisling, S., Jahreis, G., Blaut, M., & Loh, G. (2011). *Intestinal steroid profiles and microbiota composition in colitic mice* (Vol. 2).

Wymore Brand, M., Wannemuehler, M. J., Phillips, G. J., Proctor, A., Overstreet, A. M., Jergens, A. E., Orcutt, R. P., & Fox, J. G. (2015). The Altered Schaedler Flora: Continued Applications of a Defined Murine Microbial Community. *Ilar j, 56*(2), 169-178. doi:10.1093/ilar/ilv012

Zhang, W., Li, N., Tang, X., Liu, N., & Zhao, W. (2018). Changes in intestinal microbiota across an altitudinal gradient in the lizard Phrynocephalus vlangalii. *Ecol Evol, 8*(9), 4695-4703. doi:10.1002/ece3.4029

Zheng, H., Powell, J. E., Steele, M. I., Dietrich, C., & Moran, N. A. (2017). Honeybee gut microbiota promotes host weight gain via bacterial metabolism and hormonal signaling. *Proc Natl Acad Sci U S A, 114*(18), 4775-4780. doi:10.1073/pnas.1701819114

Zhu, M., Dai, X., & Wang, Y.-P. (2016). Real time determination of bacterial in vivo ribosome translation elongation speed based on LacZα complementation system. *Nucleic Acids Research, 44*(20), e155-e155. doi:10.1093/nar/gkw698

Zhu, W., Winter, M. G., Byndloss, M. X., Spiga, L., Duerkop, B. A., Hughes, E. R., Buttner, L., de Lima Romao, E., Behrendt, C. L., Lopez, C. A., Sifuentes-Dominguez, L., Huff-Hardy, K., Wilson, R. P., Gillis, C. C., Tukel, C., Koh, A. Y., Burstein, E., Hooper, L. V., Baumler, A. J., & Winter, S. E. (2018). Precision editing of the gut microbiota ameliorates colitis. *Nature, 553*(7687), 208-211. doi:10.1038/nature25172

Danksagung

Mein besonderer Dank gilt meiner Betreuerin Prof. Dr. Bärbel Stecher, die hier im Max von Pettenkofer Institut eine ganz besondere Arbeitsgruppe aufgebaut hat. Ihre Begeisterungsfähigkeit, Unterstützung und Ideen haben mich immer motiviert. Vielen herzlichen Dank.

Ich bedanke mich auch insbesondere bei meinen Arbeitskollegen: Markus Beutler, der mich in die Geheimnisse gnotobiotischen Arbeitens eingeweiht hat; Diana Ring, Problemlöserin und gute Seele des Labors ohne die die letzten Jahre extrem langweilig geworden wären; Claudia Eberl, für die stetige Motivation zum Sport; Debora Garzetti, ohne deren bioinformatisches Wissen ich schon längst verloren wäre, Stefanie Spriewald und Martin Koeppel die immer auf alle Fragen eine Antwort parat haben; Saib Hussain und dem ganzen Tierhaus-Team (Anna, Jenny, Kathi und Michi), dass sie immer das Unmögliche doch noch möglich machten; Sandrine Brugiroux, die mich an das Arbeiten mit anaeroben Bakterien herangeführt hat und Lara Jochum für die Hilfe mit der Analyse der RNAseq Daten. Weiteren Dank gilt Philipp Münch, Raphaela Götz, Patrick Schiller, Jana Glaser und Lubov Nedialkova. Vielen Dank euch allen für die schöne Zeit.

Weiterhin möchte ich mich bei allen Kooperationspartnern bedanken, insbesondere bei den Arbeitsgruppen von David Berry und Alexander Loy in Wien mit Buck Hanson, Nika Ivanova und Michaela Steinberger, der Arbeitsgruppe von Philippe Schmitt-Kopplin vom Helmholtz Zentrum München mit Alesia Walker und der Arbeitsgruppe von Roman Gerlach vom RKI in Wernigerode mit Steffi Walter.

Vielen Dank an meine Familie die mich immer unterstützt hat.